1-1-2006

Turbo multiuser detection with integrated channel estimation for differentially coded CDMA systems.

Shahram Talakoub
University of Windsor

Turbo Multiuser Detection with Integrated Channel Estimation for Differentially Coded CDMA Systems

by

Shahram Talakoub

A Dissertation
Submitted to the Faculty of Graduate Studies and Research
through Electrical Engineering
in Partial Fulfillment of the Requirements for
the Degree of Doctor of Philosophy at the
University of Windsor

Windsor, Ontario, Canada
2006

Your file Votre référence
ISBN: 978-0-494-42384-4
Our file Notre référence
ISBN: 978-0-494-42384-4

Abstract

This thesis is concerned with iterative joint multiuser detection (MUD) and channel estimation for the uplink of asynchronous direct-sequence code-division multiple-access (DS-CDMA) systems in multipath channels. For the base station of a CDMA system, it is shown that it is possible to design a receiver that can recover the multiuser information symbols of all the users within its own cell without any prior knowledge of the multipath channel or the spreading codes of users outside the cell. In this thesis, for two different scenarios, we propose two receiver structures that take all the necessary signal processing operations into account simultaneously. In other words, the proposed iterative receivers can jointly perform channel estimation, channel equalization, MUD, and channel decoding. The proposed iterative processing algorithms allow earlier stages of a receiver (e.g., the channel estimator) to refine their processing based on soft information obtained from later stages (e.g., the channel decoder) to provide a refine estimate of some signal or channel parameters.

First, a turbo (iterative) receiver structure is proposed for the uplink of coded CDMA systems in the presence of unknown interference. The proposed receiver consists of a first stage that performs soft interference cancellation and group-blind linear minimum mean-square-error (MMSE) filtering, followed by a second stage that performs channel decoding. The proposed group-blind linear MMSE filter suppresses the residual multiple-access interference (MAI) from known users based on the spreading codes and the channel characteristics of these users, while suppressing the interference from other unknown users using a

subspace-based blind method. A novel estimator is also proposed to estimate the number of unknown users in the system by exploiting the statistical properties of the received signal, since the knowledge of the number of unknown users is crucial for the proposed receiver. Simulation results demonstrate that the proposed estimator can provide the number of unknown users in heavily loaded CDMA systems with high probability, and also the proposed group-blind receiver integrated with the new estimator can significantly outperform the conventional turbo multiuser detector in the presence of intercell interference.

Second, we propose another receiver structure that performs joint iterative multiuser detection and channel estimation for the uplink of differentially coded asynchronous DS-CDMA systems in unknown multipath channels. The proposed receiver consists of two stages. The first stage performs channel estimation, soft interference cancellation and soft-in-soft-out (SISO) multiuser filtering and the second stage consists of a bank of serially concatenated single-user channel decoders and differential decoders. The single-user iterative decoder for each user consists of a powerful combination of a recursive systematic convolutional (RSC) decoder with a differential decoder, which work together in an iterative fashion. In terms of channel estimation for the first iteration, the multipath channel is estimated blindly by exploiting the orthogonality between the signal and the noise subspaces. For the next iterations the channel is estimated using the soft estimates of coded bits of each user provided by single-user iterative decoders in conjunction with the output of the multiuser detector. By exchanging soft information between different stages, the receiver performance is improved through the iteration process. Simulation results demonstrate that the performance of the proposed iterative multiuser detector with integrated channel estimator approaches the single-user bound at high SNR.

We also study the effect of an SNR mismatch on the BER performance of the Log-MAP and the Max-Log-MAP turbo equalizers, and propose an iterative online SNR estimation scheme that effectively estimates the unknown SNR from each block of data. Simulation results illustrate that the performance of this scheme is very close to that of the receiver which assumes perfect knowledge of the channel SNR even for short block lengths over high-loss channels.

To my Family

Acknowledgements

A journey is easier when you travel together. Interdependence is certainly more valuable than independence. This thesis is the result of more than four years of work whereby I have been accompanied and supported by many people. It is a pleasant aspect that I have now the opportunity to express my gratitude for all of them.

The first person I would like to thank is my direct supervisor Dr. Behnam Shahrrava. During these years I have known Behnam as a sympathetic and principle-centered person. His overly enthusiasm and integral view on research and his mission for providing "only high-quality work and not less" has made a deep impression on me. I owe him lots of gratitude for having me shown this way of research. He cannot realize how much I have learned from him. Besides of being an excellent supervisor, Behnam was as close as a relative and a good friend to me. I am really glad that I have come to get to know him in my life.

I would like to thank Dr. Majid Ahmadi who kept an eye on the progress of my work and always was available when I needed his advises. I would also like to thank the other members of my PhD committee who monitored my work and took effort in reading and providing me with valuable comments on earlier versions of this thesis: Dr. David Falconer, Dr. Scott Goodwin, and Dr. Kemal Tepe. I thank you all.

This research has been supported and funded by the Natural Sciences and Engineering Research Council of Canada. I would like to thank them for their confidence in me. I am also grateful for the department of Electrical and computer Engineering of the University of Windsor for providing me an excellent work environment during the past years and Shelby Merchand, Andria Turner, Frank Cicchello and Don Tersigni for their cheerful assistance.

In my opinion, doing a PhD is a sacred task and without the help of my close friends I believe it was impossible to come to a good end. I would like to thank my dearest friend Mohammad Reza Yazdani who I know for more than ten years now for having shared many experiences and thoughts with me throughout these years. A special thanks goes to Haniyeh Yusofpourfard, who showed to be a kind, mostly helpful and trustful friend.

I feel a deep sense of gratitude for my father and mother who formed my vision and taught me the good things that really matter in life. They still provide a persistent inspiration for my journey in this life. I am grateful for my two sisters Shadi, and Naghme for rendering me the sense and the value of sisters.

I am very grateful for my wife Leila, for her love and patience during the PhD period. Her ability to see the best in everything has been inspiration to my life. Her presence in my life is the best gift ever bestowed to me. Words cannot express my sense of gratitude to her.

Contents

List of Figures

List of Tables

Chapter 1

Intoduction

Around the mid twentieth century, Claude Shannon defined the basis of the information theory, showing that it is possible to transmit information error free as long as it occurs at a rate below the channel capacity; however, the solution to the problem remained unknown until a few years ago.

Claude Shannon was still alive when the answer was finally found at the dawn of the third millennium. Turbo coding [2] represents a new and very powerful error control coding technique, which has begun to have a significant impact, allowing communication very close to the channel capacity. The powerful error correction capability of turbo codes was recognized and accepted for almost all types of channels leading to increased data rates and improved quality of service. Turbo codes can operate at 0.1 dB from the Shannon capacity limit outperforming any coding technique known today.

Extensive research has been done in the application of turbo codes in deep space communications, satellite/cellular communications, microwave links, paging, in orthogonal frequency-division multiplexing (OFDM) and code-division multiplex-access (CDMA) architectures. The extra coding gain achieved by exploiting turbo codes may be well spent to save bandwidth or to reduce the power requirements in the link budget.

The information obtained from the decoders in the turbo code scheme contains not only

the decoded message (hard output), but also the measure of the amount of confidence in the decision (soft output).

Turbo equalization employs the turbo principle for joint equalization and decoding over frequency selective channels which produce inter-symbol interference (ISI). In [3], the turbo scheme using the soft output Viterbi algorithm (SOVA) was applied for detection and decoding of recursive systematic code over a delay dispersive channel. Turbo equalization by exploiting maximum *a posteriori* probability (MAP) algorithm was first introduced in [4].

It is known that for equalization and decoding the optimal soft-input/soft-output (SISO) algorithm in the sense of minimum bit error rate is symbol by symbol maximum *a posteriori* algorithm [1]. In practice, this algorithm is implemented in the logarithmic domain in order to reduce the numerical computation problems. The resulting algorithm is called the Log-MAP algorithm. The Max-Log-MAP algorithm [53], as will be shown later, is extracted from the Log-MAP algorithm with an approximation. Making this approximation results in the Max-Log-MAP algorithm to be suboptimal and it yields inferior results compared to the Log-MAP algorithm. In additive white Gaussian noise (AWGN) channels, the performance difference between the Log-MAP algorithm and the Max-Log-MAP algorithm is negligible. Considering the implementation complexity of the Log-MAP algorithm, the Max-Log-MAP algorithm is an attractive option. However, as it is shown in [9], the Max-Log-MAP algorithm is not suitable for turbo equalization over the high loss frequency selective channels [15].

1.0.1 Multiuser Communication Systems

Since the telephone was invented in the late nineteenth century, there has been a steady development of telephone services, and the number of subscribers has continuously increased. One of the most revolutionary developments in telephone service in the late twentieth century was the introduction of the cellular variety of mobile phone services. As the number of subscribers has explosively grown in the wireless communication systems, provision of the mobility in telephone service was made possible by the technique of wireless cellular communication. As the bandwidth over the wireless link is a scarce resource, one of the

essential functions of wireless communication systems is the multiple access technique for a large number of users to share the resource. Conceptually, there are mainly three conventional multiple-access techniques: FDMA, time-division multiple-access (TDMA), and CDMA. The multiple-access technique implemented in a practical wireless communication system is one of the main distinguishing characteristics of the system, as it determines how the common transmission medium is shared among users. FDMA divides a given frequency band into many frequency channels and assigns a separate frequency channel on demand to each user. It has been used for analog wireless communication systems. The representative FDMA wireless cellular standards include Advanced Mobile Phone System (AMPS) in the United States, Nordic Mobile Telephones (NMT) in Europe, and Total Access Communications System (TACS) in the United Kingdom [16]. TDMA is another multiple access technique employed in the digital wireless communication systems. It divides the frequency band into time slots, and only one user is allowed to either transmit or receive the information data in each slot. That is, the channelization of users in the same frequency band is obtained through separation in time. The major TDMA standards contain Global System Mobile (GSM) in Europe and Interim Standard 54/136 (IS-54/136) in North America [17]. GSM was developed in 1990 for second generation (2G) digital cellular mobile communications in Europe. Systems based on this standard were first deployed in 18 European countries in 1991. By the end of 1993, it was adopted in nine more European countries, as well as Australia, Hong Kong, much of Asia, South America, and now the United States. CDMA is another multiple access technique utilized in digital mobile communication systems. In CDMA, multiple access is achieved by assigning each user a pseudo-random code (also called pseudo-noise codes due to noise-like autocorrelation properties) with good auto- and cross-correlation properties. This code is used to transform a user's signal into a wide band spread spectrum signal. A receiver then transforms this wide band signal into the original signal bandwidth using the same pseudo-random code. The wide band signals of other users remain wide band signals. Possible narrow band interference is also suppressed in this process. The available spectrum is divided into a number of channels, each with a much higher bandwidth than the TDMA systems. However, the same carrier can now be

used in all cells, such that the unity resource factor can be achieved in CDMA systems. It assigns each user a unique code, which is a pseudo-random sequence, for multiple users to transmit their information data on the same frequency band simultaneously. The signals are separated at the receiver by using a correlator that detects only signal energy from the desired user. One of the major CDMA standards is IS-95 in North America [18]. The use of CDMA technology in wireless cellular systems began with the development of the IS-95 standard [18], one of the 2G systems, in the early 1990s. At that time, the focus was to provide an efficient alternative to systems based on the AMPS standard in providing voice services, and only a low bit rate of 9.6 Kbps was provided. The main markets of IS-95 are the United States, Japan, and Korea, the latter being the largest market, with over 25 million subscribers. The success of IS-95 in Korea is based on the adoption of IS-95 as a national standard in the early 1990s. Now, CDMA is considered as one of the fastest growing digital wireless technologies. CDMA has been adopted by almost 50 countries around the world. Furthermore, CDMA was selected as a multiple-access scheme for the third generation (3G) system [19]-[21]. In addition to FDMA, TDMA, and CDMA, orthogonal frequency division multiplexing (OFDM), a special form of multicarrier modulation, can be used for multiplexing for multiple users. In OFDM, densely spaced subcarriers with overlapping spectra are generated using fast Fourier transform (FFT), and signal waveforms are selected in such a way that the subcarriers maintain their orthogonality despite the spectral overlap. One way of applying OFDM to the multiple access is through OFDM-TDMA or OFDM-CDMA, where different users are allocated different time slots or different frequency spreading codes. However, each user has to transmit its signal over the entire spectrum. This leads to an averaged-down effect in the presence of deep fading and narrow band interference. Alternatively, one can divide the total bandwidth into traffic channels (one or a cluster of OFDM subcarriers) so that multiple access can be accommodated in a form of the combination of OFDM and FDMA, which is called orthogonal frequency division multiple access (OFDMA).

An OFDMA system is defined as one in which each user occupies a subset of subcarriers, and each carrier is assigned exclusively to only one user at any time. Advantages of OFDMA

over OFDM-TDMA and OFDM-CDMA include elimination of intracell interference and exploitation of network/multiuser diversity. Space division multiple access (SDMA) is also recognized as a promising multiple access technology for improving capacity by the spatial filtering capability of adaptive antennas. SDMA separates the users spatially, typically using beam forming techniques such that in-cell users are allowed to share the same traffic channel. SDMA is not an isolated multiple access technique, but it can be applied to all other multiple access schemes [22]. In other words, a system that provides access by dividing its users in frequency bands, time slots, codes, or any combination of them, can also reuse its resources by identifying the users' positions so that under a given criterion, they can be separated in space.

CDMA techniques offer several advantages over other multiple access techniques, such as high spectral reuse efficiency, exploitation of multipath fading through RAKE combining, soft handoff, capacity improvements by the use of cell sectorization, and flexibility for multirate services [23]- [25]. The use of the CDMA techniques in wireless cellular communications commenced with the development of the IS-95A standard [18], of which IS-95A has been designed to achieve higher capacity than the first generation (1G) systems in order to accommodate rapidly growing subscribers. Further development of IS-95A toward higher bit rate services was started in 1996. This led to the completion of the IS-95B standard in 1998. While the IS-95A standard uses only one spreading code per traffic channel, IS-95B can concatenate up to eight codes for the transmission of higher bit rates. IS-95B systems can support medium user data rates of up to 115.2 Kbps by code aggregation without changing the physical layer of IS-95A. The next evolution of CDMA systems has led to wide band CDMA. Wide band CDMA has a bandwidth of 5 MHz or more. The two wide band CDMA schemes for 3G are WCDMA, which is network asynchronous, and cdma2000, which is synchronous. In network asynchronous schemes, the base stations (BSs) are not synchronized; in network synchronous schemes, the BSs are synchronized to each other within a few microseconds. Similar to IS-95, the spreading codes of cdma2000 are generated using different phase shifts of the same M sequence. This is possible because of the synchronous network operation. Because WCDMA has an asynchronous network, different long codes

rather than different phase shifts of the same code are used for the cell and user separation. The code structure further impacts how code synchronization, cell acquisition, and handover synchronization are performed. The race of the high-speed packet data in CDMA started roughly in late 1999. Before then, WCDMA and cdma2000 systems supported packet data, but the design philosophy was still old in the sense that system resources such as power, code, and data rate were optimized to voice-like applications [26]. There has been a change since late 1999, as system designers realized that the main wireless data applications will be Internet protocol (IP) related; thus, optimum packet data performance is the primary goal for the system designers to accomplish. With the design philosophy change, some new technologies have appeared, such as 1x radio transmission technology evolution for high-speed data introduction only (1xEV-DO) and high-speed downlink packet access (HSDPA). Key concepts of these systems include adaptive and variable rate transmission, adaptive modulation and coding, and hybrid automatic repeat request (ARQ) to adapt the IP-based network for a given channel condition and workload with the objective of maximizing the system performance by using various adaptive techniques while satisfying the quality of service (QoS) constraints. First, HSDPA is a major evolution of WCDMA wireless network, where the peak data rate and throughput of the WCDMA downlink for best effort data is greatly enhanced when compared to release 99. In March 2000, a feasibility study on HSDPA was approved by 3GPP. The study report was part of release 4, and the specification phase of HSDPA was completed in release 5 at the end of 2001. By contrast, cdma2000 is followed by 1xEV-DO for the first phase, in the sense of deployment schedule, and high-bit-rate data and voice (1xEV-DV) for the second phase. It is noteworthy that 1xEV-DV does not necessarily follow 1xEV-DO. Both 1xEV-DO and 1xEV-DV allow data rates of up to 2.4 Mbps in 1.25-MHz bandwidth, compatible with the frequency plan of 2G and 3G CDMA systems based on IS-95 and cdma2000. It is not hard to see the reasons for the success of CDMA. Its advances over other multiple-access schemes include higher spectral reuse efficiency due to the unity reuse factor, greater immunity to multipath fading, gradual overload capability, and simple exploitation of sectorization and voice inactivity. Moreover, CDMA has more robust handoff procedures [27]-[30].

In this work, only direct-sequence CDMA (DS-CDMA) is studied since it is deemed to be more suitable for mobile communications [31], [32]. In DS-CDMA all users use the same bandwidth, but each transmitter is assigned a distinct sequence. DS-CDMA employs a waveform, that for all purposes, appears random to anyone but the intended receiver of the transmitter waveform. Actually, for the ease of both generation and synchronization by the receiver, the waveform is pseudorandom, meaning that it can be generated by precise rules, but statistically it nearly satisfies the requirements of a truly random sequence. The conventional receiver is the simplest suboptimum detector used in CDMA. It consists of a parallel bank of K (the number of users) filters, each matched to its own spreading waveform. Assuming that only one user is active, this matched-filter receiver is optimal for transmission over the AWGN channel. Consequently, assuming that the interference from other users is accurately modeled as additive white Gaussian noise, the matched filter receiver works as a maximum likelihood (ML) single user detector. As such, data detection for each user is accomplished independently of that performed on other users. One of the disadvantages of the conventional scheme is that it is severely affected by multiple-access interference (MAI), making such systems interference limited [33]. In practice, the conventional detector also suffers from the near-far problem, which means high power users degrade the performance of low power users, even if the spreading waveforms have very low cross-correlations (the correlations between the different spreading waveforms) [34]. Two methods have been used to overcome the near-far problem: multiuser detection and power control. Multiuser detection is concerned with designing receivers that take into account the structure of the MAI. Conversely, power control is concerned with balancing both the transmitted powers of the users and the corresponding interference experienced at the detector. Power control might result in an increase in the capacity of the system so that more users can be accommodated and more data transmitted. Power control also results in reduced energy consumption of the transmitters.

The inability of the conventional receiver to exploit the structure of the MAI results in severe performance losses. A better detection strategy is to jointly detect multiple users, where the additional structure of the MAI is exploited rather than considered as noise.

It is well-known that the computational complexity of individually optimal detection for DS-CDMA grows exponentially with the number of users [75], as the computation of the marginal posterior-mode (MPM) distribution is required. Maximum *a posteriori* probability (MAP) detection for the users is therefore far too complex for practical CDMA systems with even a moderate number of users. The exponentially growing complexity has inspired a considerable effort in finding low complexity suboptimal alternatives capable of resolving the detrimental effects of MAI. For certain special cases of the correlation matrix, it has been shown that maximum likelihood (ML) detection can be obtained by polynomial-time algorithms [35]- [37]. An iterative structure that is guaranteed to deliver ML detection on some bits was suggested in [38]. Decisions on all bits are, however, not guaranteed.

Early work on low complexity suboptimal multiuser detectors include the linear multiuser detectors, such as the decorrelating detector [34], [40] and the minimum mean-squared error (MMSE) detector [86]. The main attraction of MMSE detection lies in the direct relationship between adaptive filtering and MMSE estimation. This translates into practical implementation of MMSE detectors using well understood adaptive filtering algorithms [42]. For more information of these adaptive algorithms for multiuser detector, one can refer to [43], [44]. Another group of low complexity multiuser detector is the interference cancellation (IC) strategies [45]. Early work was focused on linear cancellation and hard decision cancellation [46], [47]. More recently, soft decision cancellation has been shown to provide performance improvements. In [48], it was shown that soft decision cancellation based on convex projections provides an iterative solution to the convex-constrained multiuser ML problem. The well-known result that the optimal nonlinear MMSE estimate is the conditional posterior-mode mean was used in [49] for a decision-feedback receiver. Similar arguments were used in [50] to arrive at a soft decision IC structure, and the same structure was derived in [51] based on neural networks arguments. Even though this cancellation structure has a low complexity of order $\mathcal{O}(K^2)$, numerical examples show that near single user performance can be achieved for large systems [51].

Intercell Interference Cancellation

The presence of both MAI and inter-symbol interference (ISI) constitute the major obstacles to reliable communications in multipath CDMA systems. Therefore, techniques to mitigate MAI and ISI have been the focus of a rigorous research effort over the past decade. The multiuser detection techniques are able to combat multiple access interference and multipath distortion effectively, thus improving the system performance. The optimal multiuser detection based on maximum likelihood algorithm was introduced in [75]. The algorithm achieves the best performance at the cost of prohibitive computational complexity. Suboptimal multiuser detectors based on linear minimum mean-square error or decorrelator were proposed in [40] and [76], respectively.

In recent years, iterative (turbo) processing techniques have received considerable attention, inspired by the discovery of turbo coding [57], [2]. Exhaustive research in related topics produced different algorithms that follow the turbo decoding approach to provide similar gain in performance. Turbo multiuser detection applies the same principle, namely the iterative exchange of soft information among different blocks to improve the system performance [58]- [64]. In such turbo multiuser detectors, the channel decoding is combined with multiuser detection in a way that the output of channel decoders is fed back to the multiuser detector to improve the system performance iteratively. The optimal turbo multiuser detector exploiting maximum *a posteriori* (MAP) algorithm for detection and decoding is proposed in [65]. In the same article, the authors propose a less complex approach based on interference cancellation, and linear MMSE filtering.

Practical wireless communication systems usually experience interference from users whose signature waveform is not known to the receiver. In CDMA downlink, a mobile receiver knows only its own spreading sequence and it is blind with respect to the other users of the system. In CDMA uplinks, however, typically the base station has knowledge of the spreading sequences of a group of users within its own cell, while it is blind with respect to users from neighboring cells. The term group blind refers to this situation. It is normal to expect some performance loss due to the presence of these users in the system over the case where all users are known to the receiver. In order to boost the performance of the system

for such scenarios, various types of detection schemes are proposed for *uncoded* CDMA systems [66]- [68], where a number of linear and nonlinear detectors were developed for synchronous CDMA systems. In [69], the ideas in [67] and [68] are generalized and several forms of group blind detectors based on different criteria are developed. Also, the blind and group blind multiuser detection and blind channel estimation in presence of correlated ambient channel noise was considered. The idea of colored noise in the context of group blind is justifiable, when the very weak interference from outside the cell is considered as noise. In [70], a nonlinear group blind method is developed for detection of known users in presence of unknown interference and multipath channel distortion. The algorithm starts by constructing a likelihood function for known users and then performs slowest descent method over such a likelihood surface. Simulation result shows that the method outperforms its linear counterpart, but increases the computational complexity. Another nonlinear group blind multiuser detection technique was introduced in [71] and [72] where the Gibbs sampler was employed to perform the Bayesian multiuser detection according to the linear group blind decorrelating output.

In *coded* CDMA, Reynolds and Wang proposed a receiver structure for uplink of asynchronous CDMA systems [73]. In this method in order to suppress the intercell and intracell interferences, the detector performs a soft interference cancellation for each user in which estimates of the multiuser interferences from the known users and an estimate for the interference caused by unknown users are subtracted from the received signal. It is shown later in this paper that this algorithm does not provide a robust performance in CDMA uplink. Another group blind turbo multiuser detection for coded asynchronous CDMA is proposed in [79], where the multiple access interference is approximated as a Gaussian random vector. The algorithm tries to improve the performance of the turbo multiuser detector by employing the variance of this noise as well as the ambient channel noise at the receiver. As the turbo multiuser detector is almost insensitive to any mismatch between actual signal to interference plus noise ratio (SINR), and the one assumed at the receiver, the method can not provide fundamental gain in performance compared to conventional turbo multiuser detector in presence of unknown interferences.

All group blind algorithms based on subspace, for both coded and uncoded CDMA, require the number of known and unknown users. It is reasonable to expect attaining the number of known users from higher layers (i.e network layer), but it is very unrealistic to expect to obtain such information regarding unknown users present in the system. A likelihood approach to estimate the number of sources based on Akaike information criterion (AIC) and minimum description length (MDL) criterion was proposed in [77]. These criteria heavily rely on the white noise assumption and they fail to correctly detect the number of sources when the noise is not perfectly white. In [78], in order to improve the estimator performance in a nonwhite noise environment a decision rule based on the intrinsic property of the eigenvalues of a correlation matrix is defined which provides a coarse estimation of the signal subspace. To further improve the estimation, a hypothesis testing criterion [89] for rank decision is proposed. While the algorithm provides better performance than those of MDL and AIC in nonwhite noise, it is very sensitive to signal to noise ratio and fails to provide the correct rank of signal subspace in the low to moderate SNR region. By employing the coding, the system usually works in this region and the method can not provide the correct number of unknown users under this circumstance.

In this work, we first consider the scheme proposed in [73] and show that the algorithm does not provide robust performance in CDMA uplink because the algorithm fails to converge under certain conditions. It is mathematically proved that when the extrinsic information at the input of the multiuser detector is large enough, the output of the detector fails to converge. We then propose a robust group blind multiuser detection scheme that combines the concept of group blind detection and turbo multiuser detection for asynchronous CDMA systems. Specifically, it consists of two stages similar to those of [65] for recursive systematic convolutionally encoded CDMA systems. The first stage consists of soft interference cancellation and combined group blind MMSE filtering, whereas the second stage consists of channel decoding. The combined group blind MMSE filtering tries to suppress the interference from known users based on the signature waveforms and the channel characteristic of these users and suppresses the interference from other unknown users using subspace-based blind methods. Simulation results show that this method preserves

its advantage in performance over the conventional turbo multiuser detection method even in the case of high intercell interference. It is also shown that because of exploiting the subspace method we can easily estimate the variance of the noise at the receiver; therefore, the knowledge of SNR is not necessary at the receiver. Furthermore, based on the statistical properties of the signal and the channel, we propose an estimation algorithm to estimate the number of unknown users which is much faster, less complex and is able to provide the number of unknown users in white and nonwhite noise environments with very high precision. Simulation results show that the proposed estimator is not sensitive to parameters such as signal to noise ratio, the over sampling factor, or the processing gain.

Channel Estimation

In the uplink CDMA systems, users have crude common timing references and are able to align their signal blocks with the slot reference of the base station. However, due to various impairments of the channel such as multipath propagation and faulty synchronization the signals at the receiver experience misalignment; therefore, the system is considered asynchronous in general. Furthermore, if the blocks are short enough with respect to channel coherence time [15], the users' channels can be assumed to be time invariant over the block duration. Various types of detection and decoding schemes have been proposed in [3]-[7] where the receiver structure relies on the assumption that the channel information is somehow available at the receiver.

The problem of channel estimation for multiuser detection requires knowledge of the spreading sequence, timing of bit/symbol epoch, carrier phase and channel impulse response for the desired user as well as other users of the system. While such information can be attained using pilot sequences, [82]- [87] for different spreading sequences, blind methods offer better spectrum efficiency by not requiring pilot signals. The blind channel estimation by exploiting the orthogonality between the signal and noise subspace is considered in [89]-[93]. Due to the finite length of the signal frame from which the channel is estimated, both types of detectors tend to exhibit an error floor at high signal to noise ratio (SNR). The problem is especially severe in the case of blind channel estimation.

Iterative multiuser detection with integrated channel estimation for the *coded* DS-CDMA system was proposed in [94]. To resolve the problem of channel estimation, an iterative receiver performing pilot symbol aided channel phase and amplitude estimation as well as data and channel symbol estimation for coded transmission was proposed. It was assumed that the delays of the path are known to the receiver. In [95], another iterative multiuser channel estimation and symbol detection is proposed and its convergence is analyzed.

1.0.2 Organization and Contribution of the Thesis

The objective of this work is to address and provide practical solutions for a number of fundamental challenges that a digital communication receiver may face in a real world environment. We particularly consider coded systems in single-user and multiuser scenarios. Unless otherwise stated, the main focus of this work is on the time dispersive or frequency selective channels.

In Chapter 2, we propose two different iterative SNR estimation algorithms which provide acceptable performance in high loss ISI channels. We start the algorithm by utilizing the Max-Log-MAP algorithm for the first iteration. The hard decision of the output of the decoder is then utilized to obtain a long sequence of virtual pilot symbols to estimate the SNR. The same approach is employed in later iterations; however, instead of the Max-Log-MAP algorithm, the Log-MAP algorithm is utilized for both equalization and decoding. A similar structure based on the soft decision feedback is developed in [56]. Due to the fact that the output of the decoder is not error free, a correction of the SNR estimate may be required based on an exhaustive search for different block lengths. Furthermore, if the frame length becomes very short, there would be a slight degradation in performance due to the use of the Max-Log-MAP algorithm in the first iteration. In [55], an approximate maximum likelihood (ML) based estimator is developed using both the pilot and data symbols simultaneously; however, owing to the approximation, the estimator is biased. This results in performance degradation of the receiver, especially in the low bit error rate region.

Alternatively, in the second part of Chapter 2, we propose another structure which is able to estimate the SNR without using pilot symbols. Our proposed estimator is able

to estimate the SNR and improve the estimation via iteration. In the first iteration an eigen decomposition is performed on the received signal from the channel. By separating the signal subspace from the noise subspace and choosing the largest eigen-value of the noise subspace, an estimate for the variance of the noise is obtained. For the first iteration we exploit the estimated variance in the Log-MAP equalization and decoding algorithm. For later iterations if the quality of the extrinsic information at the output of the decoder improves, this information is utilized as an alternative to the original subspace method to mitigate any mismatch between the actual SNR and the estimated SNR at the receiver. A hypothesis testing criterion is introduced to decide whether or not this transition is beneficial in terms of the receiver performance. Simulation results demonstrate identical performance with optimal algorithm even for very short block lengths. Furthermore, the estimator performance in terms of the normalized bias is investigated and it is shown that our proposed method is unbiased. This finding is in contrast to the method proposed in [55] where it demonstrates an error floor in terms of the estimator bias by increasing the SNR. We have also included the normalized root mean-square error (RMSE) of the proposed estimator and it is shown that the RMSE of the estimator is decreased as the iteration proceeds.

Chapters 3 and 4 are dedicated to multiuser scenarios. In Chapter 3, we consider an uplink of a coded CDMA system where two different sources of interference exist in the system: the intercell interference and the intracell interference. We first consider the scheme proposed in [73] and we show that the algorithm does not provide robust performance in CDMA uplink because the algorithm fails to converge under certain conditions. It is mathematically proved that when the extrinsic information at the input of the multiuser detector is large enough, the output of the detector fails to converge. We then propose a robust group blind multiuser detection scheme that combines the concept of group blind detection and turbo multiuser detection for asynchronous CDMA systems. Specifically, it consists of two stages similar to those of [65] for recursive systematic convolutionally encoded CDMA systems. The first stage consists of soft interference cancellation and combined group blind MMSE filtering, whereas the second stage consists of channel decoding. The combined

group blind MMSE filtering tries to suppress the interference from known users based on the signature waveforms and the channel characteristic of these users and to suppress the interference from other unknown users using subspace-based blind methods. Simulation results show that this method preserves its advantage in performance over the conventional turbo multiuser detection method even in the case of high intercell interference. It is also shown that because of exploiting the subspace method we can easily estimate the variance of the noise at the receiver; therefore, the knowledge of SNR is not necessary at the receiver. Furthermore, based on the statistical properties of the signal and the channel, we propose an estimation algorithm to estimate the number of unknown users which is much faster, less complex and is able to provide the number of unknown users in white and nonwhite noise environments with very high precision. Simulation results show that the proposed estimator is not sensitive to parameters such as signal to noise ratio, over sampling factor, or processing gain.

Joint channel estimation and multiuser detection is considered in Chapter 4. We propose an iterative receiver for uplink of differentially coded CDMA systems that perform channel estimation without using pilot symbols. We will conduct the channel estimation in conjunction with symbol detection in every iteration. For the first iteration we perform the blind channel estimation procedure to estimate the channel. Since the blind channel estimator has an arbitrary phase ambiguity, it is necessary to employ differential encoding and decoding [88]. This leads us to exploit the results of recent research on the class of error correcting codes generated by the serial concatenation of a recursive systematic convolutional (RSC) encoder, an interleaver and a differential encoder. [96]- [101] for each user. These codes are attractive because they combine the performance gain of error correcting coding with the robustness of noncoherent demodulation [101].

The receiver structure consists of a matched filter, a channel estimator, a soft interference cancellation unit, a soft output minimum mean-square error (MMSE) filter, deinterleaver, a bank of single user RSC decoders, interleavers, and finally differential decoders. The single user RSC decoder and differential decoder of each user can work in an iterative fashion to further improve the performance. At the end of inner iterations between single

user decoders, the soft estimate of coded symbols, as well as the results at the output of the MMSE filter, are combined to be sent to the channel estimator and soft interference cancellation unit. The channel estimator provides a new estimate of the channel based on this new information, and sends the channel information to the multiuser detector and the soft interference cancellation unit. The process of channel estimation, soft interference cancellation, detection, and iterative decoding is continued until a suitably chosen termination criterion (i.e. specific number of iterations), stops the iteration process.

A summery of the results obtained in this research and suggestions for further studies are given in Chapter 5.

Appendix A has been added to this thesis to show one of our contributions that is not directly related to the major trend of this thesis. We propose a method to modify the Max-Log-MAP algorithm. In terms of performance, the performance of the proposed algorithm is very close to that of the Log-MAP algorithm, even in high loss ISI channels where there is a wide gap between the performance of the Max-Log-MAP and Log-MAP algorithms. In terms of implementation, the proposed algorithm is simply implementable using adders and comparators. Whereas, direct implementation of the Log-MAP algorithm is almost impossible, and using a look-up table increases the area and power, and decreases the overall speed. Unfortunately, the knowledge of the signal to noise ratio (SNR) at the receiver side is necessary for the proposed algorithm as well as the Log-MAP turbo equalizers while the Max-Log-MAP [53] algorithm does not require this information. The problem of SNR mismatch, between the channel and the receiver is studied in [54]- [8]. For turbo equalization over high loss ISI channels [15] the performance difference between the optimal algorithm (i.e the Log-MAP) and the suboptimal Max-Log-MAP algorithm is not negligible. Therefore, an accurate estimate of the SNR is essential. In practice different approaches based on known pilot symbols or unknown data symbols are proposed to estimate the SNR. The results obtained in this part have already been reported in [105].

Chapter 2

Turbo Equalization with Integrated SNR Estimation for Time-Dispersive Channels

Theoretically, it is necessary to estimate the signal-to-noise ratio (SNR) of the channel when using a maximum *a posteriori* (MAP) or Log-MAP turbo equalizer. In this chapter, we study the effect of an SNR mismatch on the bit error rate (BER) performance of Log-MAP and Max-Log-MAP turbo equalizers, and propose an iterative online SNR estimation scheme that effectively estimates the unknown SNR from each block of data. We show that this scheme gives performance very close to that with perfect knowledge of channel SNR for even short block lengths over high-loss channels. The algorithm starts by utilizing the Max-Log-MAP algorithm for the first iteration. The hard decision of the output of the decoder is then utilized to obtain a long sequence of virtual pilot symbols to estimate the SNR. Same approach is employed in later iterations; however, instead of the Max-Log-MAP algorithm, the Log-MAP algorithm is utilized for both equalization and decoding. Due to the fact that the output of the decoder is not error free, a correction of the SNR estimate may be required based on exhaustive search for different encoder structure or different

block lengths. Furthermore, if the frame length become very short there would be a slight degradation in performance due to the use of the Max-Log-MAP algorithm in the first iteration. To resolve these dilemmas we propose an alternative turbo receiver structure with integrated SNR estimation. The proposed receiver is able to estimate the signal-to-noise ratio (SNR) and improve the estimation via iteration. Initially we exploit a subspace-based method to estimate the SNR. During the iterative process of equalization and decoding if the quality of the *a posteriori* information at the output of decoder improves, it is possible to utilize this information as an alternative to the original subspace method to mitigate any mismatch between the actual SNR and the estimated SNR at the receiver. A hypothesis testing criterion is introduced to decide whether or not this transition is beneficial in terms of the receiver performance. Simulation results demonstrate that our proposed receiver structure is able to yield a performance similar to that of the known SNR at the receiver.

This chapter is organized as follows. After reviewing the turbo equalization scheme in Section 2.1, the MAP-based turbo equalization algorithms are presented in Section 2.2. In Section 2.3 we compare the performance of Log-MAP and Max-Log-MAP turbo equalizers in moderate and high loss channels. In Section 2.4 we study the SNR sensitivity of Log-MAP and Max-Log-MAP turbo equalizers. We also provide a mathematical proof to show why the Max-Log-MAP turbo equalizer is insensitive to SNR mismatch. An iterative online SNR estimation scheme is proposed in Section 2.5. The signal model and the system description of the subspace based iterative SNR estimation is presented in Section 2.6, we then demonstrate the alternative proposed receiver structure in Section 2.6.2. In Section 2.6.3, simulation results illustrate the performance of the proposed receiver structure. Finally, a summary is given in Section 2.7.

2.1 Turbo Equalization

Turbo equalization follows the same principles as turbo decoding. Here the information bits u_k are encoded through an RSC encoder and are interleaved before transmission over an ISI channel. The transmitter filter, the impulse response of the channel, and the whitening match filter at the receiver can be considered as a finite impulse response (FIR) filter [14]-

[15]. If the channel coefficients are known at the receiver, the channel can be decoded using a MAP symbol estimator. In this manner the encoder and the channel form serially concatenated codes which can be decoded using the turbo scheme shown in Fig. 2.1.

The *SISO equalizer* observes channel values $\mathbf{y}$ and then provides the *a posteriori* probability log likelihood ratio (also called L-value) $L_E^{pos}(\hat{x})$ for all coded bits using the *a priori* information $L_E^{pri}(\hat{x})$. For the first iteration we assume $L_E^{pri}(\hat{x})$ to be zero. The extrinsic information $L_E^{ext}(\hat{x})$ is obtained by subtracting the *a priori* probabilities from the *a posteriori* L-values. After deinterleaving, the extrinsic information are passed to the *SISO decoder* as priori values $L_D^{pri}(\hat{x'})$. The decoder does not have access to the channel values. The decoder provides the *a posteriori* L-values for both the information bits and parity bits $L_D^{pos}(\hat{x'})$ using the *a priori* probabilities provided by the *SISO equalizer*. Again, the extrinsic information $L_D^{ext}(\hat{x'})$ is formed after eliminating the effect of the *a priori* L-values. After interleaving this extrinsic information is delivered to the *SISO equalizer* as the *a priori* L-values. The iterative equalization and decoding proceed until the condition of a certain number of iterations is satisfied. At this point the *a posteriori* L-values of the information bits, at the output of the decoder $L_D^{pos}(\hat{u})$, are sent to a decision device and the process is terminated.

In the next section we will present the formulation of the MAP-based turbo equalization algorithms.

2.2 MAP-Based Turbo Equalization Algorithms

In this section we present the formulation of the MAP-based turbo equalization algorithms. Given a binary input alphabet $\{-1, 1\}$, the encoder (or the channel) can be in one of the 2^M states corresponding to different contents of encoder (or channel) memories. The trellis structure can be used to compute the *a posteriori* L-values:

$$L(\hat{x}_k) = \log \frac{P(x_k = 1|\mathbf{y})}{P(x_k = -1|\mathbf{y})} = \log \frac{\sum_{(s',s),x_k=1} p(s', s, \mathbf{y})}{\sum_{(s',s),x_k=-1} p(s', s, \mathbf{y})} \tag{2.1}$$

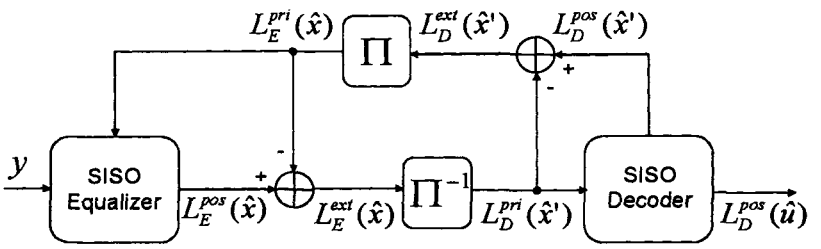

Figure 2.1: Turbo Equalizer (TEQ).

where s' and s represent the states of the encoder (or the channel input) at time $k-1$ and k, respectively, and $\mathbf{y}$ is the received sequence of length $2N$. Dividing the received sequence into three separate terms and applying the chain rule we get:

$$p(s', s, \mathbf{y}) = p(s', y_1, ..., y_{k-1})p(s, y_k|s')p(y_{k+1}, ..., y_N|s). \tag{2.2}$$

This results in the decomposition of the numerator and the denominator of equation (2.1) into three terms that can be evaluated recursively, using the forward/backward algorithm.

$$\alpha_k(s') = p(s', y_1, ..., y_{k-1}) \tag{2.3}$$

$$\beta_{k+1}(s) = p(y_{k+1}, ..., y_N|s) \tag{2.4}$$

$$\gamma_k(s', s) = p(s, y_k|s') \tag{2.5}$$

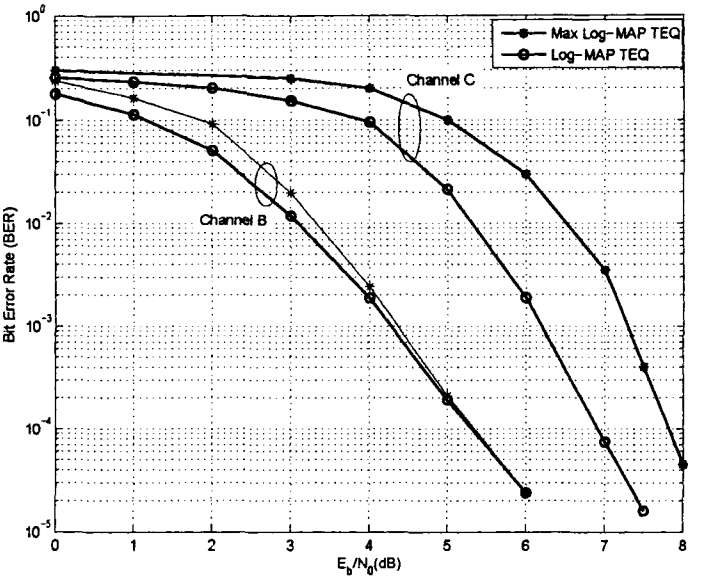

(a) Interleaver size=500

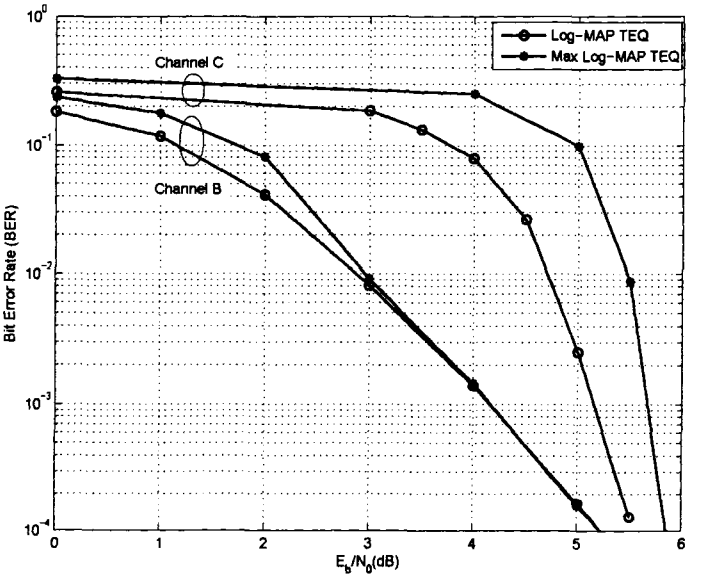

(b) Interleaver size=4096

Figure 2.2: Performance results for the Log-MAP and Max-Log-MAP turbo equalizers in moderate and high loss channels; five iterations, known SNR at the receiver.

where $\alpha_k(s)$ and $\beta_{k-1}(s')$ in (2.3) and (2.4) for both the MAP equalizer and the MAP decoder can be computed through the following forward and backward recursions [1]:

$$\alpha_k(s) = \sum_{s'} \alpha_{k-1}(s')\gamma_k(s',s) \tag{2.6}$$

$$\beta_{k-1}(s') = \sum_{s} \beta_k(s)\gamma_k(s',s) \tag{2.7}$$

with boundary conditions $\alpha_0(0)=1$, $\alpha_0(m)=0$ for $m \neq 0$; and $\beta_N(0)=1$, $\beta_N(m)=0$ for $m \neq 0$. However, the calculation of $\gamma_k(s',s)$ in (2.5) for the equalizer and the decoder will be different. According to (2.5)

$$\begin{aligned} \gamma_k(s',s) = p(s,y_k|s') &= p(y_k|s',s)P(s|s') \\ &= p(y_k|s',s)P(x_k) \end{aligned} \tag{2.8}$$

whenever there is a path on trellis between states s' and s; otherwise, $\gamma_k(s',s)$ will be zero. For the decoder, (2.8) can be obtained as follows, [4]:

$$\gamma_k(s',s) = exp(\sum_{v=1}^{2} \frac{1}{2} x_{k,v} L(\hat{x}_{k,v}) + \frac{1}{2} u_k L(u_k)) \tag{2.9}$$

where $L(\hat{x}_{k,v})$ is the extrinsic LLR passed from the equalizer to the decoder and $L(u_k)$ is the *a priori* information for the information bit u_k.

For the equalizer, (2.8) can be obtained as follows, [4]:

$$\gamma_k(s',s) = exp(-\frac{1}{2\sigma_{ch}^2}|y_k - \sum_{i=0}^{M} g_i x_{k-i}|^2 + \frac{1}{2} x_k L(x_k)) \tag{2.10}$$

where $\sigma_{ch}^2 = N_0/2$, in the case of known SNR at the input of the equalizer, and M denotes the memory length of the channel. y_k is the symbol value received at time k, the g_i values correspond to the channel coefficients and $L(x_k)$ is the *a priori* information for coded bit x_k.

The Log-MAP algorithm introduced in [52] calculates $\alpha_{k-1}(s')$, $\beta_k(s)$ and $\gamma_k(s',s)$ in logarithmic terms using the Jacobian logarithmic function. Using this approach the forward/backward recursion in (2.6) and (2.7) will change to,

$$\bar{\alpha}_k(s) = \widehat{\max}(\bar{\alpha}_{k-1}(s') + \bar{\gamma}_k(s',s)) \tag{2.11}$$

$$\bar{\beta}_{k-1}(s') = \widehat{\max}(\bar{\beta}_k(s) + \bar{\gamma}_k(s',s)) \tag{2.12}$$

where

$$\widehat{\max}(z_1 + z_2) = \max(z_1, z_2) + \log(1 + exp(-|z_1 - z_2|)) \tag{2.13}$$

and $\bar{\alpha}_k(s)$, $\bar{\beta}_k(s)$ and $\bar{\gamma}_k(s', s)$ represent the logarithmic values of $\alpha_k(s)$, $\beta_k(s)$ and $\gamma_k(s', s)$, respectively. Finally the soft output maximum *a posteriori* (LLR) of the decoder can be determined as follows:

$$\begin{aligned} L(\hat{x}_k) = & \widehat{\max}_{(s',s),x_k=1}(\bar{\alpha}_{k-1}(s') + \bar{\gamma}_k(s', s) + \bar{\beta}_k(s)) \\ & - \widehat{\max}_{(s',s),x_k=-1}(\bar{\alpha}_{k-1}(s') + \bar{\gamma}_k(s', s) + \bar{\beta}_k(s)). \end{aligned} \tag{2.14}$$

The $\widehat{\max}$ operation in the first and second parts of (2.14) is applied only to those existing transitions in the trellis structure where the coded bit x_k is 1 or -1, respectively.
The Max-Log-MAP algorithm is obtained by omitting the logarithmic part in (2.13), [53]. Using this approximation, the Max-Log-MAP algorithm is suboptimal and gives an inferior performance compared to that of the Log-MAP algorithm, which is optimal.

2.3 Performance Analysis

In this section we will compare the performance of the Log-MAP and Max-Log-MAP turbo equalizers to clearly address the performance differences in frequency selective channels. We consider two different block lengths of 250 and 2048 bits. The blocks are encoded through a recursive systematic encoder with two memories that corresponds to the generator matrix $g = [7, 5]$ in octal notation, where the first element in the matrix is the feedback part. A pseudo random interleaver is employed. It is assumed that data is transmitted over two different time-invariant Channels, B and C, with tap coefficients $B = \{.407, .815, .407\}$ and $C = \{.227, .460, .688, .460, .227\}$ corresponding to moderate and high loss channels [15], respectively. Fig. 2.2(a) shows the performance of turbo equalizers using the Log-MAP and Max-Log-MAP algorithms for both equalization and decoding. It can be seen that for the moderate loss channel B turbo equalization using the Max-Log-MAP algorithm gives performance very close to that of the Log-MAP turbo equalizer; however, in the high loss channel, the Log-MAP-based turbo equalizer outperforms the Max-Log-MAP turbo

equalizer by a factor of 1dB gain in the low bit error rate region. The same result is obtained as the length of the code increases; this is shown in Fig. 2.2(b) for interleaver of size 4096 bits.

It should be noticed that we considered that the SNR of the channel is perfectly known at the receiver. The effect of misestimation of SNR on the BER performance of turbo equalizers will be studied in the following section.

2.4 SNR Sensitivity Analysis

In order to examine the SNR sensitivity of turbo equalizer, several simulations have been performed. Fig. 2.3 shows the results for both the Log-MAP and Max-Log-MAP turbo equalizers for two different block lengths, over two different channels. The characteristics of the encoder and the channels were given in the previous section. Each figure contains three curves corresponding to different BER regions of the Log-MAP turbo equalizer and the Max-Log-MAP turbo equalizer. We have considered the effect of SNR mismatch (with an offset with respect to the true SNR) up to 8dB offset. It is noted from Fig. 2.3 that the Log-MAP turbo equalizer is more sensitive to SNR mismatch in Channel C. Also, note that for the Log-MAP turbo equalizer, an overestimation of SNR is more tolerable than an underestimation for both channels. In other words, underestimation of SNR may result in severe degradation in performance of the Log-MAP turbo equalizer while by overestimation, its BER performance is always better than that of the Max-Log-MAP turbo equalizer. From Fig. 2.3, it is evident that the Max-Log-MAP turbo equalizer is SNR independent and from a practical point of view an SNR estimation is not necessary. In other words, the Max-Log-MAP turbo equalizer does not require prior knowledge of SNR at the equalizer input; however, the soft output values (the reliability value of the bits) can be affected by SNR mismatch, as shown in the following.

Insensitivity of the Max-Log-MAP Algorithm to SNR Mismatch:

Now we prove that the Max-Log-MAP turbo equalizer is SNR independent and also show the effect of SNR mismatch on the soft output values. Based on these results an online SNR estimation method will be proposed in the next section.

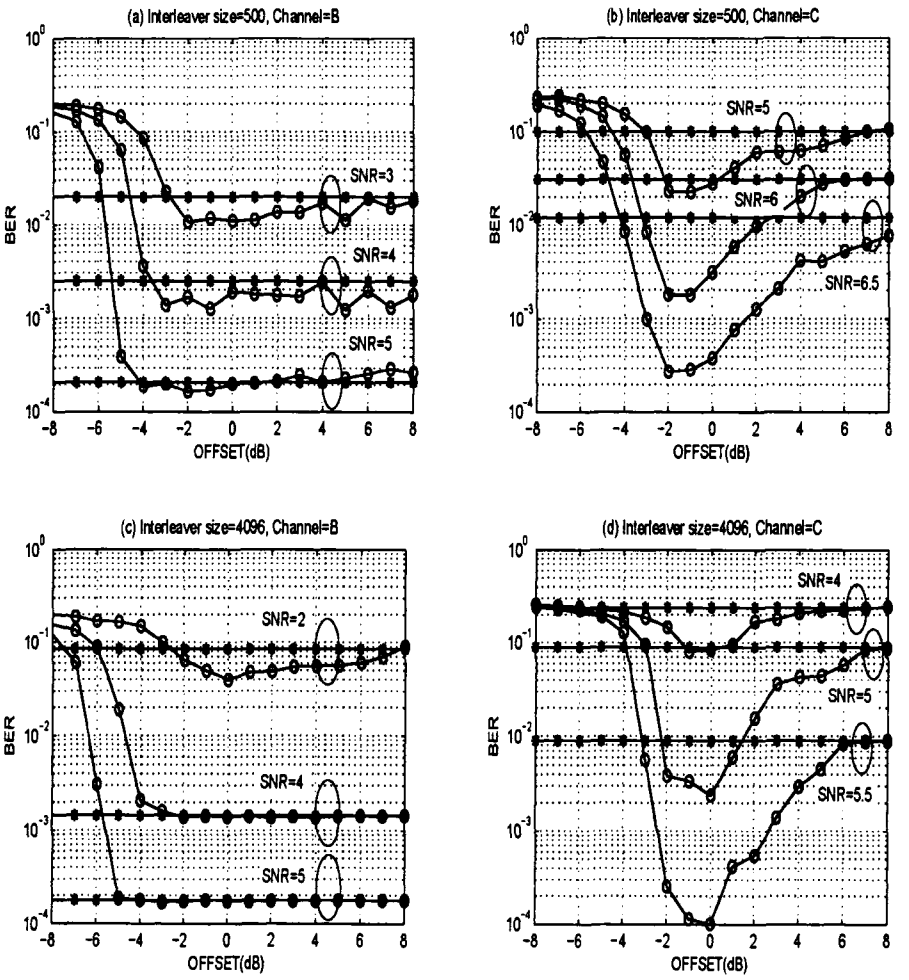

Figure 2.3: Bit error rate versus SNR mismatch; No. of iterations=5.

At this point we consider the Max-Log-MAP algorithm for both equalization and decoding and show that although the SNR mismatch affects the reliability of the *a posteriori* L-values at the output of the equalizer or the decoder, it does not affect the BER of the equalizer or the decoder. Also, we assume that the estimated SNR at the input of equalizer has an offset equal to $\Delta(\frac{E_b}{N_0})$ in decibels added to the actual value of the channel SNR $(\frac{E_b}{N_0})_{ch}$,

$$\left(\frac{E_b}{N_0}\right)_{eq} = \left(\frac{E_b}{N_0}\right)_{ch} + \Delta\left(\frac{E_b}{N_0}\right). \tag{2.15}$$

The variance of noise can be expressed in terms of the channel SNR as follows:

$$\sigma_{eq}^2 = \frac{1}{2R} 10^{-\frac{1}{10}(\frac{E_b}{N_0})_{eq}} \tag{2.16}$$

where R is the code rate. Substituting (2.15) into (2.16), and assuming a rate of 1/2, $(R = 1/2)$, leads to

$$\begin{aligned} \sigma_{eq}^2 &= 10^{-\frac{1}{10}(\frac{E_b}{N_0})_{ch}} \times 10^{-\frac{1}{10}(\Delta(\frac{E_b}{N_0}))} \\ &= K \times \sigma_{ch}^2 \end{aligned} \tag{2.17}$$

where $K = 10^{-\frac{1}{10}(\Delta(\frac{E_b}{N_0}))}$.

In the case of an SNR mismatch between the channel and the equalizer, the new branch matric $\gamma_k'(s', s)$ can be written in terms of σ_{eq}^2 instead of σ_{ch}^2 by substituting (2.17) into (2.10) as follows:

$$\gamma_k'(s', s) = exp(-\frac{1}{2K\sigma_{ch}^2}|y_k - \sum_{i=0}^{M} g_i x_{k-i}|^2 + \frac{1}{2} x_k L(x_k)). \tag{2.18}$$

After taking logarithm and assuming that the *a priori* L-values for coded bits at the input of the equalizer are zero for the first iteration, (2.18) can be rewritten as follows:

$$\log(\gamma_k'(s', s)) = -\frac{1}{2K\sigma_{ch}^2}|y_k - \sum_{i=0}^{M} g_i x_{k-i}|^2 \tag{2.19}$$

or

$$\bar{\gamma}_k'(s', s) = \frac{1}{K}\bar{\gamma}_k(s', s). \tag{2.20}$$

By considering equations (2.11) and (2.12), and changing $\widehat{\max}(.)$ with simple max(.) operation, the factor $\frac{1}{K}$ appears in $\bar{\alpha}'$ and $\bar{\beta}'$ of each time slot, shown as

$$\bar{\alpha}'_k(s) = \frac{1}{K}\bar{\alpha}_k(s) \tag{2.21}$$

$$\bar{\beta}'_k(s) = \frac{1}{K}\bar{\beta}_k(s). \tag{2.22}$$

Substituting (2.20), (2.21) and (2.22) into (2.14) leads to a new *a posteriori* LLR,

$$L'(\hat{x}_k) = \frac{1}{K}L(\hat{x}_k). \tag{2.23}$$

It is clear from (2.23) that since K is always positive, so the multiplication of the output LLR by $1/K$ does not affect our decision on a particular bit, but the reliability value of the soft output can vary. If $\Delta(\frac{E_b}{N_0})$ is greater than zero (overestimation of SNR) K will be less than one, and $1/K$ will be greater than one, hence the output LLR is greater than the actual case. Using the same reasoning, if $\Delta(\frac{E_b}{N_0})$ is less than zero (underestimation of SNR), the output LLR will be less than the actual value.

Since the *a posteriori* LLRs of the equalizer and the extrinsic information provided by the equalizer are scaled by factor $1/K$, the decoder inputs, which are the deinterleaved version of the extrinsic information, are multiplied by the same factor. The same reasoning also holds for the decoder, at the end of the first iteration, the *a posteriori* L-values at the decoder output are multiple by the same factor. For the next iteration, the *a priori* inputs of the equalizer are scaled with the same factor, $1/K$; thus the results in equations (2.20)-(2.23) are valid for both the equalizer and the decoder. The process proceeds exactly the same way for each iteration and hence the proof is complete.

2.5 Iterative Online SNR Estimation First Iteration: Using Max-Log-MAP Algorithm

Theoretically, the performance of the Log-MAP turbo equalizer is superior compared to that of the Max-Log-MAP turbo equalizer in the case of known SNR. However, any SNR misestimation may result in degradation of the BER performance of the Log-MAP turbo

equalizer so that the Log-MAP turbo equalizer can even lose its advantage over the MAX-Log-MAP turbo equalizer, particularly, in a high-loss channel.

We have used a similar method as was proposed in [9], but in an iterative fashion and with some modifications. In [9], an arbitrary SNR was assumed at the input of the Max-Log-MAP equalizer and decoder at the first iteration. At the end of the first iteration the SNR was estimated and passed to the Log-MAP equalizers and decoders used in next iterations. As is shown in Fig. 2.4, we have also used the Max-Log-MAP algorithm for both the equalization and decoding in the first iteration, but as can be seen from (2.23), the output LLRs of the Max-Log-MAP Equalizer (or decoder) are proportional to the assumed SNR at the input of the equalizer. In other words, if this SNR is greater than the actual SNR (positive offset, $\Delta(\frac{E_b}{N_0}) > 0$) the reliability values of the equalizers (or decoder) outputs will be greater that the actual values, and vice versa. This is not desirable because the high reliability value for a wrong bit is less likely to be corrected during next iterations. At the same time, if the offset goes to negative large values, the decoder will not obtain any priori knowledge form the equalizer which affects the overall performance of the system. Therefore we assume that the SNR at the input of the Max-Log-MAP Equalizer is zero. Now the output LLRs of the Max-Log-MAP decoder for both the information and parity bits are sent to a decision device to provide a hard decision on the output bits $\hat{x}_k$. Since $y_k = \sum_{i=0}^{M} g_i x_{k-i} + n_k$, if we replace $\hat{x}_k$ by x_k, we can estimate the variance of the white gaussian noise as follows:

$$\widehat{\sigma^2} = \frac{1}{2N} \sum_{k=0}^{2N} (y_k - \sum_{i=0}^{M} g_i \hat{x}_{k-i})^2. \tag{2.24}$$

In order to accomplish this process we pass the estimated symbols through the discrete channel with coefficients equal to the channel coefficients g_i (assuming the channel coefficients are known), for $i \epsilon \{0, 1, \ldots, M\}$. At each time slot the output is subtracted from the deinterleaved channel value $\mathbf{y}'$ and then the SNR is estimated using (2.24). Because of the high number of bits in error, after the first iteration, the estimated noise variance is higher than the actual value; this results in underestimation of SNR which may degrade the performance of the Log-MAP equalizer and decoder used in the second iteration. To prevent this situation we add a constant negative value to the estimated noise variance after the first

(and if necessary second) iteration(s). This value is determined using an exhaustive search method for that particular block length. This process ensures that the Log-MAP equalizer and decoder are operating in the region in which they always outperform the Max-Log-MAP-based system. It should be noted that the amount of offset added to the estimated SNR after the first (and if necessary second) iteration(s) may vary for different block lengths. Also, we have proposed an iterative scheme that can improve the performance of the system further, as shown in Fig. 2.4. In the proposed iterative SNR estimation scheme, the SNR is estimated in each iteration and then the result is passed to the next iteration. As the iterations proceed, the bit error rate is decreased and the estimated SNR is more accurate. This modification helps to achieve a better BER performance. Since we do not employ any additional hardware compared to the non-iterative scheme proposed in [9], the proposed estimation scheme does not increase the complexity of the system. Simulation results in Channel C for a block length of 250 are shown in Fig. 2.5. The advantage of using the iterative SNR estimation method over the non-iterative method proposed in [9] is evident, particularly in the low BER region. It can be shown that the constant value added here to the estimated SNR, is a function of the encoder structure, the channel coefficients and the length of the transmitted frame. Exhaustive search must be performed to determine the best value of the constant if any of these parameters changes. In the remainder of this chapter we propose a different method which is able to estimate the constant parameter based on the a priori information. Also instead of employing the Max-Log-MAP algorithm in the first iteration, which may result in performance degradation specially when the frame length becomes very short, we use the conventional log-MAP algorithm in the first iteration. The required SNR is estimated through signal decomposition in the receiver.

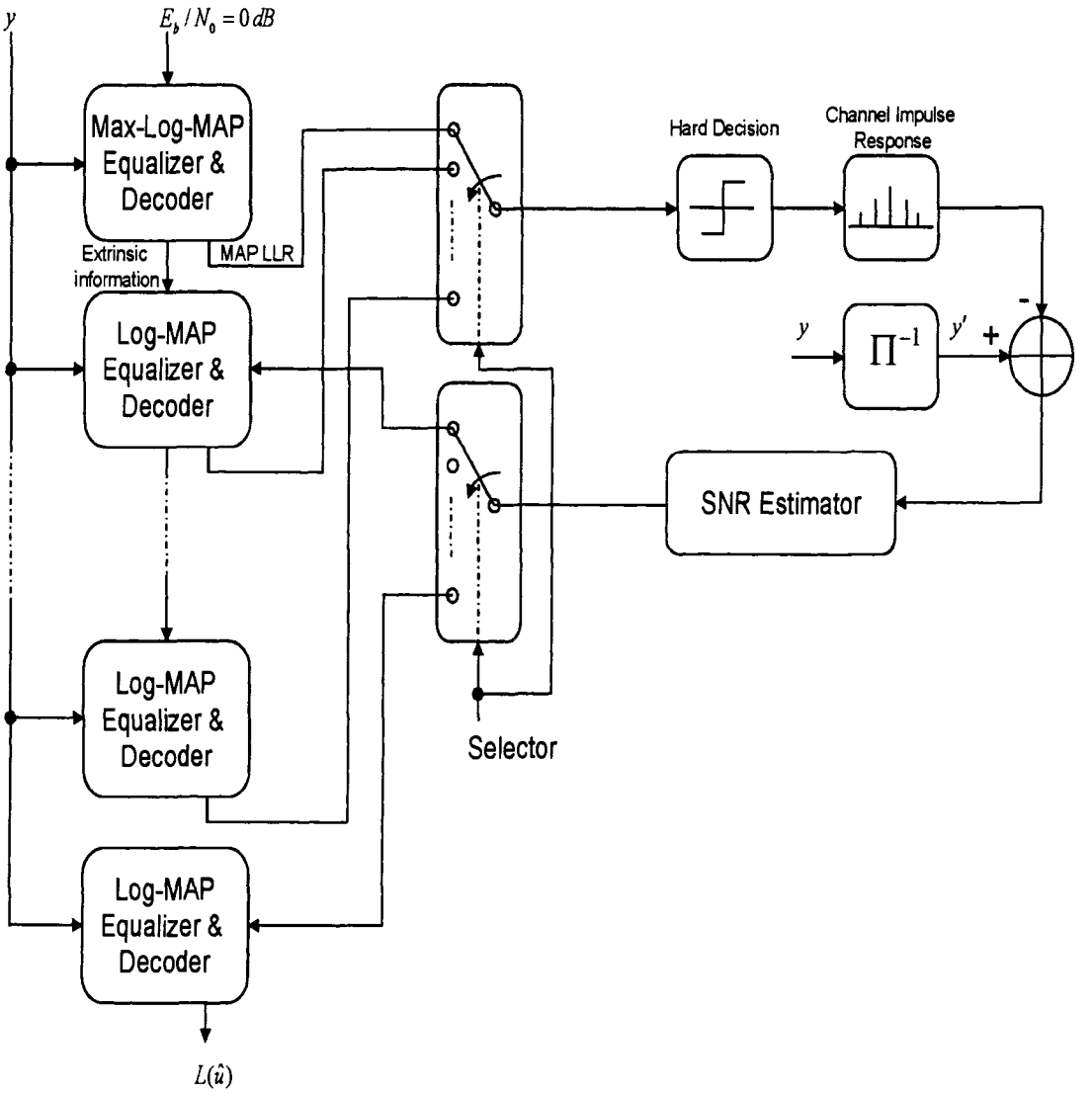

Figure 2.4: Iterative online SNR estimation scheme.

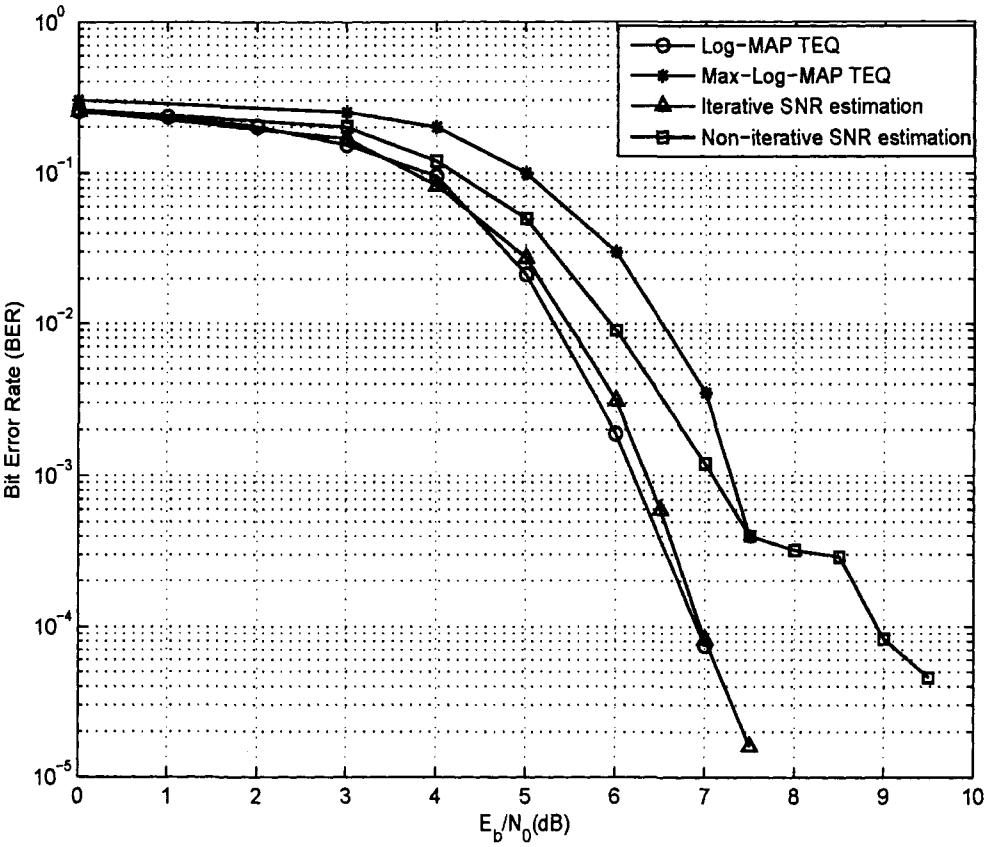

Figure 2.5: Online SNR estimation for turbo equalization; Frame size=250, five iterations, Channel C.

2.6 Subspace-Based Iterative SNR Estimation Method

2.6.1 Signal Model and the System Description

We consider a recursive systematic convolutional (RSC) encoder signaling through a frequency selective channel. The binary input information is first encoded through a recursive systematic convolutional encoder and then modulated using the binary phase shift keying (BPSK) modulation scheme. Let M' be the number of information symbols for each user, including the trellis terminating $\nu - 1$ tail bits. Thus the channel codeword of each user has length $M = M'/R_c$, and is denoted by $b[j]$ for $j = 0, 1, \ldots, M-1$, where R_c is the rate of the code. The channel encoder outputs are next interleaved by a random interleaver, and these interleaved symbols are passed through the channel. If we denote the interleaver function by $\prod$, then the interleaver output can be written as $\{b[i]\}_{i=0}^{M-1}$, where $i = \prod(j)$ for $j = 0, 1, \ldots, M-1$. The output of the interleaver is next passed through a pulse shaping filter to suppress the out-of-band interference and then transmitted through the channel. The continuous time received signal at the receiver in this case is given by

$$r(t) = x(t) \star f(t) + n(t), \tag{2.25}$$

where $x(t)$ and f(t) represent the transmitted signal and the channel impulse response, $\star$ denotes the convolution operation and $n(t)$ is a Gaussian noise process with zero mean and variance σ^2.

The transmitted signal in (2.25) is given by

$$x(t) = \sum_{i=0}^{M-1} b[i]s(t - iT), \tag{2.26}$$

where $b[i]$ refers to the transmitted symbol during the transmission interval $[iT, (i+1)T]$. The channel impulse response can be written as

$$f(t) = \sum_{l=0}^{L-1} g_l \delta(t - \tau_l), \tag{2.27}$$

where L is the number of paths in multipath channel, and g_l and τ_l are, respectively, the path gain and the delay of the lth path. It is assumed that the maximum delay of the

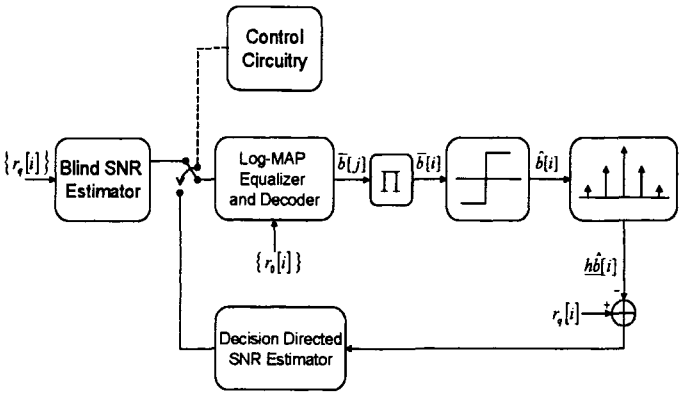

Figure 2.6: Receiver structure

channel is τ_L, and τ_l is uniformly distributed between zero and the maximum delay spread of the channel. Furthermore, we assume that the channel coefficients and the delay of each path are known to the receiver, also the average bit energy is assumed to be unity.

2.6.2 Receiver Structure and Algorithm

We modify the receiver algorithm in a way that it is able to estimate the SNR without using pilot symbols. Fig. 2.6 shows the receiver structure. The first stage of the iterative receiver performs the SNR estimation, and equalization while the second stage performs the decoding process. By exchanging the information between the first stage and the second stage the receiver performance is improved via iteration.

At the receiver, the received signal $r(t)$ is filtered by a matched filter and sampled at a multiple p of the symbol rate, where p is the number of samples per symbol period. The qth signal sample during the ith symbol interval is given by

$$r_q[i] = \sum_{n=0}^{L-1} b[i-n] \sum_{l=0}^{L-1} g_l \int_0^{T/p} s(t) \times s(t + nT - \tau_l + q\frac{T}{p})dt + \sigma n_q[i], \qquad (2.28)$$

where

$$n_q[i] \triangleq \frac{1}{\sigma}\int_{iT+q\frac{T}{p}}^{iT+(q+1)\frac{T}{p}} n(t)s(t-iT-q\frac{T}{p})dt.$$

Defining

$$h_q[n] \triangleq \sum_{l=0}^{L-1} g_l \int_0^{T/p} s(t)\times s(t+nT-\tau_l+q\frac{T}{p})dt, \tag{2.29}$$

and substituting (2.29) in (2.28), (2.28) can be written as follows:

$$r_q[i] = \sum_{n=0}^{L-1} b[i-n]h_q[n] + \sigma n_q[i], \tag{2.30}$$

By stacking m successive symbols, the following vectors can be defined

$$\mathbf{r}[i] \triangleq \begin{bmatrix} \underline{r}[i] \\ \vdots \\ \underline{r}[i+m-1] \end{bmatrix}_{pm\times 1}, \mathbf{n}[i] \triangleq \begin{bmatrix} \underline{n}[i] \\ \vdots \\ \underline{n}[i+m-1] \end{bmatrix}_{pm\times 1}, \mathbf{b}[i] \triangleq \begin{bmatrix} b[i-L+1] \\ \vdots \\ b[i+m-1] \end{bmatrix}_{(m+L-1)\times 1},$$

where $\underline{r}[i] \triangleq [r_1[i],\ldots,r_{p-1}[i]]^T$, and $\underline{n}[i] \triangleq [n_1[i],\ldots,n_{p-1}[i]]^T$. Finally the composite channel matrix is defined as follows:

$$\mathbf{H} \triangleq \begin{bmatrix} h_0[L-1] & \ldots & h_0[0] & 0 & \ldots & 0 \\ \vdots & \vdots & \vdots & \vdots & \vdots & \\ h_{p-1}[L-1] & \ldots & h_{p-1}[0] & 0 & \ldots & 0 \\ \vdots & \ddots & \ddots & \ddots & \vdots & \\ 0 & \ldots & 0 & h_0[L-1] & \ldots & h_0[0] \\ \vdots & \vdots & \vdots & \vdots & \vdots & \\ 0 & \ldots & 0 & h_{p-1}[L-1] & \ldots & h_{p-1}[0] \end{bmatrix}, \tag{2.31}$$

where $\mathbf{H}$ is a $pm \times (m+L-1)$ dimensional matrix. It should be noted that the smoothing factor m and over sampling factor p are chosen in a way that matrix $\mathbf{H}$ become a tall matrix (i.e $pm \gg m+L-1$). This is necessary in order to have separate signal and noise subspaces. The received signal at the output of the stack can be represented as

$$\mathbf{r}[i] = \mathbf{H}\mathbf{b}[i] + \sigma\mathbf{n}[i]. \tag{2.32}$$

From (2.32) it can be shown that the autocorrelation matrix for $\mathbf{r}[i]$ is equal to

$$\mathbf{C}_r \triangleq E\{\mathbf{r}[i]\mathbf{r}[i]^T\} = \begin{bmatrix}\mathbf{U}_s & \mathbf{U}_n\end{bmatrix} \begin{bmatrix}\Lambda_s & \mathbf{0} \\ \mathbf{0} & \Lambda_n\end{bmatrix} \begin{bmatrix}\mathbf{U}_s^T \\ \mathbf{U}_n^T\end{bmatrix} \tag{2.33}$$

where $\mathbf{U}_s$ and $\mathbf{U}_n$ represent the matrix of eigenvectors corresponding to the signal and the noise subspaces. $\Lambda_s \triangleq \text{diag}[\lambda_1, \ldots, \lambda_m]$ contains the m largest eigenvalues of $\mathbf{C}_r$ in descending order with $\lambda_i > \sigma^2$ for $i = 1, \ldots, m$, and $\Lambda_n \triangleq \text{diag}[\lambda_{m+1}, \ldots, \lambda_{pm}]$ contains the eigenvalues of the noise subspace with $\Lambda_n = \sigma^2 \mathbf{I}_{(p-1)m}$. In practice the expectation in (2.33) is approximated with an averaging over M successive symbols, that is

$$\mathbf{C}_r = E\{\mathbf{r}[i]\mathbf{r}[i]^T\} \approx \frac{1}{M} \sum_{i=0}^{M-1} \mathbf{r}[i]\mathbf{r}[i]^T. \tag{2.34}$$

The eigenvalues of the noise subspace in this case are decreasing in descending order with $\lambda_i > 0$ for $i = m+1, \ldots, pm$. The largest eigenvalue of the noise subspace, λ_{m+1}, is chosen as an blind estimate for the noise variance. The estimated noise variance is then applied to the Log-MAP equalizer and decoder during the first iteration. The detailed explanation on the Log-MAP algorithm for equalization and decoding is provided in [54]. For later iterations, the *a posteriori* Log-likelihood ratios (LLRs) of the coded bits are available at the output of the Log-MAP decoder. The *a priori* LLR of the ith bit delivered by the MAP decoder is given by

$$\lambda_{\text{Dec}}[b[i]] = \log \frac{\Pr[b[i] = +1]}{\Pr[b[i] = -1]}, \qquad i = 0, \ldots, M-1. \tag{2.35}$$

The hard estimates of the coded bits are denoted by $\hat{b}[i] = \text{sign}(\bar{b}[i])$, where $\bar{b}[i] \triangleq E\{b[i]\} = \tanh(\frac{1}{2}\lambda_{\text{Dec}}[b[i]])$. In the next step, we obtain an estimate of the SNR, denoted by $\widehat{\sigma_F^2}$. We

begin by forming a preliminary estimate of decision-directed SNR estimation using (2.30)

$$\begin{aligned}(\widehat{\sigma_q^2}[i])_P &= E\left\{(r_q[i]-\underline{h}_q\underline{\hat{b}}[i])(r_q[i]-\underline{h}_q\underline{\hat{b}}[i])^T\right\}\\ &= E\left\{\left(\underline{h}_q(\underline{b}[i]-\underline{\hat{b}}[i])+\sigma n_q[i]\right)\left(\underline{h}_q(\underline{b}[i]-\underline{\hat{b}}[i])+\sigma n_q[i]\right)^T\right\}\\ &= E\left\{(\underline{h}_q\underline{v}[i]+\sigma n_q[i])(\underline{h}_q\underline{v}[i]+\sigma n_q[i])^T\right\}\\ &= \underline{h}_q E\left\{\underline{v}[i]\underline{v}[i]^T\right\}\underline{h}_q^T+\sigma^2 \qquad (2.36)\end{aligned}$$

where the subscript P on $(\widehat{\sigma_q^2}[i])_P$ refers to our preliminary estimate, $\underline{b}[i] \triangleq [b[i],\ldots,b[i-L+1]]^T$, $\underline{\hat{b}}[i] \triangleq [\hat{b}[i],\ldots,\hat{b}[i-L+1]]^T$, $\underline{h}_q \triangleq [h_q[0],\ldots,h_q[L-1]]$ and $\underline{v}[i] \triangleq [v[i],\ldots,v[i-L+1]]^T$ is a random vector with each element $v[k]$ defined by

$$v[k] \triangleq b[k]-\hat{b}[k], \qquad k=i-L+1,\ldots,i. \qquad (2.37)$$

Clearly $v[k]$ can take three different values, namely $\{-2,0,+2\}$. Our ability to find the value of the correlation matrix $\Delta[i] \triangleq E\left\{\underline{v}[i]\underline{v}[i]^T\right\}$ helps us to form a more precise estimator for the SNR. Before we proceed we first find the probability distribution of the random variable $v[i]$. It should be noted that the probability that $v[i]$ is equal to zero is the probability that its hard estimate is correct, that is

$$\Pr(v[i]=0)=\Pr(b[i]=\hat{b}[i]). \qquad (2.38)$$

Using (2.35), it can be shown that [65] the *a priori* probabilities of the coded bits can be

expressed in terms of their respective LLR's, as follows:

$$\begin{aligned}\Pr(b[i] &= b) = \frac{\exp\left(b\lambda_{\mathrm{Dec}}[b[i]]\right)}{1+\exp\left(b\lambda_{\mathrm{Dec}}[b[i]]\right)} \\ &= \frac{\exp\left(+\frac{1}{2}b\lambda_{\mathrm{Dec}}[b[i]]\right)}{\exp\left(-\frac{1}{2}b\lambda_{\mathrm{Dec}}[b[i]]\right)+\exp\left(+\frac{1}{2}b\lambda_{\mathrm{Dec}}[b[i]]\right)} \\ &= \frac{\cosh\left(+\frac{1}{2}\lambda_{\mathrm{Dec}}[b[i]]\right)\left(1+b\tanh(+\frac{1}{2}\lambda_{\mathrm{Dec}}[b[i]]\right)}{2\cosh\left(+\frac{1}{2}\lambda_{\mathrm{Dec}}[b[i]]\right)} \\ &= \frac{1}{2}\left[1+b\tanh\left(+\frac{1}{2}\lambda_{\mathrm{Dec}}[b[i]]\right)\right], \end{aligned} \tag{2.39}$$

where $b \in \{+1,-1\}$. Substituting (2.38) in (2.39) we obtain

$$\Pr(v[i]=0) = \frac{1}{2}\left[1+\hat{b}[i]\tanh\left(+\frac{1}{2}\lambda_{\mathrm{Dec}}[b[i]]\right)\right], \tag{2.40}$$

again by substituting $\hat{b}[i]$ by its equivalent i.e. $\mathrm{sign}\{\tanh\left(\frac{1}{2}\lambda_{\mathrm{Dec}}[b[i]]\right)\}$ we find that

$$\begin{aligned}\Pr(v[i]=0) &= \frac{1}{2}\left[1+\mathrm{sign}\left\{\tanh\left(\frac{1}{2}\lambda_{\mathrm{Dec}}[b[i]]\right)\right\}\times\tanh\left(+\frac{1}{2}\lambda_{\mathrm{Dec}}[b[i]]\right)\right] \\ &= \frac{1}{2}\left[1+\tanh\left(\frac{1}{2}|\lambda_{\mathrm{Dec}}[b[i]]|\right)\right]; \end{aligned} \tag{2.41}$$

therefore, the probability distribution of random variable $v[i]$ may obtain as follows:

$$\Pr(v[i]=\alpha) = \begin{cases} \frac{1}{2}\left[1+\tanh\left(\frac{1}{2}|\lambda_{\mathrm{Dec}}[b[i]]|\right)\right] & \text{if } \alpha = 0; \\ \frac{1}{2}\left[1-\tanh\left(\frac{1}{2}|\lambda_{\mathrm{Dec}}[b[i]]|\right)\right] & \text{if } \alpha = 2b; \\ 0 & \text{otherwise.} \end{cases} \tag{2.42}$$

Meanwhile, assuming $b[i]$ and $b[j]$ are independent random variables for $i,j = 0,\ldots,M-1$ and $i \neq j$ due to using the interleaver, it can be proved that $v[i]$ and $v[j]$ are also independent random variables for $i,j = 0,\ldots,M-1$ and $i \neq j$. From (2.42) the probability distributions of the random variable $v[i]$ conditioned on the alternative transmitted symbols are given as follows:

$$\Pr\big(v[i]=\alpha|b[i]=+1\big)=\begin{cases}\frac{1}{2}\left[1+\tanh\left(\frac{1}{2}|\lambda_{\mathrm{Dec}}[b[i]]|\right)\right] & \text{if } \alpha=0;\\ \frac{1}{2}\left[1-\tanh\left(\frac{1}{2}|\lambda_{\mathrm{Dec}}[b[i]]|\right)\right] & \text{if } \alpha=+2;\\ 0 & \text{otherwise.}\end{cases} \tag{2.43}$$

and

$$\Pr\big(v[i]=\alpha|b[i]=-1\big)=\begin{cases}\frac{1}{2}\left[1+\tanh\left(\frac{1}{2}|\lambda_{\mathrm{Dec}}[b[i]]|\right)\right] & \text{if } \alpha=0;\\ \frac{1}{2}\left[1-\tanh\left(\frac{1}{2}|\lambda_{\mathrm{Dec}}[b[i]]|\right)\right] & \text{if } \alpha=-2;\\ 0 & \text{otherwise.}\end{cases} \tag{2.44}$$

From (2.43) and (2.44), the conditional expectations of random variable $v[i]$ can be determined as follows:

$$E\{v[i]|b[i]=+1\}=+1-\tanh\left(\frac{1}{2}|\lambda_{\mathrm{Dec}}[b[i]]|\right), \tag{2.45}$$

$$E\{v[i]|b[i]=-1\}=-1+\tanh\left(\frac{1}{2}|\lambda_{\mathrm{Dec}}[b[i]]|\right). \tag{2.46}$$

Using (2.39), (2.45) and (2.46), we may evaluate the unconditional expectation of random variable $v[i]$ after some manipulation, as

$$\begin{aligned}E\{v[i]\}&=E\{v[i]|b[i]=+1\}.\Pr\left(b[i]=+1\right)+E\{v[i]|b[i]=-1\}.\Pr\left(b[i]=-1\right)\\&=\tanh\left(\frac{1}{2}\lambda_{\mathrm{Dec}}[b[i]]\right)\cdot\left(1-\tanh\left(\frac{1}{2}|\lambda_{\mathrm{Dec}}[b[i]]|\right)\right).\end{aligned} \tag{2.47}$$

Using (2.42), the second order unconditional expectation of random variable $v[i]$ is given by

$$E\{v[i]^2\}=2\left(1-\tanh\left(\frac{1}{2}|\lambda_{\mathrm{Dec}}[b[i]]|\right)\right). \tag{2.48}$$

From (2.47) and (2.48) and bearing in mind that random variables $v[i]$ and $v[j]$ are independent random variables for $i,j=0,\ldots,M-1$ and $i\neq j$, all elements of the correlation matrix $\Delta[i]=E\left\{\underline{v}[i]\underline{v}[i]^T\right\}$ can be determined. We may now refine our preliminary estimate in (2.36) by averaging over existing samples, as

$$\begin{aligned}\widehat{\sigma_P^2}&\triangleq\frac{1}{Mp}\sum_{q=0}^{p-1}\sum_{i=0}^{M-1}(\widehat{\sigma_q^2}[i])_P\\&=\frac{1}{p}\sum_{q=0}^{p-1}\left(\underline{h}_q\left[\frac{1}{M}\sum_{i=0}^{M-1}\Delta[i]\right]\underline{h}_q^T\right)+\sigma^2.\end{aligned} \tag{2.49}$$

Therefore our final estimate is formed as follows:

$$\widehat{\sigma_F^2} = \widehat{\sigma_P^2} - \sigma_E^2 \tag{2.50}$$

where the subscript F on $\widehat{\sigma_F^2}$ refers to our final estimate, and

$$\sigma_E^2 \triangleq \frac{1}{p}\sum_{q=0}^{p-1}\left(\underline{h}_q\left[\frac{1}{M}\sum_{i=0}^{M-1}\Delta[i]\right]\underline{h}_q^T\right).$$

It should be noted that the constant value which is found through exhaustive search and subtracted out from the estimated noise variance in [54] and [56] refers to the value of $(\sigma^2)_E$, which was found here using analytical solution. The problem with those methods is that, different searches must be performed for different frame lengths, different encoder, different type of channels and different iterations, while our method here is fairly adaptive.

The proposed blind method for the first iteration provides a fairly good estimate for the SNR. Care must be taken regarding the transition from the blind method to the estimator based on the *a priori* information in (2.50) in order to achieve the best BER performance.

As we already pointed out, it is assumed that the transmitted symbols do not experience fading and therefore the received bit energy is equal to unity for all transmitted symbols. The E_b/N_0 in dB using the blind variance estimator is equal to

$$\widehat{\gamma}_B \triangleq 10\log\left(\frac{1}{2R_c\widehat{\sigma_B^2}}\right), \tag{2.51}$$

where R_c is the rate of the code and $\widehat{\sigma_B^2} \triangleq \lambda_{m+1}$. We define $\widehat{\gamma}_F \triangleq 10\log\left(\frac{1}{2R_c\widehat{\sigma_F^2}}\right)$ and interval $I \triangleq [\widehat{\gamma}_B - \epsilon_l, \widehat{\gamma}_B + \epsilon_u]$. At each iteration a new $\widehat{\gamma}_F$ is formed by exploiting a new *a posteriori* information in (2.50). If $\widehat{\gamma}_F$ lies in the interval I the corresponding $\widehat{\sigma_F^2}$ in the subsequent iteration is utilized; otherwise, we stick to our blind estimation method. It should be noted that if the blind method underestimates the SNR, the log-likelihood ratios of the coded bits for the consequent iteration, become less than their actual value. This, results in higher σ_E^2 in (2.50). Assuming that the error in the estimated SNR using the blind method is in the range that does not affect the bit error rate performance for the consequent iteration, the preliminary estimate in (2.50) remains intact; therefore, our final

estimate $\widehat{\sigma_P^2}$ is less than the actual value (i.e. SNR overestimation occurs). By the same reasoning, one concludes that the underestimation of SNR using the blind method results in the overestimation of SNR using the data-aided estimation method. The limits of the interval I depends on the number of memories of the channel while they are independent of the transmitted frame length, the constraint length of the code, and the type of modulation employed in the transmitter side. We set the boundaries to the values that the performance of the system can not be degraded due to overestimation or underestimation of SNR in the worst case scenario (i.e. high loss ISI channel). In other words we do not optimize the interval I for the best possible performance, but rather we would like to show that with fairly large interval the system performance will be well preserved at the final stage; although, slight degradation in performance is possible in the middle stages especially when we switch from the blind method to decision-directed SNR estimation method for the first time, due to the choice of interval I. furthermore, since the SNR is more susceptible to underestimation than overestimation; therefore, the interval I is chosen asymmetrically with larger allowed range for the overestimation compared to that of the underestimation, that is $\epsilon_u \geqslant \epsilon_u$. In each iteration new estimate of the SNR is formed using the new *a posteriori* information from the output of the decoder. As the iteration proceeds and the quality of the *a posteriori* information improves, the error in our estimation becomes negligible.

2.6.3 Simulation Results

We present the bit error rate performance of the proposed method and compare it to the case where the exact SNR is known to the receiver. We consider the normalized bias $\mu \triangleq E\{\frac{\widehat{\sigma_P^2}-\sigma^2}{\sigma^2}\}$ and the normalized root mean-square error (RMSE) $\eta \triangleq \sqrt{E\{(\frac{\widehat{\sigma_P^2}-\sigma^2}{\sigma^2})^2\}}$ as a figure of merit for the estimator performance using numerical examples. We consider three different block lengths of 1024, 128 and 64 bits. The blocks are encoded through a rate 1/2 constraint length 3 recursive systematic convolutional encoder with generation matrix $G = [5, 7]$, where the first element in the matrix is the feedback part. A pseudo random interleaver is employed. The oversampling factor p and the smoothing factor m are chosen to be equal to 2 and 8, respectively. The pulse shaping filter is a square waveform

with unit energy. We have chosen a symbol spaced channel model with channel coefficients equal to [.227.460.668.460.227] corresponding to a high loss ISI channel with $L = 5$ [15]. The ϵ_l and ϵ_u of the interval I are chosen to be equal to $2dB$ and $3dB$, respectively. Fig. 2.7 and 2.8 show the normalized bias and normalized RMSE bias of the proposed estimator for frame length of 1024. From these figures it can be observed that for $E_b/N_0 = 0dB$ and $E_b/N_0 = 2dB$ the estimator only utilizes the blind SNR estimator for all iterations. The reason for this is that the *a posteriori* LLRs at the output of the decoder are not reliable in such low SNRs, and the final estimate generated from the decision-directed SNR estimation (DDSNRE) method is not in the range of interval I. By increasing the SNR to $E_b/N_0 = 4dB$, we observe a slight decrease in terms of normalized bias, but a slight increase in terms of the normalized RMSE bias of the estimator in the fifth iteration. As mentioned earlier, the overestimation of the SNR by the blind SNR estimator in the previous iteration results in underestimation of the SNR in the subsequent iteration by the DDSNRE method; therefore, the mixture of overestimation (caused by the blind SNR estimation method), and underestimation (caused by the DDSNRE method) has decreased the normalized bias in the fifth iteration, but due to the fact that the magnitude of the underestimation caused by the DDSNRE method has been larger than that of the overestimation caused by the blind method, the RMSE bias of the estimator is slightly increased. Also, as the amount of normalized bias is still positive in the fifth iteration at $E_b/N_0 = 4dB$, it can be concluded that in the majority of cases the blind method has prevailed over the DDSNRE method.

By increasing the SNR from $E_b/N_0 = 4dB$ to $E_b/N_0 = 6dB$ it can be observed that the algorithm utilizes the blind method for the first and second iterations; therefore, the normalized bias and the normalized RMSE bias of the estimator remains constant. In the third iteration the system has switched to the DDSNRE method which has larger normalized RMSE bias compared to the blind method, but the normalized bias curve shows that the DDSNRE method underestimates the SNR while the blind method overestimates the SNR. The magnitude of both the normalized bias and the normalized RMSE bias is decreased for the subsequent iterations.

For $E_b/N_0 = 7dB$ it can be seen that the mixture of the blind method and DDSNRE

method is used in the second iteration. This resulted in a smaller normalized bias, but slightly larger normalized RMSE bias. Again, it can be observed that in the majority of cases, the receiver has employed the blind method. For the third, fourth and fifth iterations the receiver strictly employs the DDSNRE method and the magnitude of both the normalized bias and the normalized RMSE bias of the estimator is decreased.

A similar argument can be made with respect to the normalized bias and normalized RMSE bias as we decrease the frame length from 1024 bits to 128 and 64 bits in Figures 2.9- 2.12, respectively. It can be seen that, unlike the method proposed in [55] which demonstrates an error floor, the amount of bias for the proposed estimator is reduced by increasing the SNR and asymptotically becomes zero as the iteration proceeds. Also, it can be observed that the proposed blind SNR estimator is able to estimate the SNR with high accuracy; therefore, the magnitude of the *a posteriori* information at the output of the decoder is in the proper range. This scheme is in contrast with our proposed method in [54], where an arbitrary SNR (i.e. SNR=0) was assumed at the input of the equalizer during the first iteration. It should be noted that the small magnitude of the *a priori* information (due to this assumption) is not able to boost the performance of the equalization and decoding process in the second iteration. This becomes particularly critical for small block lengths and high loss ISI channels, since in these situations the low bit error rate region is far from the origin (i.e. SNR=0). Also, the proposed hypothesis testing criterion promises for the smooth transition from the blind method to the data-aided estimation method when the *a priori* information is reliable. From Fig. 2.8, it can be seen that a significant improvement in terms of the root mean-square error performance is achieved by utilizing the proposed iterative SNR estimation scheme; however, as we decrease the frame length to 128 and 64 bits, we observe an error floor with respect to the normalized RMSE bias performance of the estimator as shown in Fig. 2.10 and Fig. 2.12. This outcome is due to the small frame length from which the SNR is estimated. However, it is obvious that although the quality of the estimated SNR cannot be improved by iteration, still we are able to improve the receiver performance in terms of the bit error rate by performing further iterations.

Fig. 2.13 shows the performance of the proposed receiver compared to the case where the

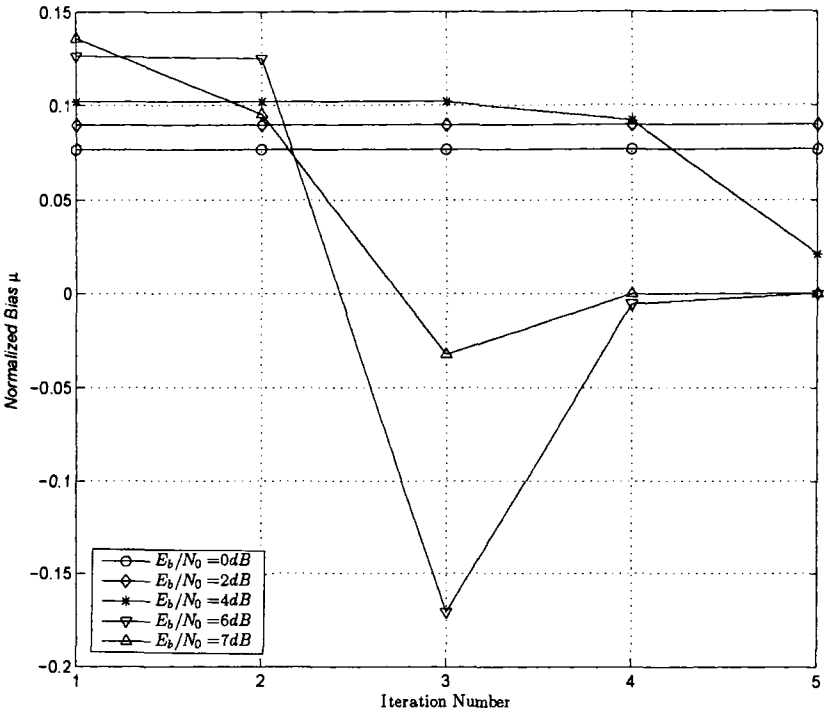

Figure 2.7: Estimator performance in terms of the normalized bias versus the number of iterations for different SNRs, Frame size=1024

actual variance of the noise is known to the receiver. From the simulation results it can be observed that the proposed SNR estimator is able to provide similar results in performance to that of the known SNR at the receiver. This is an outstanding achievement, since other methods proposed in [9], [54] or [56] are not able to do so specifically for small frame lengths.

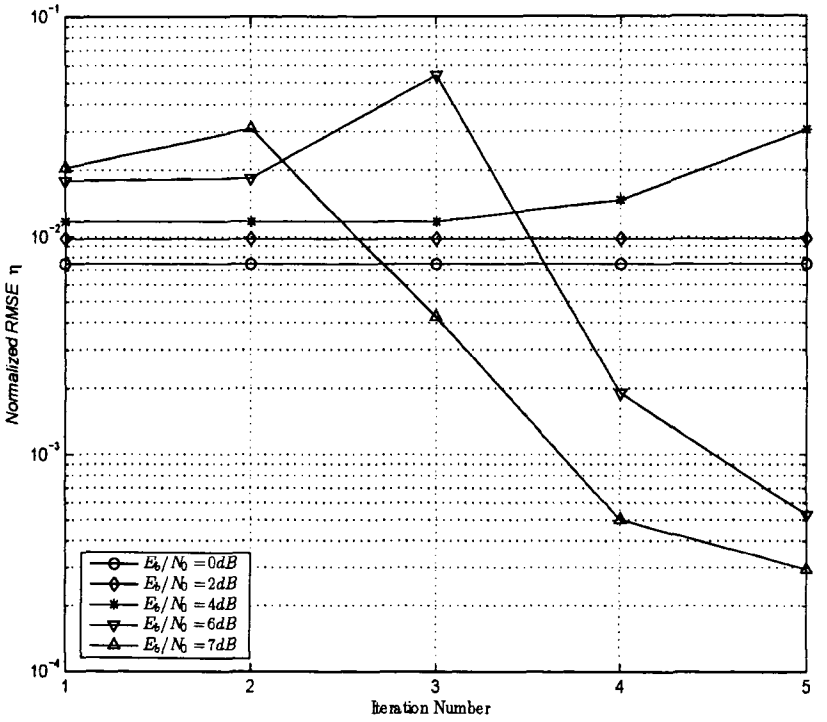

Figure 2.8: Estimator performance in terms of the normalized root mean-square error versus the number of iterations for different SNRs, Frame size=1024

2.7 Summary

The performance of the Log-MAP and the Max-Log-MAP turbo equalizers in moderate and high loss channels has been studied. Simulation results show that for moderate loss channels the Max-Log-MAP turbo equalizer is a good candidate, since it is SNR independent and its performance is very close to the Log-MAP turbo equalizer, while for high loss channels the Log-MAP turbo equalizer is a better candidate, since it shows superior performance compared to the Max-Log-MAP turbo equalizer. However, simulation results show that SNR mismatch degrades the performance of the Log-MAP turbo equalizer. Underestimation of the SNR is more detrimental than overestimation. Therefore, when there is

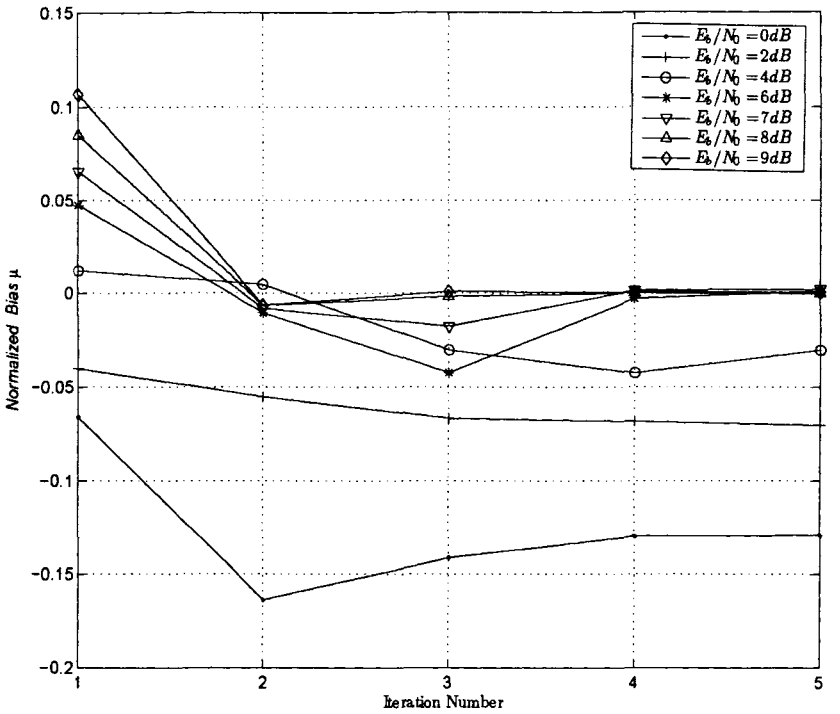

Figure 2.9: Estimator performance in terms of the normalized bias versus the number of iterations for different SNRs, Frame size=128

no information available at the receiver on SNR, an online estimation of SNR is necessary to preserve the advantage of the Log-MAP turbo equalizer over the MAX-Log-MAP turbo equalizer. We proposed an iterative SNR estimation method that demonstrates superior performance compared to the non-iterative scheme without increasing the complexity of the system. Also, the proposed iterative scheme is particularly attractive in a fast varying SNR environment, where the performance of the non-iterative method can be worse than that of the Max-Log-MAP turbo equalizer.

Furthermore We proposed an alternative iterative receiver structure with integrated SNR estimation for data transmission over frequency selective channels. For the first iteration the SNR is estimated blindly using a subspace-based method. For later iterations a decision-

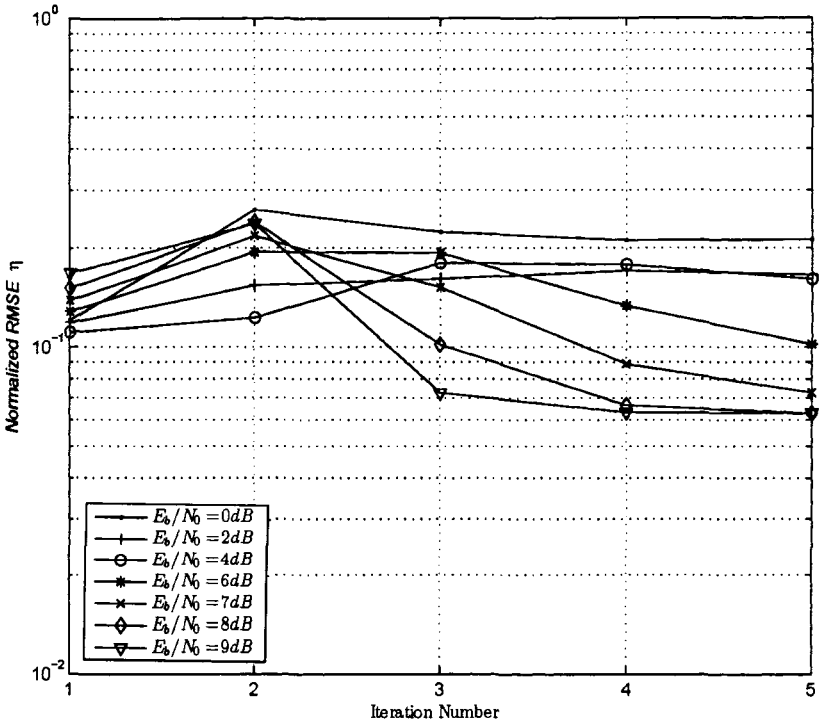

Figure 2.10: Estimator performance in terms of the normalized root mean-square error versus the number of iterations for different SNRs, Frame size=128

directed SNR estimation method is developed as an alternative to the original blind scheme. a hypothesis testing criterion is developed in order to decide whether or not this alternative is a viable option for the consequent iteration.

The performance of the receiver was examined and it is shown that our proposed receiver performance is the same as that of the known SNR case. Furthermore in terms of the estimator performance we examined the normalized bias and normalized root mean-square error of the estimator with respect to the actual value, using numerical examples. It can be seen that unlike other methods in the literature which demonstrate an error floor by increasing the SNR, our proposed estimator is virtually error free, specially in high SNR region.

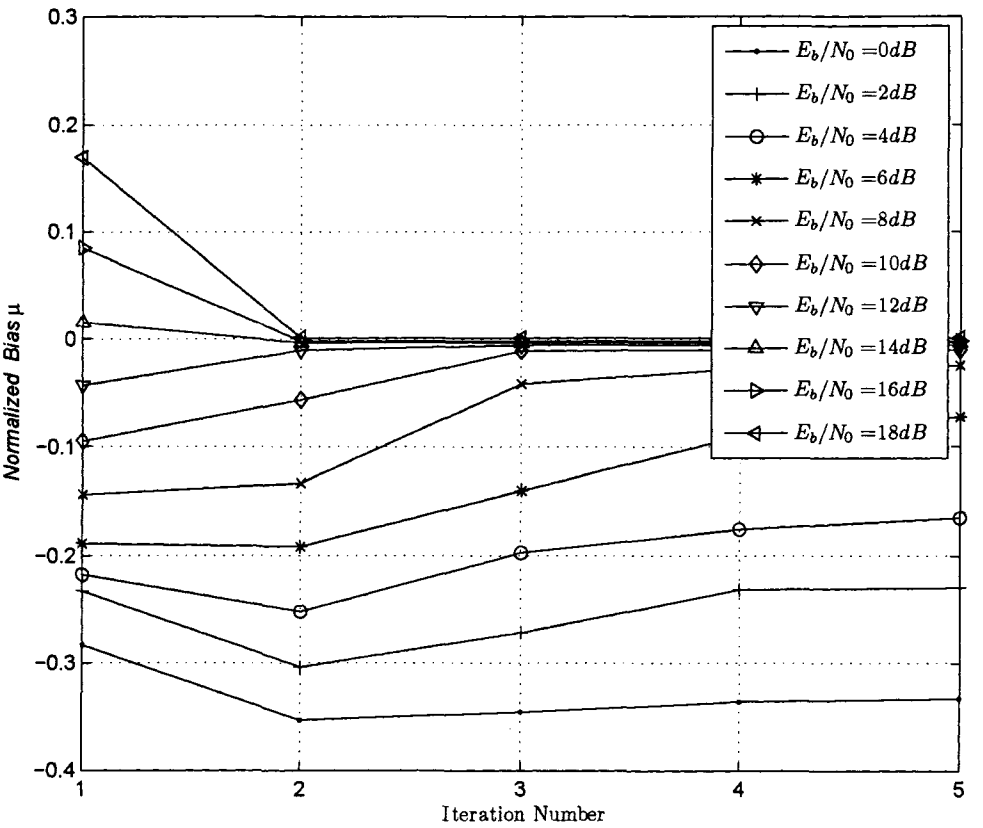

Figure 2.11: Estimator performance in terms of the normalized bias versus the number of iterations for different SNRs, Frame size=64

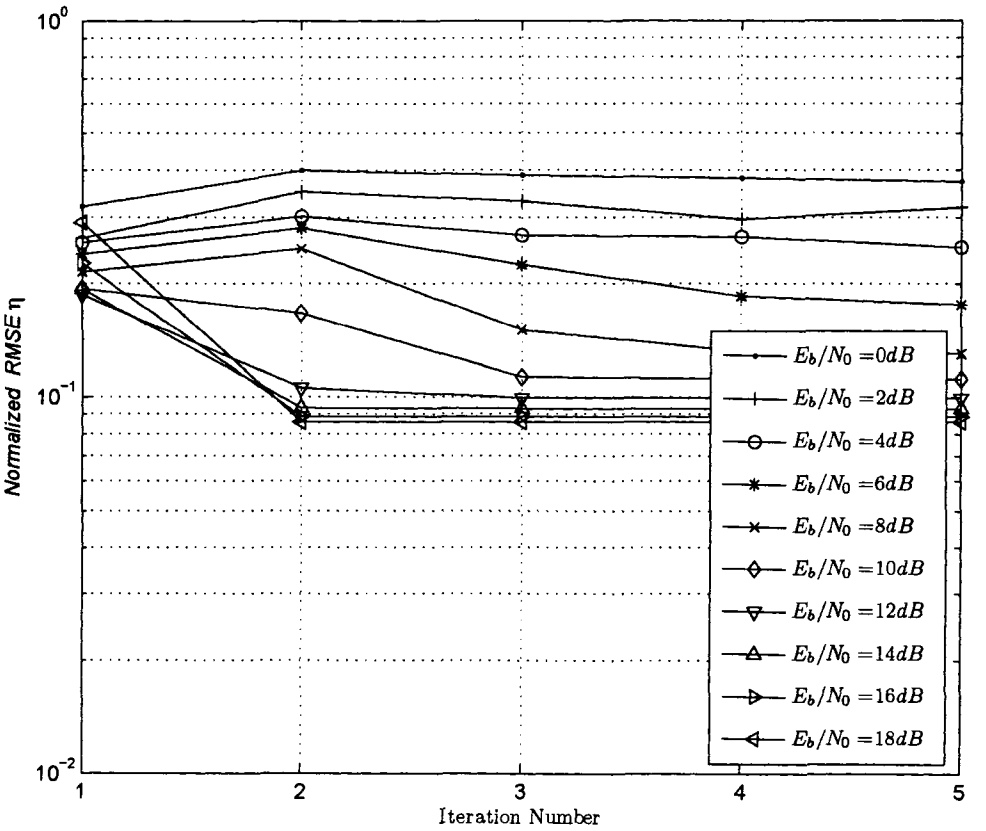

Figure 2.12: Estimator performance in terms of the normalized root mean-square error versus the number of iterations for different SNRs, Frame size=64

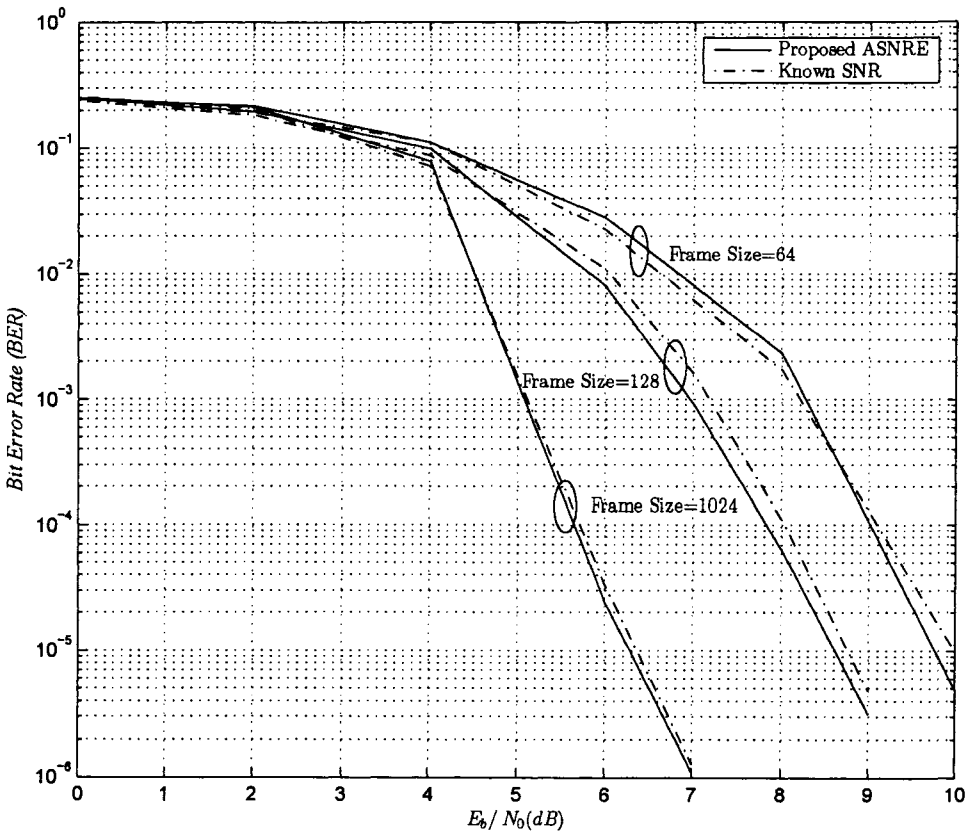

Figure 2.13: Performance of Proposed adaptive SNR estimator (ASNRE) versus known SNR for different frame lengths

Chapter 3

Turbo Group Blind Multiuser Detection with Signal Rank Estimation

In pervious chapter, we discussed single-user systems while many wireless channels, particularly in emerging systems, operate as multiple-access systems, in which multiple users share the same radio resources. As we already mentioned in Chapter 1, among different available technologies such as those based on time and or frequency division multiplexing, the code division multiple access (CDMA) technique appears to be relatively beneficial. In particular CDMA systems are intrinsically interference limited, they have higher frequency reuse potential, and are able to combat multiple access interference and multipath distortion effectively when used in conjunction with multiuser channel estimation, detection and channel decoding algorithms. In CDMA downlinks, a mobile receiver knows only its own spreading sequence and is blind with respect to the other users of the system. In CDMA uplinks, however, typically the base station has knowledge of the spreading sequences of a group of users within its own cell, while it is blind with respect to other users from neighboring cells. The term group blind refers to this situation. It is normal to expect some performance loss due to the presence of these users in the system over the case where all users are known to the receiver. In order to boost the performance of the system for such

scenarios, various types of linear and nonlinear detection schemes have been proposed for *uncoded* synchronous CDMA systems in [66]- [68]. In [69], the idea in [67] and [68] has been generalized and several forms of group blind detectors based on different criteria have been developed.

For *coded* CDMA systems, Reynolds and Wang proposed a receiver structure for the uplink of asynchronous CDMA systems [73]. In that method in order to suppress both intercell and intracell interference, the detector performs a soft interference cancellation for each user in which estimates of the multiuser interference from the known users and an estimate for the interference caused by unknown users are subtracted from the received signal.

In this chapter we first consider the scheme proposed in [73] and we show that the algorithm does not provide robust performance in CDMA uplink because the algorithm fails to converge under certain conditions. It is mathematically proved that when the extrinsic information at the input of the multiuser detector is large enough, the output of the detector fails to converge. We then propose a robust group blind multiuser detection scheme that combines the concept of group blind detection and turbo multiuser detection for asynchronous CDMA systems over frequency selective channels. Specifically, it consists of two stages similar to those of [65] for recursive systematic convolutionally encoded CDMA systems. The first stage consists of soft interference cancellation and combined group blind MMSE filtering, whereas the second stage consists of channel decoding. The combined group blind MMSE filtering tries to suppress the interference from known users based on the signature waveforms and the channel characteristic of these users and to suppress the interference from other unknown users using subspace-based blind methods. Simulation results show that this method preserves its advantage in performance over the conventional turbo multiuser detection method even in the case of high intercell interference. Furthermore, based on the statistic properties of the signal and the channel, we propose an estimation algorithm to estimate the number of unknown users which is much faster, less complex and is able to provide the number of unknown users in white and nonwhite noise environments with very high precision. Simulation results show that the proposed estimator is not sensitive to

parameters such as signal to noise ratio, over sampling factor, or processing gain.

The rest of this chapter is organized as follows. In Section 3.1, we present our signal model and the system description. In Section 3.2, we analyze the work of Reynolds and Wang in detail. Next, in Section 3.3, we derive a group blind turbo multiuser detector for asynchronous CDMA systems by modifying the receiver given in [65] for all known users. In Section 3.4, simulation results demonstrate the BER performance of the proposed method as well as its sensitivity to the number of unknown users. In Section 3.5, we propose an estimator for the number of active unknown users present in the system. Near-far situation is considered in Section 3.6. Finally, a summary is given in Section 3.7.

3.1 Signal Model And System Description

We consider a recursive systematic convolutionally (RSC) coded CDMA system with K users, employing normalized modulation waveforms $\{\mathbf{s}_1, \mathbf{s}_2, \ldots, \mathbf{s}_K\}$ and signaling through multipath channel with additive white Gaussian noise. The binary phase shift keying (BPSK) information symbol sequence $\{d_k[i']\}_{i'=0}^{\infty}$ for user k, $k = 1, \ldots, K$, is first encoded by an RSC channel encoder. For simplicity, we assume that all users employ the same encoder having constraint length ν and code rate R_c. Although this condition is not necessary for unknown users, since the base station does not decode the information from these users. Also, generalization to accommodate different channel encoders for each user with known spreading sequence is easy. Let M' be the number of information symbols for each user, including the trellis terminating $\nu - 1$ tail bits. Thus channel codeword of each user has length $M = M'/R_c$, and is denoted by $b_k[j]$ for $j = 0, 1, \ldots, M-1$.

The channel encoder outputs are next interleaved by a random interleaver, and these interleaved symbols are next modulated by the user's spreading sequence, and transmitted through the channel. If we denote the interleaver function of user k by $\prod_k$, then the interleaver output can be written as $\{b_k[i]\}_{i=0}^{M-1}$, where $i = \prod_k(j)$ for $j = 0, 1, \ldots, M-1$. The spreading waveform of user k is assumed to be of the form $s_k(t) = \frac{1}{\sqrt{N}} \sum_{j'=0}^{N-1} s_k[j']\psi(t - j'Tc)$, where N is the processing gain, $\{s_k[j']\}_{j'=0}^{N-1}$ is a signature sequence of ± 1's assigned

to the kth user, and $\psi(t)$ is a chip waveform of duration $T_c = T/N$ and unit energy [i.e., $\int_0^{T_c} \psi^2(t)dt = 1$].

It is assumed that the receiver has knowledge of the signature waveforms of the first $\tilde{K}$ users ($\tilde{K} \leq K$), whereas the signature waveforms of the remaining $K - \tilde{K}$ users are unknown to the receiver.

We now consider a general multiple-access signal model where the users are asynchronous, and a channel that exhibits dispersion due to multipath effects. In particular, the multipath channel impulse response of the kth user is modeled as $f_k(t) = \sum_{l=1}^{L} g_{l,k}\delta(t - \tau_{l,k})$, where L is the total number of pathes in the channel, and $g_{l,k}$ and $\tau_{l,k}$ are, respectively, the complex path gain and the delay of the kth user's lth path. It is also assumed that the number of paths in all channels between transmit antenna of each user and the base station is constant and is equal to L, the maximum delay spread of each user channel is $\tau_{L,k}$, and $\tau_{l,k}$ for each user is uniformly distributed between zero and the maximum delay spread of the channel.

The continuous-time signal received at the base station receiver is given by

$$r(t) = \sum_{k=1}^{K}\sum_{i=0}^{M} b_k[i]\sum_{l=1}^{L} g_{l,k}s_k(t - iT - \tau_{l,k}) + n(t), \tag{3.1}$$

where $n(t)$ is a zero-mean complex white Gaussian noise process with independent real and imaginary components and with power spectral density σ^2.

Following the approach proposed in [69], at the receiver, the received signal $r(t)$ is filtered by a chip matched filter and sampled at a multiple p of the chip rate. Let us define $P \triangleq Np$ as the number of samples per symbol period, and $\iota \triangleq \max_{1\leq k\leq K}\{\lceil\frac{\tau_{L,k}+T_c}{T}\rceil\}$ be the maximum delay spread in terms of symbol interval. The impulse response of the matched filter is given as follows:

$$g(t) \triangleq \begin{cases} \frac{1}{\sqrt{E_p}}\psi\left(\frac{T_c}{p} - t\right), & \text{if } 0 \leq t \leq \frac{T_c}{p}; \\ 0, & \text{otherwise;} \end{cases} \tag{3.2}$$

where $E_p = \int_0^{T_c/p} \psi^2(t)dt$. It is shown in Appendix B that the qth signal sample during the

ith symbol interval is given by

$$r_q[i] = \sum_{k=1}^{K}\sum_{n=0}^{\iota} b_k[i-n]\frac{1}{\sqrt{NE_P}}\sum_{j'=0}^{N-1} s_k[j']\sum_{l=1}^{L} g_{l,k}\int_0^{T_c/p} \psi(t)\psi(t-\tau_{l,k}+nT-j'Tc+q\frac{T_c}{p})dt+\sigma n_q[i], \tag{3.3}$$

where

$$n_q[i] = \frac{1}{\sqrt{\sigma^2 E_p}}\int_{iT+q\frac{T_c}{p}}^{iT+(q+1)\frac{T_c}{p}} n(t)\psi(t-iT-q\frac{T_c}{p})dt.$$

Denote $\underline{r}[i] \triangleq [r_0[i],\ldots,r_{P-1}[i]]^T$, $\underline{b}[i] \triangleq [b_1[i],\ldots,b_K[i]]^T$, and $\underline{n}[i] \triangleq [n_0[i],\ldots,n_{P-1}[i]]^T$.

Define the overall impulse response of the kth user as:

$$h_k[n] \triangleq \frac{1}{\sqrt{NE_P}}\sum_{j'=0}^{N-1} s_k[j']\sum_{l=1}^{L} g_{l,k}\int_0^{T_c/p} \psi(t)\psi(t-\tau_{l,k}+n\frac{T_c}{p}-j'T_c)dt \tag{3.4}$$

Then matrix $\underline{H}(j)$ can be defined as follows:

$$\underline{H}[j] \triangleq \begin{bmatrix} h_1[jP] & \ldots & h_K[jP] \\ \vdots & \vdots & \vdots \\ h_1[jP+P-1] & \ldots & h_K[jP+P-1] \end{bmatrix}, \quad j=0,\ldots,\iota.$$

Then, (3.3) can be written in terms of vector convolution as

$$\underline{r}[i] = \underline{H}[i] \star \underline{b}[i] + \sigma\underline{n}[i]. \tag{3.5}$$

By stacking m successive sample vectors, we define the following vectors:

$$\underbrace{\mathbf{r}[i]}_{Pm\times 1} \triangleq \begin{bmatrix} \underline{r}[i] \\ \vdots \\ \underline{r}[i+m-1] \end{bmatrix}, \underbrace{\mathbf{n}[i]}_{Pm\times 1} \triangleq \begin{bmatrix} \underline{n}[i] \\ \vdots \\ \underline{n}[i+m-1] \end{bmatrix}, \underbrace{\mathbf{b}[i]}_{K(m+\iota)\times 1} \triangleq \begin{bmatrix} \underline{b}[i-\iota] \\ \vdots \\ \underline{b}[i+m-1] \end{bmatrix}.$$

Finally matrix $\mathbf{H}$ is defined as follows:

$$\underbrace{\mathbf{H}}_{Pm\times K(m+\iota)} \triangleq \begin{bmatrix} \underline{H}[\iota] & \ldots & \underline{H}[0] & \ldots & \mathbf{0} \\ \vdots & \ddots & \ddots & \ddots & \vdots \\ \mathbf{0} & \ldots & \underline{H}[\iota] & \ldots & \underline{H}[0] \end{bmatrix},$$

where the smoothing factor m is chosen according to $m = \lceil\frac{P+K}{P-K}\rceil\iota$, [69]. Using these quantities, (3.5) can be written in matrix form as

$$\mathbf{r}[i] = \mathbf{H}\mathbf{b}[i] + \sigma\mathbf{n}[i]. \tag{3.6}$$

Now (3.6) can be rewritten as

$$\mathbf{r}[i] = \tilde{\mathbf{H}}\tilde{\mathbf{b}}[i] + \bar{\mathbf{H}}\bar{\mathbf{b}}[i] + \sigma\mathbf{n}[i], \tag{3.7}$$

where $\tilde{\mathbf{b}}[i]$ and $\bar{\mathbf{b}}[i]$ contain the data bits in $\mathbf{b}[i]$ corresponding to sets of known and unknown users, respectively; $\tilde{\mathbf{H}}$ and $\bar{\mathbf{H}}$ contain columns of $\mathbf{H}$ corresponding to known and unknown users, respectively.

3.2 Turbo Multiuser Detection with Unknown Interferers

In this section we first review in detail the receiver structure proposed in [73]. Then we show that such a multiuser detector fails to converge when the *a priori* information provided by the single-user decoders, at the input of the detector, is large enough. This situation may happen at both high and low signal-to-noise ratios after only a few iterations when the single-user decoders converge to the right or wrong code words.

As explained in [73], the detector accepts, as inputs, the *a priori* log likelihood ratios (LLR's) for the code bits of the known users delivered by the SISO MAP channel decoders of these users and produces, as outputs, updated LLR's for these code bits. This is accomplished by soft interference cancellation and MMSE filtering. Specifically, using the *a priori* LLR's, knowledge of channel coefficients as well as the delay of each path and signature sequence of the known users and the number of unknown users present in the system, the detector performs a soft interference cancellation for each known user, in which estimates of the multiuser interference from known users and an estimate of the interference caused by unknown users are subtracted from the received signal. Residual interference is suppressed by passing the resulting signal through an instantaneous MMSE filter. The *a posteriori* LLR can then be computed from the MMSE filter output. The detector first forms soft estimates of the known users' code bits as

$$\hat{b}_k[i] = E\{b_k[i]\} = \tanh\left(\frac{1}{2}\lambda_1[k,i]\right), \tag{3.8}$$

for $k = 1, \ldots, \tilde{K}$ and $i = 0, \ldots, M-1$, where $\lambda_1[k,i]$ is the *a priori* LLR of the kth user's ith bit delivered by the MAP channel decoder. We denote hard estimates of the code bits

as

$$\check{b}_k[i] = \text{sign}(\hat{b}_k[i]) \qquad \text{for} \quad k = 1, \ldots, \tilde{K}, \tag{3.9}$$

and define $\check{\tilde{\mathbf{b}}}[i] = \left[\check{\underline{b}}[i-\iota]^T, \ldots, \check{\underline{b}}[i+m-1]^T\right]^T$, where $\check{\underline{b}}[i] \triangleq \left[\check{b}_1[i], \ldots, \check{b}_{\tilde{K}}[i]\right]^T$. In the next step, an estimate of interference of the unknown users, $\hat{\mathbf{I}}[i]$, is formed. The first estimate is formed by

$$\gamma[i] = \mathbf{r}[i] - \tilde{\mathbf{H}}\check{\tilde{\mathbf{b}}}[i] = \tilde{\mathbf{H}}(\underbrace{\tilde{\mathbf{b}}[i] - \check{\tilde{\mathbf{b}}}[i]}_{\mathbf{d}[i]}) + \bar{\mathbf{H}}\bar{\mathbf{b}}[i] + \sigma\mathbf{n}[i], \tag{3.10}$$

where $\mathbf{d}[i] = \left[\underline{d}[i-\iota]^T, \ldots, \underline{d}[i+m-1]^T\right]^T$, $\underline{d}[i] \triangleq \left[d_1[i], d_2[i], \ldots, d_{\tilde{K}}[i]\right]^T$, and $d_k[i] \triangleq b_k[i] - \check{b}_k[i]$ for $k = 1, \ldots, \tilde{K}$ and can be given by

$$d_k[i] = \begin{cases} 0 & \text{with probability } \frac{1}{2} + \frac{1}{2}\tanh\left[\frac{1}{2}|\lambda_1[k,i]|\right]; \\ 2b_k[i] & \text{with probability } \frac{1}{2} - \frac{1}{2}\tanh\left[\frac{1}{2}|\lambda_1[k,i]|\right]. \end{cases}$$

Defining $\Gamma = [\gamma[0], \ldots, \gamma[M-1]]$ and performing an eigendecomposition on $\Gamma\Gamma^H/M$ yields

$$\Gamma\Gamma^H/M = U\Lambda U^H, \tag{3.11}$$

where U is the matrix of orthonormal basis of $\mathcal{C}^{Pm}$ which can be partitioned as follows: $U = [U_u \mid U_l]$, where U_u denotes the matrix of eigenvectors corresponding to the $\tilde{K}(m+\iota)$ largest eigenvalues, and U_l denotes the matrix of eigenvectors corresponding to the $Pm - \tilde{K}(m+\iota)$ smallest eigenvalues. The span of the columns of U_u represents an estimate of the subspace of the unknown users (i.e. the interference subspace). In the case of $b_k[i] = \check{b}_k[i]$ for $i = 0, \ldots, M-1$ and $k = 1, \ldots, \tilde{K}$, U_u contains the signal subspace spanned by the unknown interference $\tilde{\mathbf{H}}$. To refine the estimate of the unknown users interference, $\gamma[i]$ is projected onto U_u. The result is

$$\hat{\mathbf{I}}[i] = U_u U_u^H \left[\tilde{\mathbf{H}}\mathbf{d}[i] + \bar{\mathbf{H}}\bar{\mathbf{b}}[i] + \sigma\mathbf{n}[i]\right]. \tag{3.12}$$

Denoting $\tilde{\mathbf{H}}_u \triangleq U_u U_u^H \tilde{\mathbf{H}}$ and $\mathbf{n}_u[i] \triangleq U_u U_u^H \mathbf{n}[i]$, then (3.12) can be written as

$$\hat{\mathbf{I}}[i] = \tilde{\mathbf{H}}_u\mathbf{d}[i] + \bar{\mathbf{H}}\bar{\mathbf{b}}[i] + \sigma\mathbf{n}_u[i]. \tag{3.13}$$

Subtracting the interference estimate in (3.13) from the received signal in (3.7), a new signal is obtained as follows:

$$\zeta[i] = \mathbf{r}[i] - \hat{\mathbf{I}}[i] = \tilde{\mathbf{H}}\tilde{\mathbf{b}}[i] - \tilde{\mathbf{H}}_u\mathbf{d}[i] + \mathbf{v}[i], \tag{3.14}$$

where $\mathbf{v}[i] \triangleq \mathbf{n}[i] - \mathbf{n}_u[i] \sim \mathcal{N}(\mathbf{0}, \Sigma_v)$, with

$$\Sigma_v = \sigma^2(\mathbf{I}_{Pm} - U_u U_u^H), \tag{3.15}$$

where $\mathbf{I}_{Pm}$ is a $Pm \times Pm$ identity matrix.

The soft interference cancellation on $\zeta[i]$ is performed as follows:

$$\mathbf{r}_k[i] = \zeta[i] - \tilde{\mathbf{H}}\hat{\tilde{\mathbf{b}}}_k[i] + \tilde{\mathbf{H}}_u\hat{\mathbf{d}}[i], \tag{3.16}$$

where $\hat{\tilde{\mathbf{b}}}_k[i] \triangleq \left[\underline{\hat{b}}[i-\iota]^T, \ldots, \underline{\hat{b}}_k[i]^T, \ldots, \underline{\hat{b}}[i+m-1]^T\right]^T$, $\hat{\mathbf{d}}[i] \triangleq \left[\underline{\hat{d}}[i-\iota]^T, \ldots, \underline{\hat{d}}[i+m-1]^T\right]^T$, with $\underline{\hat{b}}_k[i] \triangleq \left[\hat{b}_1[i], \ldots, \hat{b}_{k-1}[i], 0, \hat{b}_{k+1}[i], \ldots, \hat{b}_{\tilde{K}}[i]\right]^T$, $\underline{\hat{d}}[i] \triangleq \left[\hat{d}_1[i], \ldots, \hat{d}_{\tilde{K}}[i]\right]^T$, and

$$\hat{d}_k[i] = \hat{b}_k[i]\left\{1 - \tanh\left(\frac{1}{2}|\lambda_1[k,i]|\right)\right\} \quad \text{for} \quad k = 1, \ldots, \tilde{K}. \tag{3.17}$$

Substituting (3.14) into (3.16), gives

$$\mathbf{r}_k[i] = \tilde{\mathbf{H}}(\tilde{\mathbf{b}}[i] - \hat{\tilde{\mathbf{b}}}_k[i]) - \tilde{\mathbf{H}}_u(\mathbf{d}[i] - \hat{\mathbf{d}}[i]) + \mathbf{v}[i]. \tag{3.18}$$

An instantaneous MMSE filter is then applied to $\mathbf{r}_k[i]$ to minimize the mean-square error between the code bit $b_k[i]$ and the filter output $z_k[i]$, i.e.

$$\mathbf{w}_k[i] \triangleq \arg \min_{\mathbf{w} \in \mathcal{C}^{Pm}} E\{|b_k[i] - \mathbf{w}^H\mathbf{r}_k[i]|^2\}. \tag{3.19}$$

The answer to the optimization problem in (3.19) for user k is given by

$$\mathbf{w}_k[i] = (\mathcal{H}\Delta_k[i]\mathcal{H}^H + \Sigma_v)^{-1}\mathbf{p}_k[i], \tag{3.20}$$

where $\mathcal{H} \triangleq \left[\tilde{\mathbf{H}} \quad \tilde{\mathbf{H}}_u\right]$, and

$$\Delta_k[i] \triangleq \mathrm{Cov}\left\{\begin{bmatrix} -(\hat{\tilde{\mathbf{b}}}[i] - \hat{\tilde{\mathbf{b}}}_k[i]) \\ \mathbf{d}[i] - \tilde{\mathbf{d}}[i] \end{bmatrix}\right\} = \begin{bmatrix} \Delta_{11}^k[i] & \Delta_{12}^k[i] \\ \Delta_{21}^k[i] & \Delta_{22}^k[i] \end{bmatrix}, \tag{3.21}$$

where $\Delta_{11}^k[i] \triangleq \mathrm{Cov}\{\tilde{\mathbf{b}}[i] - \hat{\tilde{\mathbf{b}}}_k[i]\} = \mathrm{diag}\left[\underline{\delta}_{11}^k[i-\iota], \ldots, \underline{\delta}_{11}^k[i], \ldots, \underline{\delta}_{11}^k[i+m-1]\right]$, and

$$\begin{aligned} \underline{\delta}_{11}^k[i+l] &\triangleq \mathrm{diag}\left[1 - \tilde{b}_1[i+l]^2, \ldots, 1 - \tilde{b}_{\tilde{K}}[i+l]^2\right] \quad l = -\iota, \ldots, m-1 \quad \text{and} \quad l \neq 0, \\ \underline{\delta}_{11}^k[i] &\triangleq \mathrm{diag}\left[1 - \tilde{b}_1[i]^2, \ldots, 1 - \tilde{b}_{k-1}[i]^2, 1, 1 - \tilde{b}_{k+1}[i]^2, \ldots, 1 - \tilde{b}_{\tilde{K}}[i]^2\right]. \end{aligned}$$

In a similar way, $\Delta_{22}^k[i]$ is given by $\Delta_{22}^k[i] \triangleq \text{Var}\{\tilde{\mathbf{d}}[i]\} = \text{diag}[\underline{\delta}_{22}^k[i-\iota],\ldots,\underline{\delta}_{22}^k[i+m-1]]$, where $\underline{\delta}_{22}^k[j] \triangleq \text{diag}[\beta_1[j],\ldots,\beta_{\tilde{K}}[j]]$, for $j = i-\iota,\ldots,i+m-1$, $\beta_k[j] = 2\alpha_k[j] - \tilde{b}_k[j]^2\alpha_k[j]^2$, and $\alpha_k[i] \triangleq 1-\tanh\left(\frac{1}{2}|\lambda_1[k,i]|\right)$. Also,

$$\Delta_{21}^k[i] = \Delta_{12}^k[i] \triangleq \text{Cov}\{\tilde{\mathbf{b}}[i],\tilde{\mathbf{d}}[i]\} = \text{diag}[\underline{\delta}_{12}^k[i-\iota],\ldots,\underline{\delta}_{12}^k[i+m-1]], \tag{3.22}$$

where $\underline{\delta}_{12}^k[j] \triangleq \text{diag}[\alpha_1[j](\tilde{b}_1[j]^2-1),\ldots,\alpha_{\tilde{K}}[j](\tilde{b}_{\tilde{K}}[j]^2-1)]$, for $j = i-\iota,\ldots,i+m-1$.

Finally, $\mathbf{p}_k[i]$ is defined as

$$\mathbf{p}_k[i] \triangleq E\{b_k[i]\mathbf{r}_k[i]\} = \tilde{\mathbf{H}}\mathbf{e}_{\tilde{K}\iota+k} - \alpha_k[i](1-\hat{b}_k[i]^2)\tilde{\mathbf{H}}_u\mathbf{e}_{\tilde{K}\iota+k}, \tag{3.23}$$

where $\mathbf{e}_{\tilde{K}\iota+k}$ is a $\tilde{K}(m+\iota)$-component column vector with 1 in the $(\tilde{K}\iota+k)$th position and 0 elsewhere. Making the assumption that the MMSE filter output is Gaussian [74], the extrinsic information $\lambda_2[k,i]$, delivered by SISO multiuser detector is given by

$$\lambda_2[k,i] = \frac{4\Re\{z_k[i]\}}{1-\mu_k[i]}, \quad k = 1,\ldots,\tilde{K} \tag{3.24}$$

where $z_k[i] \triangleq \mathbf{w}_k[i]^H\mathbf{r}_k[i]$ and $\mu_k[i] \triangleq \mathbf{p}_k[i]^H(\mathcal{H}\Delta_k[i]\mathcal{H}^H + \Sigma_v)^{-1}\mathbf{p}_k[i]$.

When the *a priori* information on the code bits of known interfering users becomes large enough (i.e $\lambda_1[j,i] = \pm\infty$ for $j = 1,\ldots,\tilde{K}, j \neq k$), (3.20) can be simplified as follows:

$$\mathbf{w}_k[i] = (\tilde{\mathbf{H}}\mathbf{e}_{\tilde{K}\iota+k}\mathbf{e}_{\tilde{K}\iota+k}^H\tilde{\mathbf{H}}^H + \Sigma_v)^{-1}\tilde{\mathbf{H}}\mathbf{e}_{\tilde{K}\iota+k}. \tag{3.25}$$

Since $\tilde{\mathbf{H}}\mathbf{e}_{\tilde{K}\iota+k}$ is a column vector, the rank of $\tilde{\mathbf{H}}\mathbf{e}_{\tilde{K}\iota+k}\mathbf{e}_{\tilde{K}\iota+k}^H\tilde{\mathbf{H}}^H$ is 1. Using the proposition below, it is easy to see that the rank of Σ_v is $Pm - \tilde{K}(m+\iota)$.

Proposition: *The rank of* $\Sigma_v = \sigma^2(\mathbf{I}_{Pm} - U_uU_u^H)$ *is* $Pm - \tilde{K}(m+\iota)$.

Proof: Since the matrix U is unitary, $UU^H = \mathbf{I}_{Pm}$. Partitioning U as before, $[U_u \mid U_l][U_u \mid U_l]^H = \mathbf{I}_{Pm}$ or $\mathbf{I}_{Pm} - U_uU_u^H = U_lU_l^H$. Therefore, $\text{rank}\{\Sigma_v\} = \text{rank}\{\mathbf{I}_{Pm} - U_uU_u^H\} = \text{rank}\{U_lU_l^H\}$. Since the columns of U_l consists of $Pm - \tilde{K}(m+\iota)$ orthogonal vectors, $\text{rank}\{U_lU_l^H\} = Pm-\tilde{K}(m+\iota)$. It therefore follows that the rank of $\Sigma_v = \sigma^2(\mathbf{I}_{Pm}-U_uU_u^H)$ is $Pm-\tilde{K}(m+\iota)$.

Therefore, the rank of $(\tilde{\mathbf{H}}\mathbf{e}_{\tilde{K}\iota+k}\mathbf{e}_{\tilde{K}\iota+k}^H\tilde{\mathbf{H}}^H + \Sigma_v)$ is less than or equal to $Pm - \tilde{K}(m+\iota)+1$; thus, this matrix is singular and its inverse does not exist. In practice, this situation might happen when the single-user decoders converge to the right or wrong code words which

produces large extrinsic information at the output of these decoders. In the next iteration this large *a priori* information at the input of multiuser detector results in convergence failure of the multiuser detector. This is in contrast with the result reported in [65], where the detector converges to the correct code words in the case of perfect *a priori* information. Our simulation results confirm our analytical discussion. We observed that multiuser detector fails to converge after only two or three iterations at both high and low signal-to-noise ratios.

3.3 Group-blind Turbo Multiuser Detector For Asynchronous CDMA Systems

In this section, we consider a general multiple access signal model where the users are asynchronous, and a channel that exhibits dispersion due to multipath effects. Then, we generalize the turbo multiuser detector (TMUD) proposed in [65] for group-blind CDMA systems. Instead of modifying the soft interference unit by estimating the interference form the unknown users and subtracting it from the received signal, as it is done in [73], we revise the MMSE-based filter in a way that the receiver can suppress the multiple-access interference (MAI) from unknown users, at the expense of adding computational complexity. The structure of the proposed receiver is shown in Fig. 3.1. The first stage of the iterative receiver performs soft detection on all known users' symbols. The second stage of the receiver consists of a bank of $\tilde{K}$ single-user channel decoders. In the first stage of the receiver, it is assumed that the *a priori* information about the coded symbols $b_k[i]$ for $k = 1, \ldots, \tilde{K}$ and $i = 0, \ldots, M-1$ is available. For the first iteration, it is assumed that the *a priori* information has a uniform distribution, while for the next iterations the *a priori* information is provided by the second stage of the receiver (i.e. the channel decoders). The iterative group-blind multiuser detection proceeds until the condition of a certain number of iterations is satisfied. At this point the *a posteriori* information at the output of the decoder is sent to a decision device and the process is terminated. The proposed group-blind multiuser detector consists of soft interference cancellation for known users and a combined

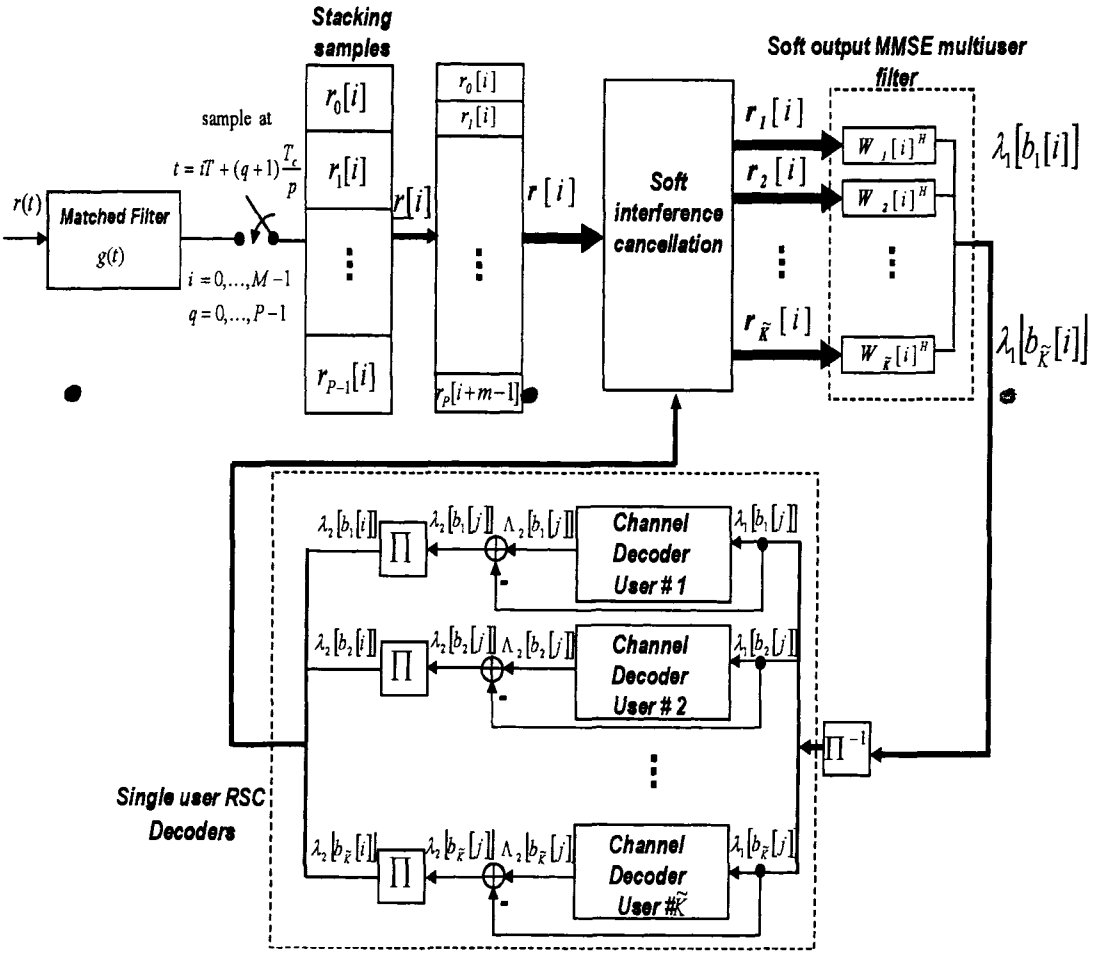

Figure 3.1: Block diagram of the proposed receiver structure

MMSE filtering, which minimizes both the intracell and intercell interference using MMSE criterion. The unknown users' signals are suppressed by identifying the subspace spanned by these users followed by a linear transformation in this subspace, based on MMSE criterion.

Soft Interference Cancellation

The soft interference cancellation at the first stage of the proposed receiver is similar to what was proposed in [65]. Suppose that at the first stage of the receiver we have available *a priori* log likelihood ratios $\lambda_1[k,i]$ of known users' transmitted symbols. These values are in fact generated by the single-user channel decoders at the previous iteration, which are fed to the group-blind multiuser detector after appropriate interleaving.The soft estimate of the known user's transmitted symbol is given by (3.8) for $k = 1,\ldots,\tilde{K}$, and $i = 0,\ldots,M-1$. The partially interference-canceled signal corresponding to the kth user's symbol is then obtained by subtracting a soft-estimate of the multiple-access interference of known users from the received signal

$$\mathbf{r}_k[i] = \mathbf{r}[i] - \tilde{\mathbf{H}}\hat{\tilde{\mathbf{b}}}_k[i] = \tilde{\mathbf{H}}(\tilde{\mathbf{b}}[i] - \hat{\tilde{\mathbf{b}}}_k[i]) + \bar{\mathbf{H}}\bar{\mathbf{b}}[i] + \sigma\mathbf{n}[i], \tag{3.26}$$

where $\hat{\tilde{\mathbf{b}}}_k[i] = \hat{\tilde{\mathbf{b}}}[i] - \hat{b}_k[i]\mathbf{e}_{\tilde{K}\iota+k}$, $\mathbf{e}_{\tilde{K}\iota+k}$ is an $\tilde{K}(m+\iota)$ vector of all zero except for the single unity element at the $\tilde{K}\iota + k$ position. $\hat{b}_k[i]$ is the soft estimate of the kth user's symbol, and $\hat{\tilde{\mathbf{b}}}[i]$ is a vector of the soft estimate of known users' coded bits. We further define $\tilde{\mathbf{r}}_k[i] = \tilde{\mathbf{H}}(\tilde{\mathbf{b}}[i] - \hat{\tilde{\mathbf{b}}}_k[i]) + \sigma\mathbf{n}[i]$ to be the component of $\mathbf{r}_k[i]$ in (3.26) consisting of signals from known users plus noise.

Group-blind Linear MMSE Filtering

In order to further suppress the MAI from known users and unknown users a combined instantaneous linear MMSE filter $\mathbf{w}_k[i]$ is applied to $\mathbf{r}_k[i]$, such that

$$z_k[i] = \mathbf{w}_k[i]^H\mathbf{r}_k[i]. \tag{3.27}$$

The purpose of using group-blind MMSE filtering is to suppress the remaining MAI from known users based on the spreading sequences and channel characteristics of these users and

to suppress the interference from other unknown users using subspace-based blind method. The weight vector of the group-blind linear MMSE detector for user k is given by

$$\mathbf{w}_k[i] = \tilde{\mathbf{w}}_k[i] + \bar{\mathbf{w}}_k[i], \qquad 1 \le k \le \tilde{K}$$

where $\tilde{\mathbf{w}}_k[i] \in \text{range}(\tilde{\mathbf{H}})$, and $\bar{\mathbf{w}}_k[i] \in \{\text{range}(\mathbf{H}) \cap \text{null}(\tilde{\mathbf{H}}^H)\}$ such that

$$\tilde{\mathbf{w}}_k[i] = \arg \min_{\mathbf{w} \in \text{range}(\tilde{\mathbf{H}})} E\{|b_k[i] - \mathbf{w}^H \tilde{\mathbf{r}}_k[i]|^2\} \tag{3.28}$$

$$\bar{\mathbf{w}}_k[i] = \arg \min_{\mathbf{w} \in \Omega} E\{|b_k[i] - (\mathbf{w} + \tilde{\mathbf{w}}_k[i])^H \mathbf{r}_k[i]|^2\} \tag{3.29}$$

where $\Omega \triangleq \{\text{range}(\mathbf{H}) \cap \text{null}(\tilde{\mathbf{H}}^H)\}$. (3.28) can be rewritten as

$$\tilde{\mathbf{w}}_k[i] = \arg \min_{\mathbf{w} \in \text{range}(\tilde{\mathbf{H}})} \mathbf{w}^H E\{\tilde{\mathbf{r}}_k[i]\tilde{\mathbf{r}}_k[i]^H\}\mathbf{w} - \mathbf{w}^H E\{b_k[i]\tilde{\mathbf{r}}_k[i]\} - E\{b_k[i]\tilde{\mathbf{r}}_k[i]\}^H \mathbf{w} \tag{3.30}$$

where

$$E\{\tilde{\mathbf{r}}_k[i]\tilde{\mathbf{r}}_k[i]^H\} = \tilde{\mathbf{H}}\Delta_k[i]\tilde{\mathbf{H}}^H + \sigma^2 \mathbf{I}_{Pm} \tag{3.31}$$

$$E\{b_k[i]\tilde{\mathbf{r}}_k[i]\} = \tilde{\mathbf{H}}\mathbf{e}_{\tilde{K}\iota+k}, \tag{3.32}$$

and $\Delta_k[i] \triangleq \text{Cov}\{\tilde{\mathbf{b}}[i] - \hat{\tilde{\mathbf{b}}}_k[i]\} = \text{diag}[\underline{\delta}_k[i-\iota], \ldots, \underline{\delta}_k[i], \ldots, \underline{\delta}_k[i+m-1]]$, where

$$\underline{\delta}_k[i+l] \triangleq \text{diag}[1 - \tilde{b}_1[i+l]^2, \ldots, 1 - \tilde{b}_{\tilde{K}}[i+l]^2] \quad l = -\iota, \ldots, m-1 \quad \textit{and} \quad l \neq 0,$$

$$\delta_k[i] \triangleq \text{diag}[1 - \tilde{b}_1[i]^2, \ldots, 1 - \tilde{b}_{k-1}[i]^2, 1, 1 - \tilde{b}_{k+1}[i]^2, \ldots, 1 - \tilde{b}_{\tilde{K}}[i]^2].$$

The solution to the optimization problem (3.30) is given by

$$\tilde{\mathbf{w}}_k[i] = \tilde{\mathbf{H}}(\Delta_k[i]\tilde{\mathbf{H}}^H\tilde{\mathbf{H}} + \sigma^2 \mathbf{I}_{\tilde{K}(m+\iota)})^{-1}\mathbf{e}_{\tilde{K}\iota+k}. \tag{3.33}$$

In the same way, (3.29) can be simplified as follows:

$$\begin{aligned}\bar{\mathbf{w}}_k[i] = \arg \min_{\mathbf{w} \in \Omega} \{&(\mathbf{w} + \tilde{\mathbf{w}}_k[i])^H E\{\mathbf{r}_k[i]\mathbf{r}_k[i]^H\}(\mathbf{w} + \tilde{\mathbf{w}}_k[i]) \\ &-(\mathbf{w} + \tilde{\mathbf{w}}_k[i])^H E\{b_k[i]\mathbf{r}_k[i]\} - E\{b_k[i]\mathbf{r}_k[i]\}^H(\mathbf{w} + \tilde{\mathbf{w}}_k[i])\},\end{aligned} \tag{3.34}$$

where $E\{\mathbf{r}_k[i]\mathbf{r}_k[i]^H\} = \tilde{\mathbf{H}}\Delta_k[i]\tilde{\mathbf{H}}^H + \bar{\mathbf{H}}\bar{\mathbf{H}}^H + \sigma^2\mathbf{I}_{Pm}$ and $E\{b_k[i]\mathbf{r}_k[i]\} = \tilde{\mathbf{H}}\mathbf{e}_{\tilde{K}\iota+k}$. To solve the optimization problem (3.34), we first introduce the projection matrix $\mathbf{P}$, which is defined

in a way that projects any signal onto the null subspace of $\tilde{\mathbf{H}}^H$; in this way $\mathbf{P}$ is defined as follows:

$$\mathbf{P} \triangleq \mathbf{I}_{Pm} - \tilde{\mathbf{H}}(\tilde{\mathbf{H}}^H\tilde{\mathbf{H}})^{-1}\tilde{\mathbf{H}}^H. \tag{3.35}$$

The autocorrelation matrix of $\mathbf{r}[i]$ is given by

$$E\{\mathbf{r}[i]\mathbf{r}[i]^H\} = \tilde{\mathbf{H}}\tilde{\mathbf{H}}^H + \bar{\mathbf{H}}\bar{\mathbf{H}}^H + \sigma^2\mathbf{I}_{Pm}. \tag{3.36}$$

It is then easily seen that the matrix $\mathbf{P}E\{\mathbf{r}[i]\mathbf{r}[i]^H\}\mathbf{P}$ has an eigen-structure of the form

$$\mathbf{P}E\{\mathbf{r}[i]\mathbf{r}[i]^H\}\mathbf{P} = \begin{bmatrix}\bar{U}_s & \bar{U}_n & \bar{U}_0\end{bmatrix}\begin{bmatrix}\bar{\Lambda}_s & 0 & 0\\ 0 & \bar{\Lambda}_n & 0\\ 0 & 0 & 0\end{bmatrix}\begin{bmatrix}\bar{U}_s^H\\ \bar{U}_n^H\\ \bar{U}_0^H\end{bmatrix}, \tag{3.37}$$

where $\bar{\Lambda}_s \triangleq \text{diag}[\lambda_1,\ldots,\lambda_{(K-\tilde{K})(m+\iota)}]$, and $\bar{\Lambda}_n \triangleq \sigma^2\mathbf{I}_{Pm-K(m+\iota)}$, with $\lambda_i > \sigma^2$ for $i = 1,\ldots,(K-\tilde{K})(m+\iota)$. The columns of $\bar{U}_s$ form an orthogonal basis of the subspace range($\mathbf{H}$) $\cap$ null($\mathbf{H}^H$). An approximation for autocorrelation matrices $E\{\mathbf{r}[i]\mathbf{r}[i]^H\}$ and $E\{\mathbf{r}_k[i]\mathbf{r}_k[i]^H\}$ can be formed as follows:

$$\mathbf{C}_r \triangleq E\{\mathbf{r}[i]\mathbf{r}[i]^H\} \approx \frac{1}{M}\sum_{i=0}^{M-1}\mathbf{r}[i]\mathbf{r}[i]^H \tag{3.38}$$

$$\mathbf{C}_{r_k}[i] \triangleq E\{\mathbf{r}_k[i]\mathbf{r}_k[i]^H\} \approx \mathbf{C}_r - \tilde{\mathbf{H}}\tilde{\mathbf{H}}^H + \tilde{\mathbf{H}}\Delta_k[i]\tilde{\mathbf{H}}. \tag{3.39}$$

The solution to the optimization problem (3.34) is given by

$$\bar{\mathbf{w}}_k[i] = -\bar{U}_s\bar{\Lambda}_s^{-1}\bar{U}_s^H\mathbf{C}_{r_k}[i]\tilde{\mathbf{w}}_k[i]. \tag{3.40}$$

The combined group-blind MMSE filter is defined as

$$\mathbf{w}_k[i] = \tilde{\mathbf{w}}_k[i]+\bar{\mathbf{w}}_k[i] = (\mathbf{I}_{Pm}-\bar{U}_s\bar{\Lambda}_s^{-1}\bar{U}_s^H\mathbf{C}_{r_k}[i])\tilde{\mathbf{H}}(\Delta_k[i]\tilde{\mathbf{H}}^H\tilde{\mathbf{H}}+\sigma^2\mathbf{I}_{\tilde{K}(m+\iota)})^{-1}\mathbf{e}_{\tilde{K}\iota+k}. \tag{3.41}$$

In [74], it is shown that the residual MAI plus the background receiver noise at the output of a linear MMSE multiuser detector can be well modeled as being Gaussian. It is reasonable to expect the same property to hold in this situation. Thus, we may model the combined MMSE filter output as

$$z_k[i] = \mu_k[i]b_k[i] + \eta_k[i], \tag{3.42}$$

where $\mu_k[i] \triangleq E\{z_k[i]b_k[i]\} = \mathbf{w}_k[i]^H\tilde{\mathbf{H}}\mathbf{e}_{\tilde{K}\iota+k}$, and $v_k[i]^2 \triangleq \mathrm{Var}\{z_k[i]\} = \mu_k[i] - \mu_k[i]^2$. Model (3.42) is used to compute the soft outputs from the first stage of the receiver. It can be shown that the extrinsic log likelihood ratio corresponding to the kth user's signal $k \in \{1,\ldots,\tilde{K}\}$, delivered by the soft instantaneous group-blind MMSE filter is given by [65]

$$\lambda_2[k,i] = \frac{4\Re\{z_k[i]\}}{1-\mu_k[i]}. \tag{3.43}$$

Then, the set of soft outputs $\{\lambda_2[k,i]\}_{i=0}^{M-1}$, $k = 0,\ldots,\tilde{K}$ are deinterleaved and passed on to the bank of single-user channel decoders to serve as the *a priori* information.

3.4 Simulation Results

3.4.1 BER performance of the proposed method

We present bit error rate (BER) performance results by simulating data transmission using the receiver introduced in Section 3.3 part A. We consider an asynchronous CDMA system with seven users ($K = 7$). The number of known users in this system are 5,4,3 or 2, as noted on the figures. The spreading sequences of the users are random sequences of length 7 and the same set of spreading sequences is used for all the simulations. The number of paths between each user and the base station is $L_k = 3$, and the maximum delay in symbol interval is 1. The complex path gains for each user channel are generated from a complex Gaussian distribution and normalized such that the composite signature of each user (i.e user k) satisfies $||\mathbf{H}\mathbf{e}_{\tilde{K}\iota+k}|| = 1$. All users employ the same rate 1/2 constraint length 5 recursive systematic convolutional encoder with generator matrix $g = [23, 35]$ in octal notation, where the first element in the matrix is the feedback part. Each user uses a different interleaver generated randomly. The block size of information bits for each user is 128. In the simulation, we consider the worst case scenario where all users have equal power. The chip pulse waveform is a raised cosine with roll-off factor of 0.5. For the sake of comparison, in each figure, we have included three sets of graphs, the proposed turbo group-blind multiuser detector (Pm-GBMUD), the conventional turbo multiuser detector as proposed in [65], in the presence of unknown interference and conventional turbo multi user detector when all users are known to the receiver. We have considered the sampling

rate at the output of the matched filter to be T_c/p where $p = 3$ for our method as well as the conventional turbo multiuser detector [65]. For this reason we named the conventional turbo multiuser detector as Pm-TMUD. It should be noted that, the transmitter, the multipath channel, the channel decoder, and the interleaver/deinterleaver structure are identical for all systems. The only difference resides in the SISO multiuser detector structure.

Fig. 3.2 illustrates the average bit error rate performance of the 5 known users, out of the total number of 7 users, for the proposed turbo group-blind receiver and the conventional turbo multiuser receiver. As is shown in this figure, the performance of both methods is very close in the presence of low intercell interference . Almost same results are obtained for 4 known users out of the total number of 7 users, as shown in Fig. 3.3 except that, the Pm-GBMUD preserves its advantage over conventional Pm-TMUD even in high SNR region. As the intercell interference increases or equivalently number of known users decreases to 3 and 2, as shown in Fig. 3.4 and Fig. 3.5, respectively, the conventional Pm-TMUD tends to exhibit an error floor at high SNR. This is mostly because the detector fails to suppress the multiple access interference from unknown users, while the proposed method continues to provide the lower BER as the SNR increases. Also as we would expect, by increasing the number of unknown users the performance gain due to iteration decreases. This is because the decoder only provides soft information for the known users signals, and soft interference cancellation is only done for these users, while the interference from unknown users is suppressed blindly, which is not improved through the iteration.

3.4.2 BER Performance Sensitivity to the Number of Unknown Users

It is worth noting that both the algorithms presented in Section 3.2 and 3.3 assume perfect knowledge of the number of unknown users at the receiver. In this section, several simulations have been performed in order to examine the effect of mismatch of the number of unknown users on the BER performance of the proposed method. Fig. 3.6 and Fig. 3.7 show the simulation results when the number of known users is equal to 5 and 2, respectively. The total number of active users in the system is 7. The characteristics of the encoders, spreading sequences, and the multipath channels are the same as those given in

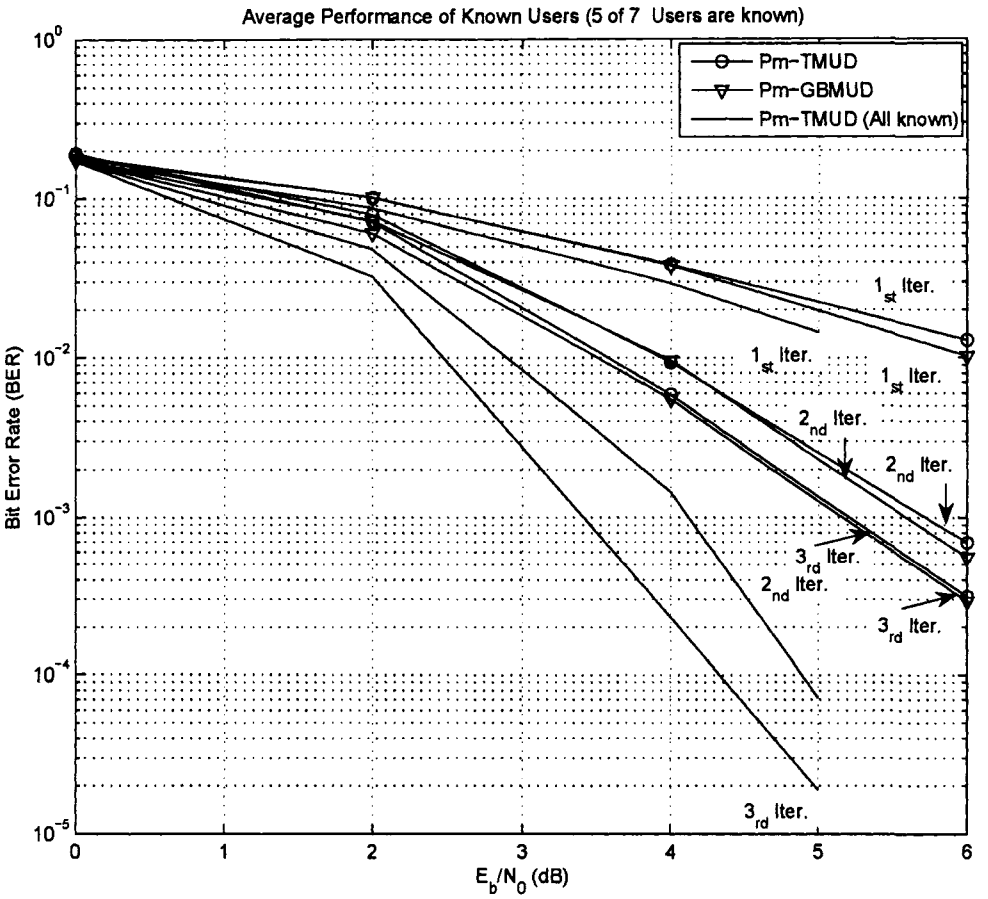

Figure 3.2: Performance comparison between different methods when 5out of 7 users are known to the receiver

the previous section.

Each figure contains a number of curves corresponding to different signal to noise ratios. We consider the effect of the number of unknown users mismatch with an offset with respect to the true number of unknown users present in the system. It is noted from these figures that both overestimation and underestimation of the number of unknown users result in performance degradation of the receiver; nevertheless, as far as we are able to determine the presence of unknown users, the system performance is better than that of the conven-

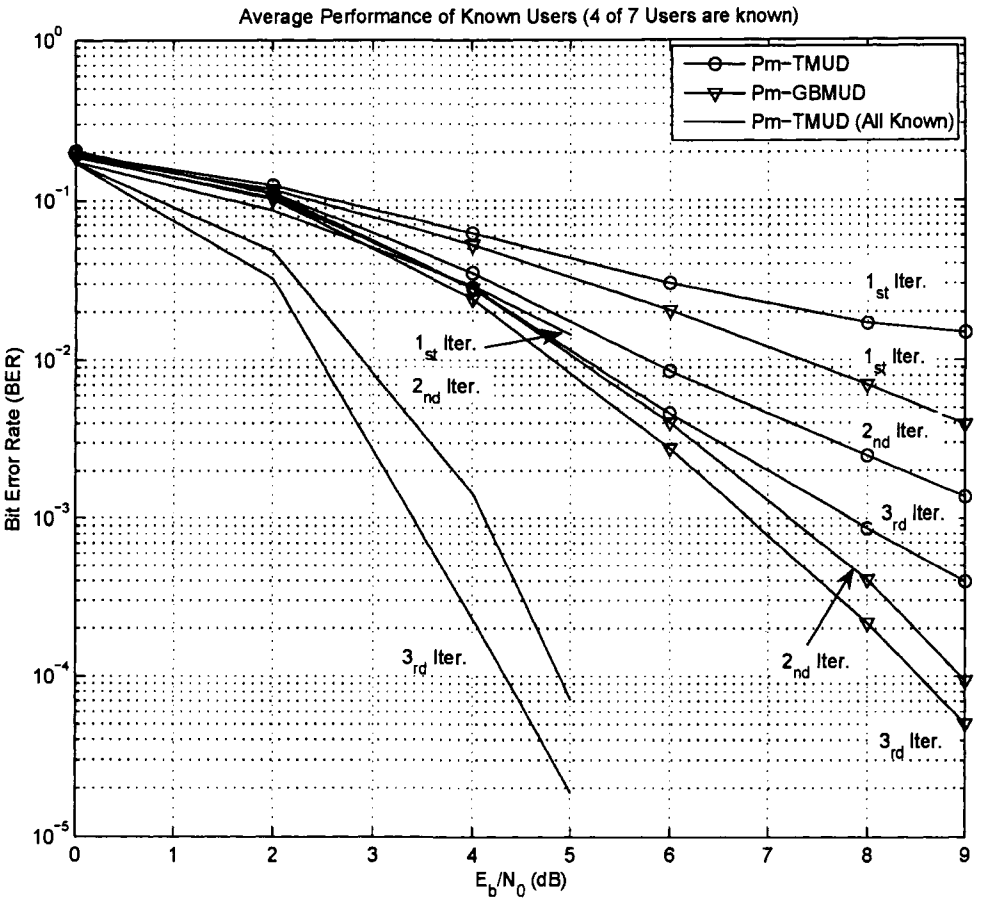

Figure 3.3: Performance comparison between different methods when 4 out of 7 users are known to the receiver

tional turbo multiuser detector. However, in order to attain the best performance from the proposed receiver, accurate estimation of the active number of unknown users in the system is essential.

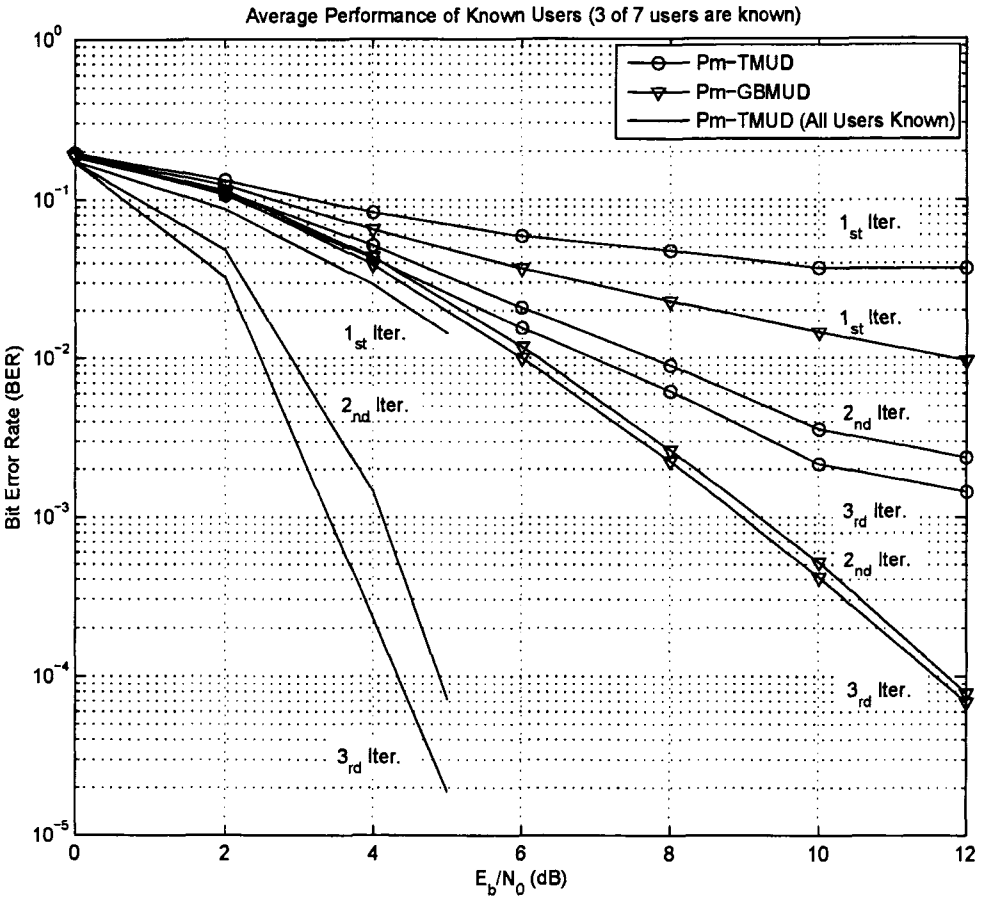

Figure 3.4: Performance comparison between different methods when 3 out of 7 users are known to the receiver

3.5 Estimation of the Number of Unknown Users

The adaptive rank estimation algorithm (AREA) proposed in [78] for signal rank estimation exploits the intrinsic property of the eigenvalues of the correlation matrix $\mathbf{C}_r = \mathbf{V}_s\mathbf{D}_s\mathbf{V}_s^H + \sigma^2\mathbf{V}_n\mathbf{V}_n^H$ to define a decision rule. In this method, which is similar to the work in [77], a

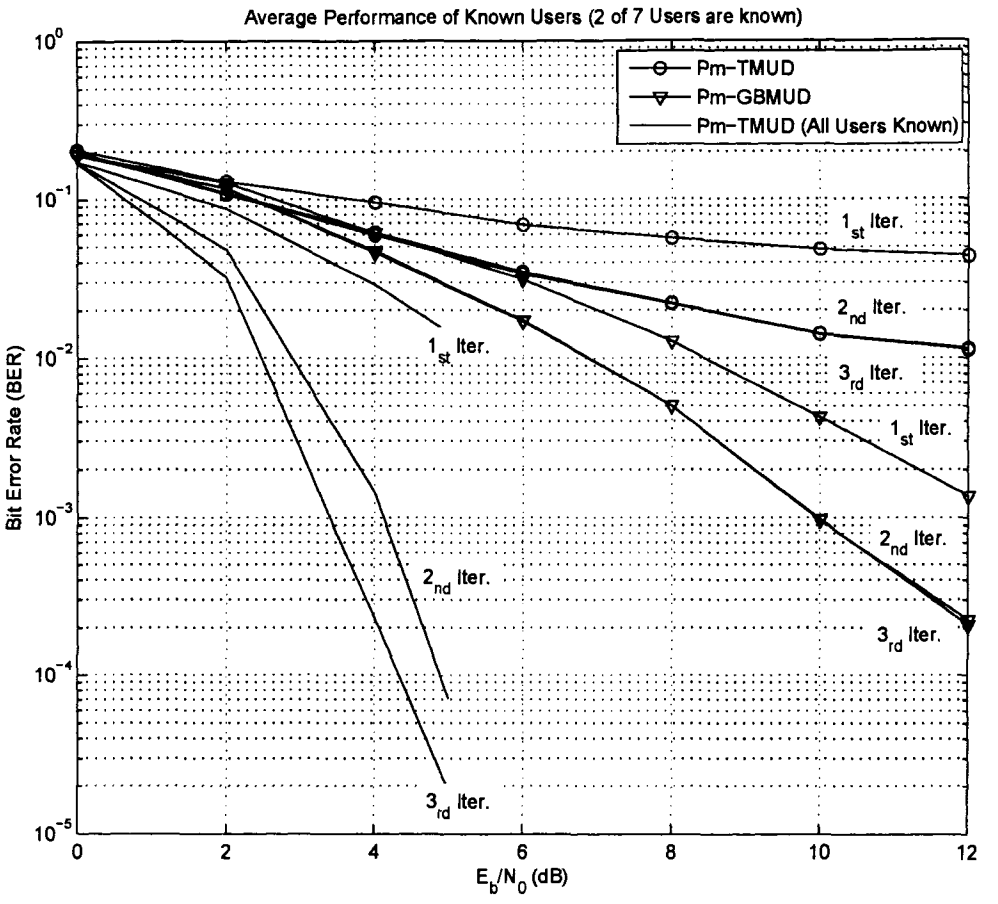

Figure 3.5: Performance comparison between different methods when 2 out of 7 users are known to the receiver

likelihood function plus a penalty function is given by

$$HDL(k) = M(D-k)\ln\left\{\frac{\frac{1}{D-k}\sum_{j=k+1}^{D}\lambda_j}{(\prod_{j=k+1}^{D}\lambda_j)^{\frac{1}{D-k}}}\right\} + P(D,k,\lambda), \tag{3.44}$$

where λ_j for $j = 1, 2, \ldots, D$ are the estimated eigenvalues of correlation matrix decomposition in descending order and $D \triangleq Pm$ is the dimension of the received signal vector in our

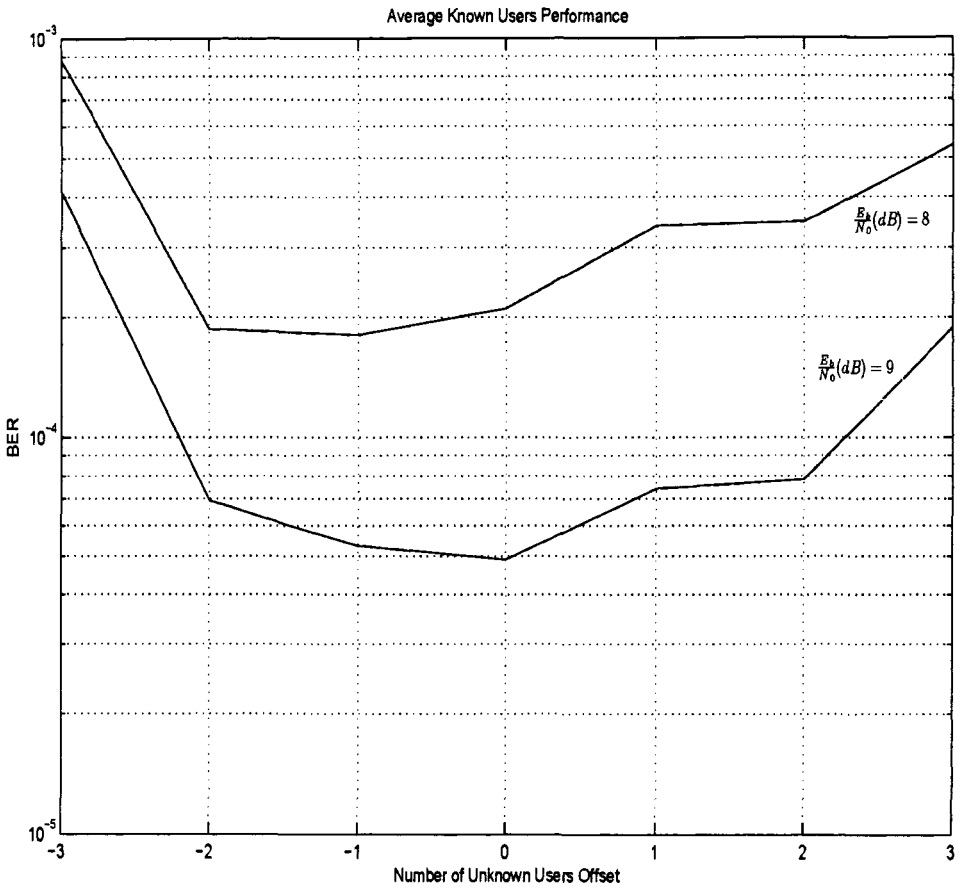

Figure 3.6: Bit error rate versus number of unknown users mismatch after 3 iterations, $K = 7$, $\tilde{K} = 4$, and $\bar{K} = 3$

model. In [78], the penalty function, however, is chosen in a different way in comparison with the Akaike information criterion and minimum description length criterion in [77] to correctly detect the number of sources for colored noise, and is given by

$$P(D, k, \lambda) = -M \sum_{j=k+1}^{D} \ln \frac{\lambda_1}{\lambda_j}. \tag{3.45}$$

The rank of the signal subspace is determined coarsely by a k that minimizes the cost function in (3.44). For further improvement of the estimation, in [78], a hypothesis testing

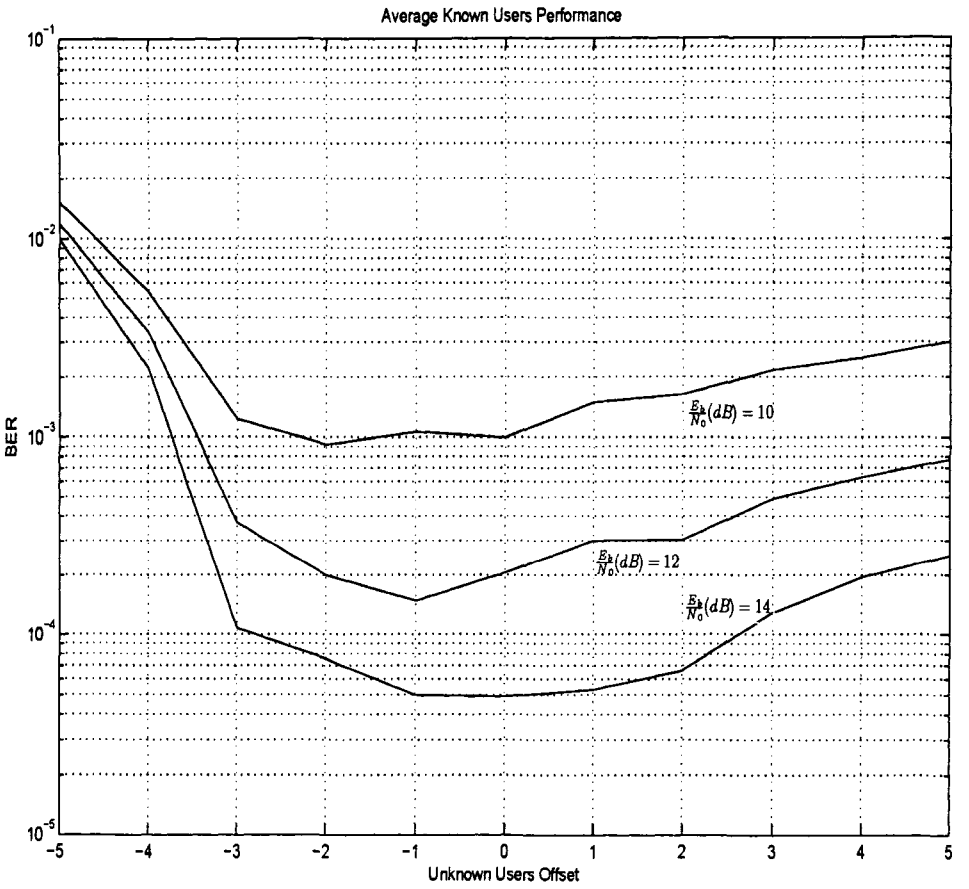

Figure 3.7: Bit error rate versus number of unknown users mismatch after 3 iterations, $K = 7$, $\tilde{K} = 2$, and $\bar{K} = 5$

criterion has been proposed based on the method in [?]. The criterion is to find a rank that minimizes the hypothesis criterion

$$Y^j \triangleq \frac{(\mathbf{h}_k^j)^H \hat{\mathbf{V}}_n^j (\hat{\mathbf{V}}_n^j)^H \mathbf{h}_k^j}{(\mathbf{h}_k^j)^H \mathbf{h}_k^j}, \qquad \hat{r} - d \leq j \leq \hat{r} + d,$$

where $\hat{r}$ is the estimated rank using the cost function in (3.44), d is the adjusting factor, $\hat{\mathbf{V}}_n^j$ is the corresponding matrix of the noise eigenvectors when the rank of the signal subspace is j, and $\mathbf{h}_k^j$ is the blind estimation of the kth user's channel, when the rank of the noise

subspace is $Pm - j$.

Fig. 3.8 shows the performance of the AREA. The frame size, and the encoder structures are the same as in previous sections. The spreading sequences are randomly generated and different sequences are used for each transmitted frame. As before, each user's channel has $L = 3$ paths. The fading gain of each path in each user's channel is generated from a complex Gaussian distribution and is fixed over the duration of one signal frame, and changes independently thereafter. The delay of each path is uniformly distributed on $[0, NT_c]$. The smoothing factor is $m = 2$. The noise at the receiver is modeled by a first-order autoregressive model with coefficient $a = 0$ or $a = 0.8$, corresponding to white or highly correlated noise samples. The noise is generated according to,

$$\mathbf{v}[i] = \pm\sqrt{|a|}\mathbf{v}[i-1] + \sqrt{1-|a|}\mathbf{n}[i], \tag{3.46}$$

where $\mathbf{v}[i]$ is the noise sample at sample i and $\mathbf{n}$[i] is a complex Gaussian noise vector. In each simulation the number of transmitted frames is 1000. From Fig. 3.8(a), it is evident that the AREA does not provide the correct number of unknown users in the low to moderate SNR regions, even when a large adjusting factor d for hypothesis testing is chosen; also, when the total number of users is larger than the maximum number of users that the system can accommodate, the AREA method provides incorrect estimation of the number of unknown users as shown in Fig. 3.8(b). In contrast, in the high SNR region, when the total number of users present in the system is less than the maximum number of users that the system can accommodate, the AREA is able to estimate the number of unknown users accurately in both colored and white noise as shown in 3.8(c) and 3.8(d), respectively; however, in a coded CDMA system, the system usually works in low to moderate SNR, and for heavily loaded CDMA systems, there is always a possibility that the sum of the number of interfering users from outside the cell plus the number of users inside the cell exceed the total number of users that the system can accommodate. In such scenarios, if we can detect the correct rank of the signal subspace, we can increase the over sampling factor p for the next frames such that all active users can be accommodated in the system. This way we can effectively eliminate the interference from unknown users, using the group-blind receiver structure. Based on these conditions, we propose a novel signal rank estimation

method that can estimate the number of unknown users with high probability.

In order to estimate the number of unknown users, we assume the number of known users and the variance of the noise are known to the receiver, and as before, we assume all users have equal power. We start by rewriting (3.7) in terms of known and unknown users' signals as

$$\mathbf{r}[i] = \tilde{\mathbf{H}}\tilde{\mathbf{b}}[i] + \bar{\mathbf{H}}\bar{\mathbf{b}}[i] + \sigma\mathbf{n}[i] = \mathbf{X}[i] + \mathbf{I}[i] + \sigma\mathbf{n}[i], \tag{3.47}$$

where $\mathbf{X}[i] \triangleq \tilde{\mathbf{H}}\tilde{\mathbf{b}}[i]$ and $\mathbf{I}[i] \triangleq \bar{\mathbf{H}}\bar{\mathbf{b}}[i]$. It is possible to approximate the interference from unknown users by a zero mean Gaussian noise vector which is independent from the additive white Gaussian noise and the known users signal $\mathbf{X}[i]$; therefore, the sum of the interference from unknown users and the additive white Gaussian noise is also a complex Gaussian noise with zero mean and covariance matrix

$$\text{Cov}\{\mathbf{v}[i]\} = E\{\mathbf{r}[i]\mathbf{r}[i]^H\} - \tilde{\mathbf{H}}\tilde{\mathbf{H}}^H = \frac{1}{M}\sum_{i=0}^{M-1}\mathbf{r}[i]\mathbf{r}[i]^H - \tilde{\mathbf{H}}\tilde{\mathbf{H}}^H, \tag{3.48}$$

where $\mathbf{v}[i] \triangleq \mathbf{I}[i] + \sigma\mathbf{n}[i]$. It is feasible to further estimate the variance of $\mathbf{v}[i]$ as

$$\widehat{\sigma_{\mathbf{v}}^2} = \frac{\text{Trace}\left\{\frac{1}{M}\sum_{i=0}^{M-1}\mathbf{r}[i]\mathbf{r}[i]^H - \tilde{\mathbf{H}}\tilde{\mathbf{H}}^H\right\}}{2Pm}. \tag{3.49}$$

Extending the same methodology to the known users, enables us to approximate the known users' signal as a complex Gaussian vector with zero mean and covariance matrix $\text{Cov}\{\mathbf{X}[i]\} = \tilde{\mathbf{H}}\tilde{\mathbf{H}}^H$. An estimate of the variance of $\mathbf{X}[i]$ is given by $\widehat{\sigma_{\mathbf{X}}^2} = \frac{\text{Trace}\{\tilde{\mathbf{H}}\tilde{\mathbf{H}}^H\}}{2Pm}$. Since $\widehat{\sigma_{\mathbf{X}}^2}$ depends on the number of known users, and seeing that all users contribute equally to form this variance, the variance of the Gaussian signal corresponding to each known user is equal to $\frac{\widehat{\sigma_{\mathbf{X}}^2}}{\tilde{K}}$. Finally, the number of unknown users in the system can be found as follows:

$$\hat{\bar{K}} = \text{round}\left(\frac{\tilde{K}\widehat{\sigma_{\mathbf{I}}^2}}{\widehat{\sigma_{\mathbf{X}}^2}}\right) = \text{round}\left(\frac{\tilde{K}\text{Trace}\left\{(\frac{1}{M}\sum_{i=0}^{M-1}\mathbf{r}[i]\mathbf{r}[i]^H) - \tilde{\mathbf{H}}\tilde{\mathbf{H}}^H - \sigma^2\mathbf{I}_{Pm}\right\}}{\text{Trace}\left\{\tilde{\mathbf{H}}\tilde{\mathbf{H}}^H\right\}}\right), \tag{3.50}$$

where round(x) rounds x to the nearest integer.

Fig. 3.9 shows the the performance of the proposed estimator in systems with different parameters such as processing gain, the over sampling factor p, the number of known and

unknown users, the autoregressive coefficient, and the signal to noise ratios. Figures 3.9(a)-(d) represent our proposed estimator performance with the exact same parameters as those in Fig. 3.8. As it is evident from the graphs, the estimator is able to provide an accurate estimate of the number of unknown users with high probability. The worst performance occurred in $\frac{E_b}{N_0} = 0$ dB, but the estimation error is almost always limited to ± 1 in the number of unknown users. The application of the proposed method is not limited to the uplink of CDMA systems. Such an estimator can be applied to the blind receiver for the downlink of CDMA systems, where the knowledge of the number of unknown users that are present in the system is crucial for subspace-based detectors. In addition, the proposed estimator can also be employed with aperiodic spreading sequences. The alternative methods based on singular value or eigenvalue decomposition usually set a threshold to separate the unknown users from the variance of the noise, or sometimes it is claimed that the gap between the smallest eigenvalue of signal subspace and the largest eigenvalue of the noise subspace is much greater than the gap between other adjacent eigenvalues. While theoretically this is true; in practice the magnitude of singular values (or eigenvalues) depends on different parameters such as SNR, and the processing gain; therefore, any predetermined threshold might result in a huge error in the estimation. Also, the magnitude of singular values or eigenvalues changes very smoothly, thus it is not reliable to split the signal and the noise subspaces based on the gap between their eigenvalues.

3.6 Near-Far Situation

We consider a near-far situation, where there are four equal power strong known users and three equal power weak unknown users present in the system. The known users are 3 dB stronger than the unknown users. Fig. 3.10 shows the average performance of known users under the proposed group-blind receiver. We consider two situations. First, when the exact number of unknown users is available to the receiver, and second, when the proposed estimation method (which assumes equal-power users) is used to estimate the number of unknown users. For the sake of comparison, we have included curves corresponding to group-blind case, when 4 out of 7 users are known and all users have equal power, as well as the case

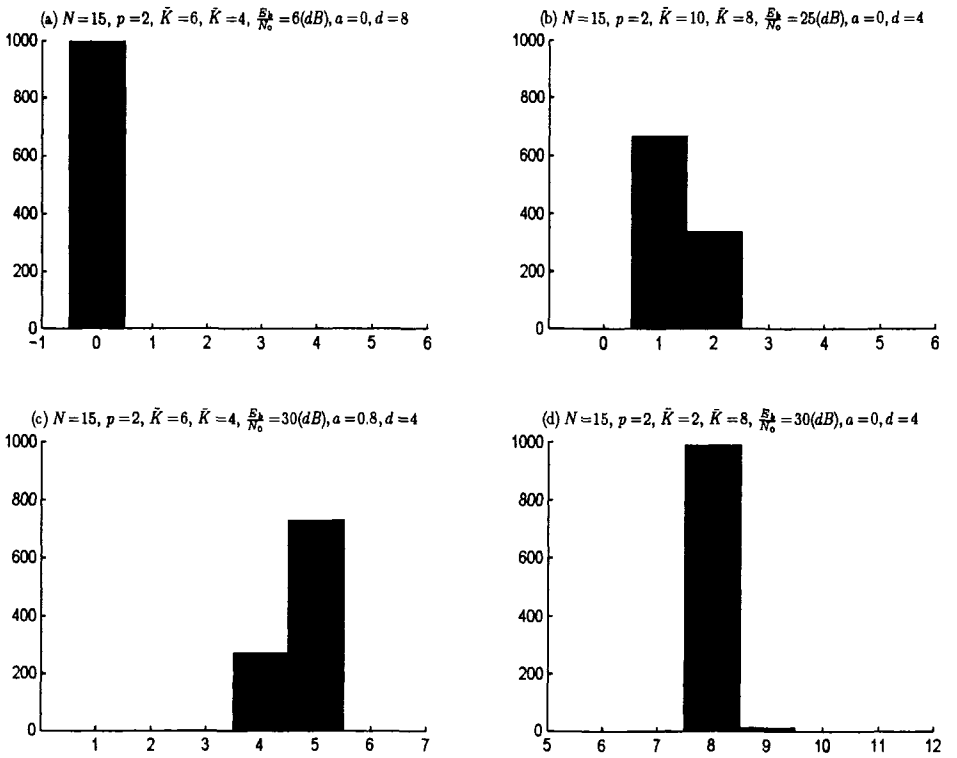

Figure 3.8: AERA rank estimation performance in systems with different parameters. Horizontal: estimated number of unknown users; vertical: number of frames

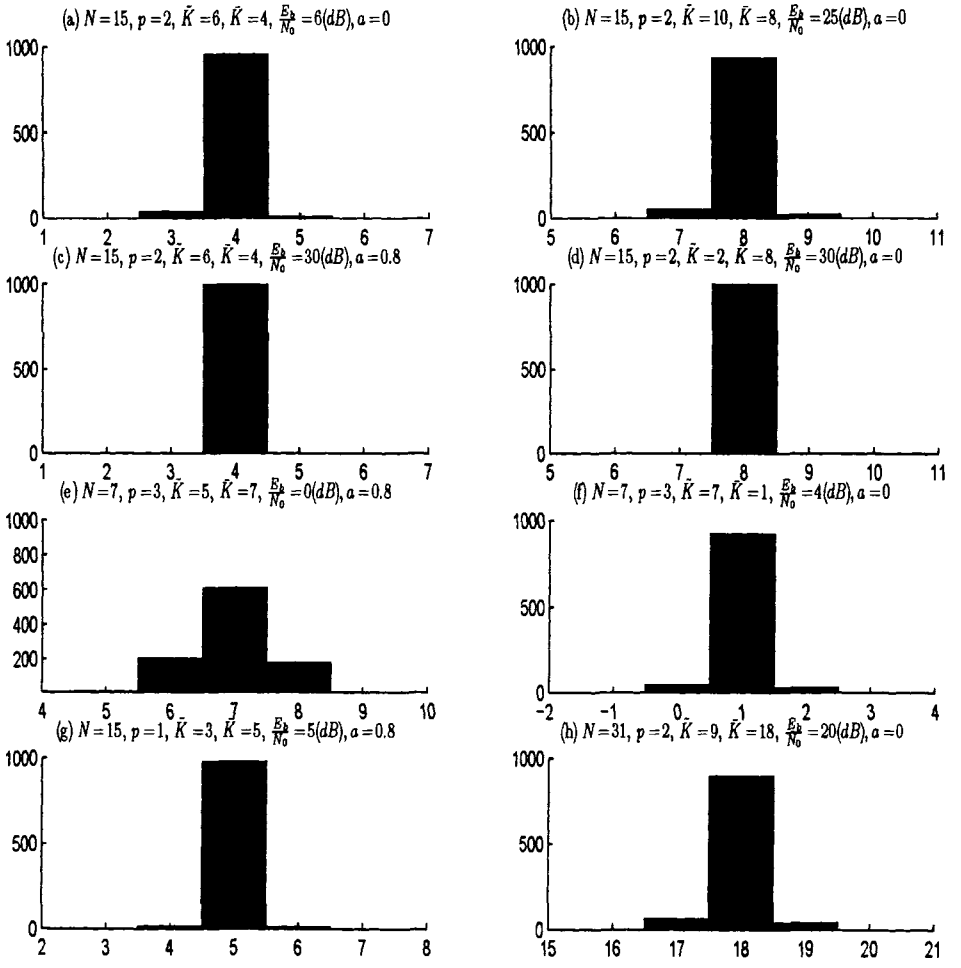

Figure 3.9: Proposed estimator performance in systems with different parameters. Horizontal: estimated number of unknown users; vertical: number of frames

where all 7 users are known to the receiver after 3 iterations. The system specifications are exactly the same as those given in Section 3.3. As seen, the performance of the strong users does not degrade from the weak interference, a phenomenon which was previously observed in the conventional turbo multiuser detector [65]. Intuitively this makes sense, since in the group-blind situation, we treat the unknown users from the prospect of complex Gaussian noise vector; therefore, we can expect the system to achieve better performance when the noise has lower power spectral density, compared to the equal power case. Therefore, it is evident that the proposed receiver has robust performance in near-far situations. Also, the performance degradation due to unknown users with weak power is not severe. Note that in the case of near-far situation, our proposed signal rank estimation method underestimates the number of weak unknown users by a factor proportional to the known users versus unknown users power ratio, but as it can be seen from the simulation results, this effect is in fact beneficial and the turbo multiuser detector performance integrated with the proposed signal rank estimation outperforms the performance of a system when the number of unknown users is available to the receiver. Such an effect has been reported in [77] as well.

3.7 Summary

By generalizing the turbo multiuser receiver proposed in [65] for the group blind case, we have proposed an iterative uplink receiver for multiuser block coded CDMA systems in multipath channels. The iterative receiver consists of a first stage that performs soft interference cancellation and combined group blind filtering based on MMSE criterion to suppress the MAI from known and unknown users, followed by a second stage of channel decoders. In order to reduce the effect of intercell interference we proposed a modified scheme that can be used to suppress the effect of MAI from unknown users in high intercell interference systems. The modified scheme performs the interference suppression and channel decoding in different stages. More specifically, after soft interference cancellation on the coded bits of known users, this soft information is sent to a combined group blind multiuser detector. The proposed group blind filter satisfies the MMSE criterion in a way that it suppresses

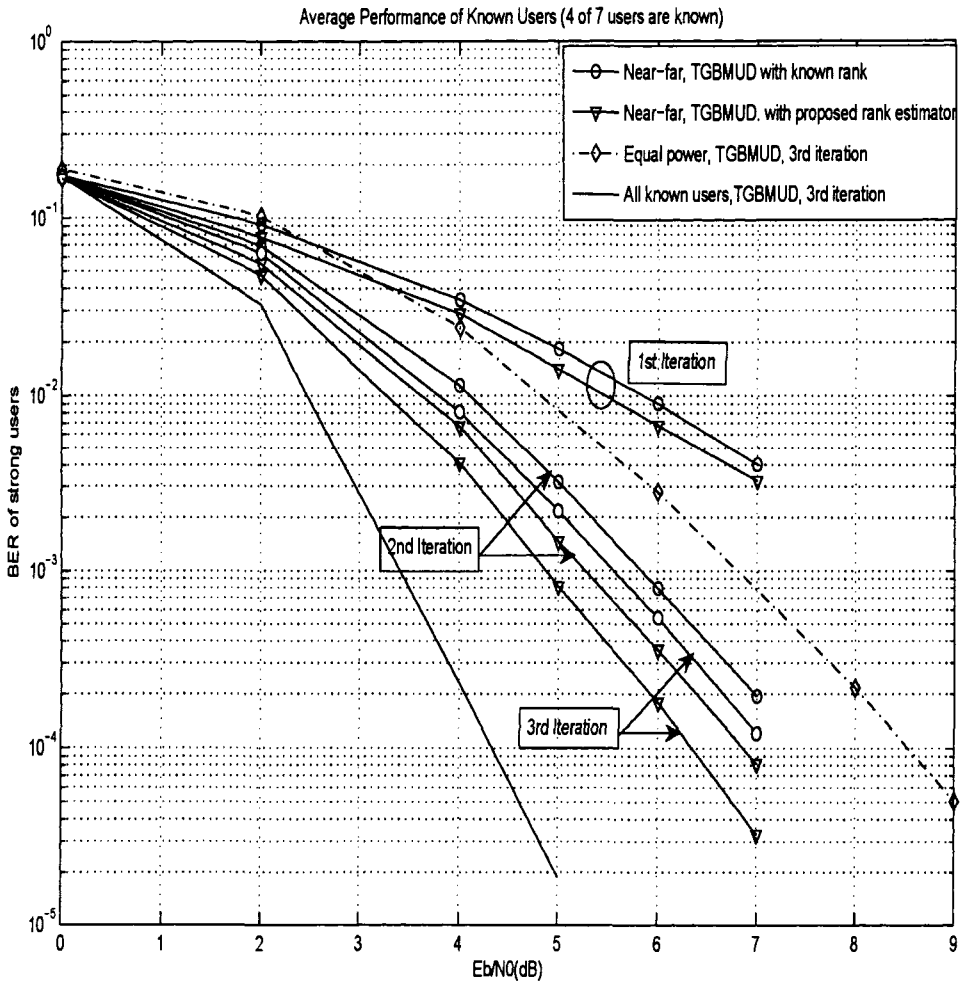

Figure 3.10: Average Bit error rate of unknown users under the proposed receiver structure, when the known users are $3dB$ stronger than the unknown users. Number of iterations= 3, $K = 7$, $\tilde{K} = 4$, and $\bar{K} = 3$

the remained MAI from known users based on the spreading sequences and the channel characteristics of these users, while suppressing the MAI from other unknown users, using subspace-based blind method. Simulation results show that the proposed method significantly outperforms systems that ignore the effect of interference from unknown users.

The knowledge of the number of unknown users is crucial for proposed receiver structure. For this reason we proposed an estimator structure by exploiting the statistical properties of the signal. Unlike other schemes in the literature, the proposed estimator is able to estimate the number of unknown users in low to moderate signal to noise ratio with highly correlated noise samples. Furthermore, if the number of known users plus the number of unknown users exceed the number of users that the system can accommodate, the estimator is able to accurately estimate the number of unknown users in such scenarios. By increasing the over sampling factor for later frames, we are able to eliminate the interference from these users effectively.

Chapter 4

Joint Iterative Multiuser Detection and Channel Estimation

In this chapter we propose an iterative receiver that performs channel estimation without using pilot symbols. We will estimate the channel in conjunction with symbol detection at each iteration. For the first iteration, we perform the blind channel estimation procedure to estimate the channel. Since the blind channel estimator has an arbitrary phase ambiguity, we employ differential encoding and decoding [88]. We exploit the result of recent research on the class of error correcting codes generated by the serial concatenation of a recursive systematic convolutional (RSC) encoder, an interleaver and a differential encoder [96]- [101] for each user. These codes are attractive because they combine the performance gain of error correcting coding with the robustness of noncoherent demodulation [101]. The receiver structure consists of a matched filter, a channel estimator, a soft interference cancellation unit, a minimum mean-square error filter, a soft output differential detector, distinct deinterleaver for each user, a bank of single-user RSC decoders, corresponding interleaver, and finally differential decoders. The single-user RSC decoder and differential decoder of each user can work in an iterative fashion to further improve the performance. At the end of inner iterations between single-user decoders, the soft estimate of coded symbols, as well

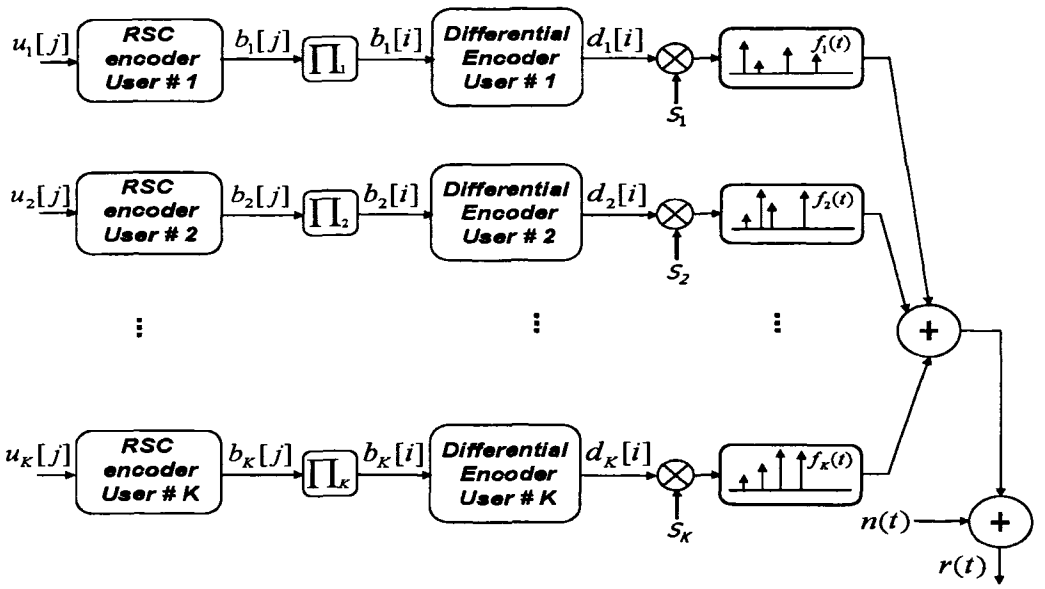

Figure 4.1: Block diagram of the transmitter structure

as the results at the output of the MMSE filter are combined to be sent to the channel estimator and soft interference cancellation unit. The channel estimator provides a new estimate of the channel based on this new information, and sends the channel information to the multiuser detector and the soft interference cancellation unit. The process of channel estimation, soft interference cancellation, detection, and iterative decoding is continued until a suitably chosen termination criterion (i.e. specific number of iterations), stops the iteration process.

The rest of this chapter is organized as follows. In section 4.1 we present our signal model and the system description. Next, in Section 4.2, we derive the receiver structure for asynchronous CDMA systems. In section 4.3, we demonstrate the performance results obtained via computer simulation. Finally summaries of this chapter are given in Section 4.4.

4.1 Signal Model and the System Description

We consider an asynchronous coded CDMA system of K users employing normalized modulation waveforms $\{\mathbf{s}_1, \mathbf{s}_2, ..., \mathbf{s}_k\}$ with binary differential phase shift keying (DPSK) modulation signaling through a multipath channel with additive white Gaussian noise. Fig.4.1 shows the structure of such a system. The binary phase shift keying (BPSK) information symbol sequence of $\{u_k[i]\}_{i=0}^{\infty}$ of user k for $k = 1, ..., K$ is first encoded by an RSC channel encoder. For simplicity we assume that all users employ the same encoder having constraint length ν and rate R_c, although this condition is not necessary, and generalization to accommodate different channel encoders for each user with known spreading sequence is easy. Let M' be the number of information symbols for each user, including the trellis terminating $\nu - 1$ tail bits. Thus the channel codeword of each user has length $M = M'/R_c$, and is denoted by $b_k[j]$ for $j = 0, 1, ..., M-1$. The channel encoder outputs are next interleaved by a random interleaver, and these interleaved symbols are passed through a differential encoder. Each user employ a different interleaver. If we denote the interleaver function of user k by $\prod_k$, then the interleaver output can be written as $\{b_k[i]\}_{i=0}^{M-1}$, where $i = \prod_k[j]$ for $j = 0, 1, ..., M-1$. The output of the differential encoder is given by

$$d_k[i] = -b_k[i]d_k[i-1]. \tag{4.1}$$

The differential encoder is assumed to start at the reference symbol $d_k[0] = 1$. The differential encoder outputs are next modulated by the user's spreading sequence, and transmitted through the channel. The spreading waveform of user k is assumed to be of the form

$$s_k(t) = \frac{1}{\sqrt{N}} \sum_{j'=0}^{N-1} s_k[j']\psi(t - j'Tc), \tag{4.2}$$

where N denotes the processing gain of the CDMA system, $\mathbf{s}_k = [s_k[0], ..., s_k[N-1]]^T$ denotes the kth user's spreading code, T_c denotes the chip period, $s_k[j'] \in \{(+1), (-1)\}$, and $\psi(t)$ is the normalized chip waveform (i.e. $\int_0^{T_c} \psi^2(t)dt = 1$).

The transmitted signal $x_k(t)$ in (4.5) is given by

$$x_k(t) = \sum_{i=0}^{M-1} d_k[i]s_k(t - iT), \tag{4.3}$$

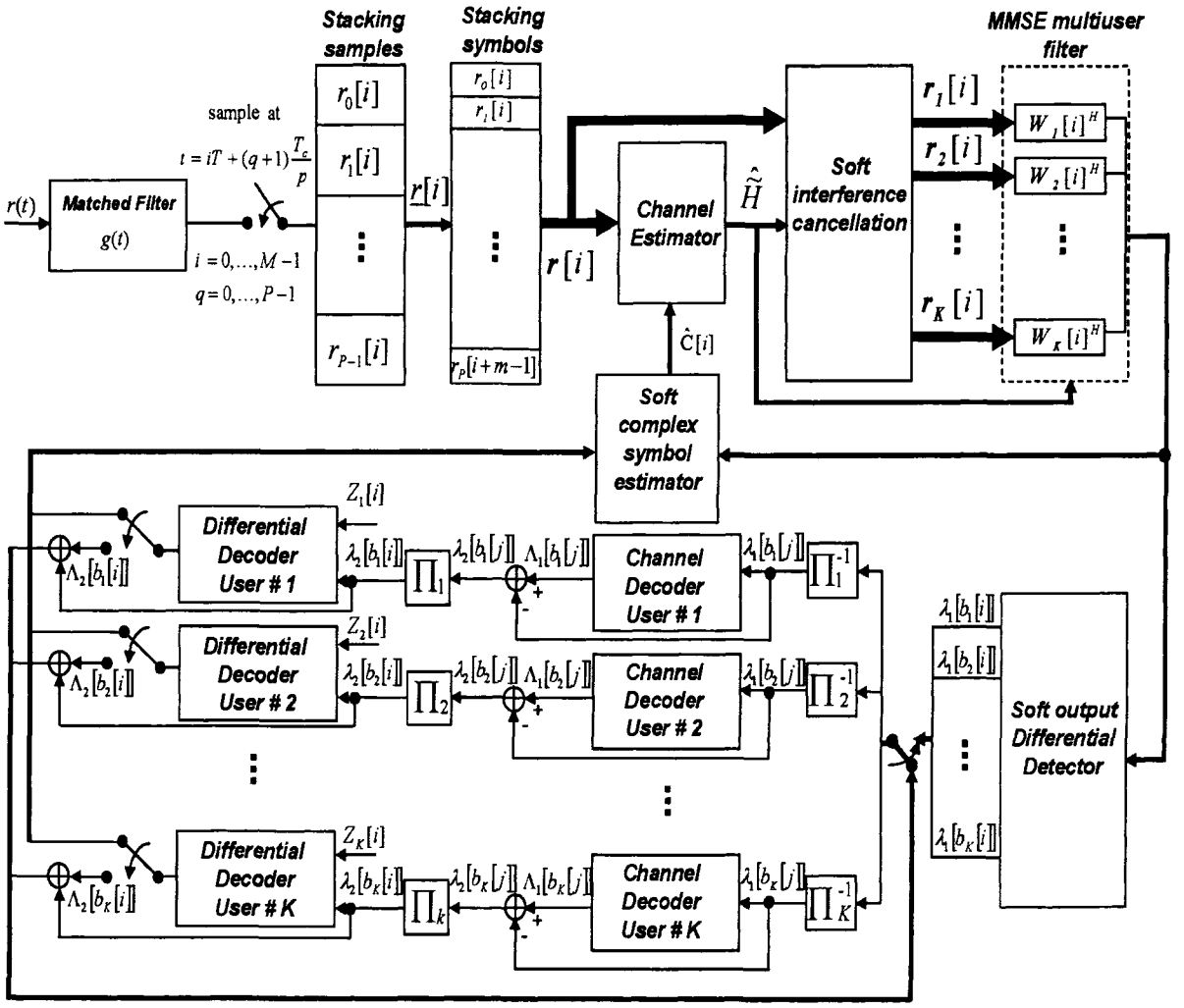

Figure 4.2: Block diagram of the receiver structure

where $d_k[i]$ denotes the transmitted symbol of user k during the transmission interval $[iT, (i+1)T]$. The channel impulse response can be written as

$$f_k(t) = \sum_{l=1}^{L} g_{l,k}\delta(t - \tau_{l,k}), \tag{4.4}$$

where L is the number of paths in multipath channel, $g_{l,k}$ denotes the corresponding complex path gain of the channel for user k, and $\tau_{l,k}$ is the delay of the lth path of the kth user's signal.

The continuous time received signal can be written as

$$r(t) = \sum_{k=1}^{K}[x_k(t) \star f_k(t)] + n(t), \tag{4.5}$$

where $\star$ denotes the convolution operation and $n(t)$ is complex white Gaussian noise process with zero mean and variance σ^2.

We have assumed that the number of paths in all channels between transmit antenna of each user and the base station is constant and is equal to L, that the maximum delay spread of each user channel is $\tau_{L,k}$, and $\tau_{l,k}$ for each user is uniformly distributed between zero and the maximum delay spread of the channel.

4.2 Receiver Structure and Algorithms

In this section, we incorporate the channel estimation procedure into the turbo multiuser detection algorithm. We modify the receiver structure in a way that it is able to estimate the channel without using pilot sequences. Fig.4.2 shows the receiver structure. The first stage of the iterative receiver performs channel estimation, and soft symbol detection for all users in the system. The second stage of the receiver consists of a bank of single-user RSC decoders serially concatenated with single-user differential decoders.

We consider a general multiple access signal model where the users are asynchronous, and the channel exhibits multipath distortion effects. From (4.5) and (4.4), the continuous signal received in this case is given by

$$r(t) = \sum_{k=1}^{K}\sum_{i=0}^{M} d_k[i] \sum_{l=1}^{L} g_{l,k}s_k(t - iT - \tau_{l,k}) + n(t). \tag{4.6}$$

At the receiver, the received signal $r(t)$ is filtered by a chip matched filter with the following impulse response:

$$g(t) \triangleq \begin{cases} \frac{1}{\sqrt{E_P}}\psi\left(\frac{T_c}{p} - t\right) & \text{if } 0 \le t \le \frac{T_c}{p}; \\ 0 & \text{otherwise.} \end{cases} \tag{4.7}$$

where $E_P \triangleq \int_0^{T_c/p} \psi^2(t)dt$. The output of the matched filter is then sampled at a multiple p of the chip rate. The over-sampling of the output of the matched filter can increase the number of users that the system can accommodate [104]. Let define $P \triangleq Np$ as the number of samples per symbol period, and $\iota \triangleq \max_{1\le k\le K}\{\lceil \frac{\tau_{L,k}+T_c}{T} \rceil\}$ be the maximum delay spread in terms of symbol interval. The qth signal sample during the ith symbol interval is given by

$$r_q[i] = \sum_{k=1}^{K}\sum_{n=0}^{\iota} d_k[i-n]\frac{1}{\sqrt{N}}\sum_{j'=0}^{N-1} s_k[j']\sum_{l=1}^{L} g_{l,k}$$
$$\times\frac{1}{\sqrt{E_P}}\int_0^{T_c/p} \psi(t)\psi(t - \tau_{l,k} + nT - j'Tc + q\frac{T_c}{p})dt + \sigma n_q[i], \tag{4.8}$$

where

$$n_q[i] = \frac{1}{\sqrt{\sigma^2 E_P}}\int_{iT+q\frac{T_c}{p}}^{iT+(q+1)\frac{T_c}{p}} n(t)\psi(t - iT - q\frac{T_c}{p})dt.$$

Denote

$$\underline{r}[i] \triangleq \begin{bmatrix} r_0[i] \\ \vdots \\ r_{P-1}[i] \end{bmatrix}, \quad \underline{d}[i] \triangleq \begin{bmatrix} d_1[i] \\ \vdots \\ d_K[i] \end{bmatrix}, \quad \underline{n}[i] \triangleq \begin{bmatrix} n_0[i] \\ \vdots \\ n_{P-1}[i] \end{bmatrix},$$

and

$$h_k[n] \triangleq \frac{1}{\sqrt{NE_P}}\sum_{j'=0}^{N-1} s_k[j']\sum_{l=1}^{L} g_{l,k}\int_0^{T_c/p} \psi(t)\psi(t - \tau_{l,k} + n\frac{T_c}{p} - j'T_c)dt. \tag{4.9}$$

Then matrix $\underline{H}(j)$ can be defined as follows:

$$\underline{H}[j] \triangleq \begin{bmatrix} h_1[jP] & \dots & h_K[jP] \\ \vdots & \vdots & \vdots \\ h_1[jP+P-1] & \dots & h_K[jP+P-1] \end{bmatrix}$$

$$j = 0, ..., \iota.$$

Using these quantities, (4.8) can be written in terms of vector convolution as

$$\underline{r}[i] = \underline{H}[i] \star \underline{d}[i] + \sigma \underline{n}[i] \tag{4.10}$$

where $\underline{H}[i] \star \underline{d}[i] \triangleq \sum_{j=0}^{\iota} \underline{H}[j]\underline{d}[i-j]$. By stacking m successive sample vectors, we define the following vectors:

$$\mathbf{r}[i] \triangleq \begin{bmatrix} \underline{r}[i] \\ \vdots \\ \underline{r}[i+m-1] \end{bmatrix}_{Pm\times 1}, \mathbf{n}[i] \triangleq \begin{bmatrix} \underline{n}[i] \\ \vdots \\ \underline{n}[i+m-1] \end{bmatrix}_{Pm\times 1}, \mathbf{d}[i] \triangleq \begin{bmatrix} \underline{d}[i-\iota] \\ \vdots \\ \underline{d}[i+m-1] \end{bmatrix}_{K(m+\iota)\times 1}.$$

Finally matrix $\mathbf{H}$ is defined as follow,

$$\mathbf{H} \triangleq \begin{bmatrix} \underline{H}[\iota] & \dots & \underline{H}[0] & \dots & \mathbf{0} \\ \vdots & \ddots & \ddots & \ddots & \vdots \\ \mathbf{0} & \dots & \underline{H}[\iota] & \dots & \underline{H}[0] \end{bmatrix}_{Pm\times K(m+\iota)} \tag{4.11}$$

where the smoothing factor m is chosen according to $m = \lceil \frac{P+K}{P-K} \rceil \iota$ [88]. Using these quantities, (4.10) can be written as follows:

$$\mathbf{r}[i] = \mathbf{H}\mathbf{d}[i] + \sigma \mathbf{n}[i], \tag{4.12}$$

where $\mathbf{n}[i]$ is a complex Gaussian noise vector of dimension Pm, $\mathbf{n}[i] \sim \mathcal{N}(\mathbf{0}, \mathbf{I}_{Pm})$. As mentioned earlier, the blind channel estimator always introduces an arbitrary phase ambiguity to the system. To incorporate this phase ambiguity in our model, (4.12) can be written as follows:

$$\mathbf{r}[i] = \tilde{\mathbf{H}}\mathbf{a}\mathbf{d}[i] + \sigma \mathbf{n}[i], \tag{4.13}$$

where

$$\mathbf{a} = \mathrm{diag}\big[[\underline{a}, ..., \underline{a}]_{1\times K(m+\iota)}\big],$$
$$\underline{a} = [a_1, ..., a_K],$$

and $a_k = \exp j\theta_k$ is the phase ambiguity compensator. The parameter θ_k of user k remains constant over one frame and changes independently for each frame. Using (4.13), it can be

assumed that the channel estimator, estimates the matrix $\tilde{\mathbf{H}}$, and the random vector $\mathbf{a}$ can be eliminated using differential detection. We define the following complex symbol vector:

$$\mathbf{c}[i] \triangleq \mathbf{a}\mathbf{d}[i] \tag{4.14}$$

with elements $c_k[i] \triangleq a_k d_k[i]$. Now, (4.13) can be rewritten in terms of complex symbol vector $\mathbf{c}[i]$ as

$$\mathbf{r}[i] = \tilde{\mathbf{H}}\mathbf{c}[i] + \sigma\mathbf{n}[i]. \tag{4.15}$$

At this point in order to explain the structure of the first stage of the receiver including channel estimator, soft interference cancellation unit, and soft output MMSE multiuser detector, it is assumed that the soft estimate of complex symbols $c_k[i]$ are known to the receiver.

4.2.1 Channel Estimation

For the first iteration we assume that soft estimates of complex symbols have uniform distribution. In the first iteration the channel is estimated by exploiting the orthogonality between the signal and noise subspaces. This is similar to what is proposed in [93]. Define

$$\begin{aligned} \alpha_k[m] &\triangleq \frac{1}{\sqrt{NE_P}} \sum_{l=1}^{L} g_{l,k} \int_0^{T_c/p} \psi(t)\psi(t - \tau_{l,k} + m\frac{T_c}{p})dt, \\ & m = 0, 1, ..., p\mu - 1, \end{aligned} \tag{4.16}$$

where μ is the maximum length of the channel response, defined as

$$\mu \triangleq \max_{1 \le k \le K} \lceil \frac{\tau_{L,k}}{T_c} \rceil \le \iota N. \tag{4.17}$$

From (4.9), we can write

$$\begin{aligned} h_k[n] &= \sum_{j'=0}^{N-1} s_k[j']\alpha_k[n - j'p], \\ & n = 0, 1, ..., (\mu + N - 2)p + p - 1. \end{aligned} \tag{4.18}$$

By decimating $\alpha_k[m]$ and $h_k[n]$ into p subsequences, we get

$$\begin{aligned} \alpha_{k,q}[m] &\triangleq \alpha_k[q+mp] \\ &\quad m=0,...,\mu-1; q=0,...,p-1. \\ h_{k,q}[n] &\triangleq h_k[q+np] = \sum_{j'=0}^{N-1} s_k[j']\alpha_k[q+(n-j')p]. \\ &\quad n=0,...,\mu+N-2; q=0,...,p-1. \end{aligned} \tag{4.19}$$

From (4.18), we can write

$$\{h_{k,q}[n]\}_{n=0}^{\mu+N-2} = \{s_k[j']\}_{j'=0}^{N-1} \star \{\alpha_{k,q}[m]\}_{m=0}^{\mu-1}. \tag{4.20}$$

Define

$$\underline{h}_{k,q} \triangleq \begin{bmatrix} h_{k,q}[0] \\ \vdots \\ h_{k,q}[\mu+N-2] \end{bmatrix}, \underline{\alpha}_{k,q} \triangleq \begin{bmatrix} \alpha_{k,q}[0] \\ \vdots \\ \alpha_{k,q}[\mu-1] \end{bmatrix}, \text{ and}$$

$$\Omega_k \triangleq \begin{bmatrix} s_k[0] & 0 & \dots & 0 \\ s_k[1] & s_k[0] & 0 & \vdots \\ \vdots & s_k[1] & \ddots & 0 \\ \vdots & \vdots & \ddots & s_k[0] \\ s_k[N-1] & \vdots & \ddots & s_k[1] \\ 0 & s_k[N-1] & \ddots & \vdots \\ \vdots & 0 & \ddots & \vdots \\ 0 & \dots & 0 & s_k[N-1] \end{bmatrix}_{(\mu+N-1)\times\mu},$$

Then (4.20) can be written as

$$\underline{h}_{k,q} = \Omega_k \underline{\alpha}_{k,q}. \tag{4.21}$$

Finally, defining:

$$\underline{h}_k \triangleq \begin{bmatrix} h_{k,0}[0] \\ \vdots \\ h_{k,p-1}[0] \\ \vdots \\ h_{k,0}[\mu+N-2] \\ \vdots \\ h_{k,p-1}[\mu+N-2] \end{bmatrix}, \qquad \underline{\alpha}_k \triangleq \begin{bmatrix} \alpha_{k,0}[0] \\ \vdots \\ \alpha_{k,p-1}[0] \\ \vdots \\ \alpha_{k,0}[\mu-1] \\ \vdots \\ \alpha_{k,p-1}[\mu-1] \end{bmatrix},$$

we can write

$$\underline{h}_k = \underline{\Omega}_k \underline{\alpha}_k, \tag{4.22}$$

where

$$\underline{\Omega}_k \triangleq \Omega_k \otimes \mathbf{I}_p,$$

and $\otimes$ denotes the Kronecker product and $\mathbf{I}_p$ is the $p \times p$ identity matrix. Using (4.12), the autocorrelation matrix for $\mathbf{r}[i]$ is given by

$$\mathbf{C}_r \triangleq E\{\mathbf{r}[i]\mathbf{r}[i]^H\} = \mathbf{H}\mathbf{H}^H + \sigma^2 \mathbf{I}_{Pm}. \tag{4.23}$$

By performing an eigen-decomposition of the matrix $\mathbf{C}_r$, we obtain

$$E\{\mathbf{r}[i]\mathbf{r}[i]^H\} = \begin{bmatrix} U_s & U_n \end{bmatrix} \begin{bmatrix} \Lambda_s & 0 \\ 0 & \Lambda_n \end{bmatrix} \begin{bmatrix} U_s^H \\ U_n^H \end{bmatrix}, \tag{4.24}$$

where $\Lambda_s \triangleq \text{diag}[\lambda_1, ..., \lambda_{K(m+\iota)}]$ contains the $K(m+\iota)$ largest eigenvalues of $\mathbf{C}_r$ in descending order; $\Lambda_n \triangleq \sigma^2 \mathbf{I}_{Pm-K(m+\iota)}$, with $\lambda_i > \sigma^2$ for $i = 1, ..., K(m+\iota)$. The column of U_n form an orthogonal basis to the column space of $\mathbf{H}$. Specifically $\tilde{\underline{h}}_k \triangleq \mathbf{H}\mathbf{e}_{K\iota+k}$ is in the column space of $\mathbf{H}$, where $\mathbf{e}_{K\iota+k}$ is an $K(m+\iota)$ vector of all zero except for the single unity element at the $K\iota + k$ position. In other words,

$$U_n^H \tilde{\underline{h}}_k = U_n^H \tilde{\underline{\Omega}}_k \underline{\alpha}_k = \mathbf{0}, \tag{4.25}$$

where

$$\tilde{\underline{h}}_k = \tilde{\underline{\Omega}}_k \underline{\alpha}_k, \tag{4.26}$$

and

$$\tilde{\underline{h}}_k = \begin{bmatrix} \underline{h}_k \\ \mathbf{0}_{((m-\iota-1)P+p)\times 1} \end{bmatrix}, \tag{4.27}$$

$$\tilde{\underline{\Omega}}_k = \begin{bmatrix} \underline{\Omega}_k \\ \mathbf{0}_{((m-\iota-1)P+p)\times p\mu} \end{bmatrix}. \tag{4.28}$$

From (4.25), an estimate for the channel response $\underline{\alpha}_k$ can be obtained by computing the eigenvector corresponding to the minimum eigenvalue of the matrix $\tilde{\underline{\Omega}}_k^H U_n U_n^H \tilde{\underline{\Omega}}_k$. Using (4.26), and the estimated channel response (i.e. $\hat{\underline{\alpha}}_k$), we can estimate the vector $\tilde{\underline{h}}_k$ for $k = 1, ..., K$. Finally, an estimate of the matrix $\tilde{\mathbf{H}}$ is formed with the same structure given in 4.11. The condition for the channel estimation obtained in this way to be unique is that the matrix $U_n^H \tilde{\underline{\Omega}}_k$ has rank $p\mu - 1$ which necessitates that $[Pm - K(m + \iota)] \geq p\mu$. Thus the total number of users that can be accommodated in this system is upper-bounded by $\min\left(\lceil P(m-\iota)/(m+\iota)\rceil, K_{\max}\right)$, where $\min(.,.)$ selects the smaller value of the two, and $K_{\max}$ is the total number of users that can be accommodated in a CDMA system and is a function of the total bandwidth, the coding rate, the processing gain, and the information bit signal to noise ratio [103].

For later iterations when the soft estimates of complex symbols $c_k[i]$ for $k = 1, ...K$ and $i = 0, ..., M-1$ are available to the channel estimator, the channel can be estimated differently.

Multiplying both sides of (4.15) by the complex symbol vector $\mathbf{c}[i]^H$ and taking the expected values of both sides, we get

$$\tilde{\mathbf{H}} = E\{\mathbf{r}[i]\mathbf{c}[i]^H\}. \tag{4.29}$$

Replacing $\mathbf{c}[i]$ in (4.29) with the soft estimated vector (i.e. $\hat{\mathbf{c}}[i]$), the matrix $\tilde{\mathbf{H}}$ can be estimated as follows:

$$\hat{\tilde{\mathbf{H}}} = \frac{1}{M} \sum_{i=0}^{M-1} \mathbf{r}[i]\hat{\mathbf{c}}[i]^H. \tag{4.30}$$

The estimation can be refined further by averaging different values in the estimated matrix $\hat{\tilde{\mathbf{H}}}$, that represents the same quantity, using the structure given in (4.11).

4.2.2 Soft Interference Cancellation

Consider that we would like to detect the kth user's complex symbol at time i. Now, (4.10) can be written as

$$\underline{r}[i] = \underline{\tilde{H}}^k[0]c_k[i] + \sum_{j=1}^{\iota} \underline{\tilde{H}}^k[j]c_k[i-j] + \sum_{n=1,n\neq k}^{K} \sum_{j=0}^{\iota} \underline{\tilde{H}}^n[j]c_n[i-j] + \sigma\underline{n}[i], \tag{4.31}$$

where $\underline{\tilde{H}}[m] \triangleq \underline{H}[m].(\text{diag}[\underline{a}])^{-1}$, and $\underline{\tilde{H}}^l[m]$ denotes the lth column of $\underline{\tilde{H}}[m]$. The first term in (4.31) contains the complex symbol of the desired user (i.e. user k) at time i; the second term contains the previous complex symbols of the desired user which results in intersymbol interference (ISI), and the third term contains the complex symbols of other users in the system which contributes to the multiple access interference.

The function of soft interference cancellation unit is to partially remove the ISI and the MAI from the received signal by utilizing the soft information on the complex symbols. The proposed soft interference cancellation unit is similar to what is proposed in [65]. The partially interference-canceled signal corresponding to the kth user's symbol is then obtained by subtracting out the soft-estimates of the intersymbol interference of the desired user as well as the multiple access interference of other users.

$$\mathbf{r}_k[i] = \mathbf{r}[i] - \tilde{\mathbf{H}}\hat{\mathbf{c}}_k[i] \tag{4.32}$$

where $\hat{\mathbf{c}}_k[i] = \hat{\mathbf{c}}[i] - \hat{c}_k[i]\mathbf{e}_{K\iota+k}$, $\mathbf{e}_{K\iota+k}$ is an $K(m+\iota)$ vector of all zero except for the single unity element at the $K\iota+k$ position. $\hat{c}_k[i]$ is the soft estimate of the kth user's complex symbol, and $\hat{\mathbf{c}}[i]$ is a vector of the soft estimate of all users' ith complex symbol.

4.2.3 Soft Output MMSE Filtering

In order to further suppress the ISI from previous symbols of intended user as well as the MAI from other users in the system, an instantaneous linear MMSE filter $\mathbf{w}_k[i]$ is applied to $\mathbf{r}_k[i]$, such that

$$z_k[i] = \mathbf{w}_k[i]^H\mathbf{r}_k[i]. \tag{4.33}$$

The purpose of employing an instantaneous MMSE filter is to suppress the remaining ISI and MAI based on the spreading sequences and channel characteristics of all users in the

system. The filter $\mathbf{w}_k[i] \in \mathcal{C}^{Pm}$ is chosen to minimize the mean square error between the complex symbol $c_k[i]$ and the filter output $z_k[i]$, i.e.,

$$\mathbf{w}_k[i] = \arg \min_{\mathbf{w} \in \mathcal{C}^{Pm}} E\{|c_k[i] - \mathbf{w}^H \mathbf{r}_k[i]|^2\} \tag{4.34}$$

Then, (4.34) can be simplified to

$$\begin{aligned} \mathbf{w}_k[i] &= \arg \min_{\mathbf{w} \in \mathcal{C}^{Pm}} \mathbf{w}^H E\{\mathbf{r}_k[i]\mathbf{r}_k[i]^H\}\mathbf{w} \\ &\quad -\mathbf{w}^H E\{c_k[i]\mathbf{r}_k[i]\} - E\{c_k[i]\mathbf{r}_k[i]\}^H \mathbf{w} \end{aligned} \tag{4.35}$$

where

$$E\{\mathbf{r}_k[i]\mathbf{r}_k[i]^H\} = \tilde{\mathbf{H}}\Delta_k[i]\tilde{\mathbf{H}}^H + \sigma^2 \mathbf{I}_{Pm} \tag{4.36}$$

$$E\{c_k[i]\mathbf{r}_k[i]\} = \tilde{\mathbf{H}}\mathbf{e}_{K\iota+k}, \tag{4.37}$$

and

$$\begin{aligned} \Delta_k[i] &\triangleq \mathrm{Cov}\{\mathbf{c}[i] - \hat{\mathbf{c}}_k[i]\} \\ &= \mathrm{diag}\big[\underline{\delta}_k[i-\iota], ..., \underline{\delta}_k[i], ..., \underline{\delta}_k[i+m-1]\big], \end{aligned} \tag{4.38}$$

where $\hat{\mathbf{c}}_k[i] \triangleq \hat{\mathbf{c}}[i] - \hat{c}_k[i]\mathbf{e}_{K\iota+k}$ and,

$$\begin{aligned} \underline{\delta}_k[i+l] &\triangleq \mathrm{diag}\big[1 - |\hat{c}_1[i+l]|^2, ..., 1 - |\hat{c}_K[i+l]|^2\big] \\ &\qquad l = -\iota, ..., m-1 \quad \text{and} \quad l \neq 0, \\ \delta_k[i] &\triangleq \mathrm{diag}\big[1 - |\hat{c}_1[i]|^2, ..., 1 - |\hat{c}_{k-1}[i]|^2, 1, \\ &\qquad 1 - |\hat{c}_{k+1}[i]|^2, ..., 1 - |\hat{c}_K[i]|^2\big]. \end{aligned}$$

The solution to (4.35) is given by

$$\mathbf{w}_k[i] = (\tilde{\mathbf{H}}\Delta_k[i]\tilde{\mathbf{H}}^H + \sigma^2 \mathbf{I}_{Pm})^{-1}\tilde{\mathbf{H}}\mathbf{e}_{K\iota+k}. \tag{4.39}$$

It should be noted that in (4.39) we require an estimate of the noise variance σ^2. A simple estimate of σ^2 is obtained by averaging on the eigenvalues of Λ_n given in (4.24).

In [74] it is shown that the residual interference plus the background receiver noise at the output of a linear MMSE multiuser detector can be well modeled as being Gaussian. It is reasonable to expect the same property to hold in this situation. Thus, we may model the combined MMSE filter output as

$$z_k[i] = \mu_k[i]c_k[i] + \eta_k[i], \tag{4.40}$$

where

$$\begin{aligned} \mu_k[i] &\triangleq E\{z_k[i]c_k[i]\} \\ &= \mathbf{w}_k[i]^H \tilde{\mathbf{H}}\mathbf{e}_{K\iota+k}, \end{aligned} \tag{4.41}$$

and

$$\begin{aligned} \upsilon_k^2[i] &\triangleq \mathrm{var}\{z_k[i]\} \\ &= \mu_k[i] - \mu_k^2[i]. \end{aligned} \tag{4.42}$$

In order to obtain the extrinsic information of the coded symbol $b_k[i]$ at the output of the filter, we need to perform differential detection. More specifically using (4.40) and (4.1) and defining $\tilde{z}_k[i] \triangleq -z_k[i]z_k^*[i-1]$ we can write,

$$\begin{aligned} \tilde{z}_k[i] &= \mu_k[i]\mu_k^*[i-1]b_k[i] - \mu_k[i]c_k[i]\eta_k^*[i-1] \\ &\quad -\mu_k^*[i-1]c_k^*[i-1]\eta_k[i] - \eta_k[i]\eta_k^*[i-1]. \end{aligned} \tag{4.43}$$

From (4.43), it can be seen that $\tilde{z}_k[i]$ is the sum of three different random variables. Substituting $c_k[i]$ with $\exp(j\theta)d_k[i]$, and $c_k^*[i-1]$ with $\exp(-j\theta)d_k[i-1]$, one may obtain the individual distribution of the random variables on the right hand side of equation (4.43). The second term on the right hand side of equation (4.43) is the product of two independent random variables namely $d_k[i]$ and $\eta_k^*[i-1]$. The random variable $X \triangleq d_k[i]$ has the following distribution:

$$f_X(x) = \xi\delta(x-1) + (1-\xi)\delta(x+1),$$

where we assumed $\Pr(d_k[i] = +1) = \xi$ and $\delta(.)$ is the Dirac's delta function. The product of the zero mean, complex Gaussian distribution $Y \triangleq \eta_k^*[i-1]$ with $d_k[i]$ has the following

distribution:

$$\begin{aligned} f_Z(z) &= \int_{-\infty}^{+\infty} \frac{1}{|w|} f_{X,Y}\left(w, \frac{z}{w}\right) dw \\ &= \int_{-\infty}^{+\infty} \frac{1}{|w|} f_X(w).f_Y\left(\frac{z}{w}\right) dw \\ &= \int_{-\infty}^{+\infty} \frac{1}{|w|} (\xi\delta(w-1) + (1-\xi)\delta(w+1)).f_Y\left(\frac{z}{w}\right) dw \\ &= \xi f_Y(z) + (1-\xi) f_Y(-z) = f_Y(z), \end{aligned} \tag{4.44}$$

where the last equality is obtained since the zero-mean Gaussian distribution has even symmetry. The distribution of the third term can be obtained by exploiting the same analysis. The fourth term is the product of two independent zero mean complex Gaussian distributions. It can be shown that the product of two independent zero mean Gaussian random variables with distinct variances σ_x^2 and σ_y^2 is given by $f_Z(z) = \frac{1}{\pi\sigma_x\sigma_y} K_0\left(\frac{z}{\sigma_x\sigma_y}\right)$, where K_0 is the modified Bessel function. Using the central limit theorem it is possible to approximate the sum of the above distributions with a Gaussian distribution having the same mean and variance, i.e., $\tilde{z}_k[i] \sim \mathcal{N}_c(\tilde{\mu}_k[i]b_k[i], \tilde{v}_k^2[i])$, where

$$\tilde{\mu}_k[i] \triangleq E\{\tilde{z}_k[i]b_k[i]\} = \mu_k[i]\mu_k[i-1], \tag{4.45}$$

and

$$\begin{aligned} \tilde{v}_k^2[i] &\triangleq \text{var}\{\tilde{z}_k[i]\} = E\{\tilde{z}_k^2[i]\} - (E\{\tilde{z}_k[i]\})^2 \\ &= \mu_k[i]\mu_k[i-1] - \mu_k^2[i]\mu_k^2[i-1]. \end{aligned} \tag{4.46}$$

Therefore, the log-likelihood ratio (LLR) of the extrinsic information $\lambda_1[b_k[i]]$ delivered by the differential soft instantaneous MMSE filter is given by

$$\begin{aligned} \lambda_1[b_k[i]] &= -\frac{|\tilde{z}_k[i] - \tilde{\mu}_k[i]|^2}{\tilde{v}_k^2[i]} + \frac{|\tilde{z}_k[i] + \tilde{\mu}_k[i]|^2}{\tilde{v}_k^2[i]} \\ &= \frac{4\Re\{\tilde{\mu}_k[i]\tilde{z}_k[i]\}}{\tilde{v}_k^2[i]} \\ &= \frac{4\Re\{\tilde{z}_k[i]\}}{1 - \mu_k[i]\mu_k[i-1]}. \end{aligned} \tag{4.47}$$

The set of soft outputs $\{\lambda_1[b_k[i]]\}$ for $k = 1, ..., K$ and $i = 0, ..., M-1$ are next deinterleaved and passed on to the bank of single-user channel decoders to serve as the *a priori* information.

The second stage of the receiver consists of a bank of K independent serially concatenated SISO single-user channel decoders and differential decoders. As shown in Fig. 4.2, the inputs to the kth SISO channel decoder are the *a priori* LLR's of the code bits of the kth user. For the first inner iteration this information is provided by SISO multiuser detector as given in (4.47); however, for later iterations between the two decoders, the information is provided to the channel decoder by the differential decoder. Next we briefly review the concept of channel decoding and differential decoding.

4.2.4 Channel Decoding

Given the binary input alphabet $\{-1, +1\}$, the encoder can be in one of the $2^{\nu-1}$ states corresponding to different contents of encoder memories. The trellis structure can be employed to compute the *a posteriori* LLRs [1],

$$\begin{aligned}
\Lambda_1[b_k[j]] &\triangleq \log \frac{P\left[b_k[j] = +1 | \{\lambda_1[b_k[n]]\}_{n=0}^{M-1}\right]}{P\left[b_k[j] = -1 | \{\lambda_1[b_k[n]]\}_{n=0}^{M-1}\right]} \\
&= \log \frac{P[\{\lambda_1[b_k[n]]\}_{n=0}^{M-1} | b_k[j] = +1]}{P[\{\lambda_1[b_k[n]]\}_{n=0}^{M-1} | b_k[j] = -1]} + \log \frac{P[b_k[j] = +1]}{P[b_k[j] = -1]} \\
&= \lambda_2[b_k[j]] + \lambda_1[b_k[j]] \\
k &= 1, ..., K \qquad j = 0, ..., M-1
\end{aligned} \tag{4.48}$$

where $\lambda_2[b_k[j]]$ and $\lambda_1[b_k[j]]$ refer to the extrinsic LLR and the *a priori* LLR of the coded bit $b_k[i]$, respectively. The extrinsic information is the information about the code bit $b_k[i]$ gleaned from the prior information about the other code bits based on the trellis structure of the code. The *a priori* LLR of $b_k[i]$ is computed by the multiuser detector or differential decoder of the kth user, deinterleaved and then fed back to the channel decoder.

Finally the extrinsic information at the output of the decoder is obtained by subtracting

Table 4.1: Simulated Multipath CDMA System

User No.	Signature	Multipath delay (T_c)			Multipath gain		
k	$\{s_k[j']\}$	$\tau_{1,k}$	$\tau_{2,k}$	$\tau_{3,k}$	$g_{1,k}$	$g_{2,k}$	$g_{3,k}$
1	1-1-1-1-1 1-1 1-1-1 1-1 1-1 1	0.4943	1.5442	6.3966	$-0.2910 + j0.5010$	$0.3610 - j0.5060$	$0.5280 - j0.0080$
2	-1 1-1 1-1-1-1-1 1-1 1-1-1 1 1	0.2097	7.8899	8.3667	$-0.5780 - j0.0570$	$-0.5230 - j0.5820$	$0.2070 + j0.0930$
3	-1-1 1-1 1-1 1 1-1 1-1-1 1-1-1	5.7937	8.3178	9.5788	$-0.1780 - j0.4690$	$0.3070 + j0.6290$	$0.3620 - j0.3580$
4	1 1 1-1-1 1 1-1-1-1-1-1-1 1-1	0.2535	2.0265	8.3214	$0.7120 + j0.5290$	$1.2900 + j0.2190$	$0.6690 - j0.9220$
5	1 1 1 1-1 1-1-1 1-1-1 1-1-1 1	0.5679	7.9975	8.4917	$-0.0400 + j0.5587$	$-0.3480 - j0.2987$	$0.1231 - j0.6788$
6	1-1 1 1 1-1-1 1 1 1-1-1-1 1-1	1.6180	2.8400	4.2480	$-0.2488 + j0.5732$	$0.3086 + j0.5183$	$0.4510 - j0.2054$
7	-1-1 1-1 1 1-1-1 1 1 1-1 1 1-1	1.3362	4.0040	5.9678	$0.5065 + j0.0667$	$-0.5114 + j0.6822$	$-0.0084 - j0.1094$
8	1 1-1 1 1-1 1-1 1-1-1 1-1 1-1	2.8625	3.6942	5.0833	$-0.6535 + j0.1480$	$0.4108 + j1.2638$	$0.9724 - j0.2241$

the *a priori* LLR from the *a posteriori* LLR in (4.48), that is

$$\lambda_2[b_k[j]] = \Lambda_1[b_k[j]] - \lambda_1[b_k[j]]. \tag{4.49}$$

4.2.5 SISO Differential decoder

The purpose of the differential decoder is to calculate the *a posteriori* LLRs of the coded symbols $b_k[i]$ entering the differential encoder. In [101] it is shown that the *a posteriori* probabilities (APPs) $P_r\{b_k[i] = b|\{z_k[m]\}_{m=0}^{N-1}\}$ where $b \in \{(+1),(-1)\}$, can be calculated by utilizing the original algorithm introduced in [1] for each user. The inputs to the kth differential decoder are $\{z_k[i]\}$ provided at the output of the multiuser MMSE filter as given in (4.40), and the *a priori* information on coded bits $\lambda_2[b_k[i]]$ that are formed by interleaving the extrinsic information provided by the corresponding single-user channel decoder. It should be noted that there are slight differences between our proposed differential encoder and the one proposed in [101]. In [101] the inputs to the noncoherent decoder are first modulo-M added to the previous coded symbol and then the outputs of the encoder are modulated using M-PSK modulation. Keeping the difference in mind it can be seen that for the same set of input data, the outputs of the proposed differential encoder are exactly the same of those proposed in [101] and thus the same decoding structure can be employed.

Using (4.40) and knowing that there is a one-to-one mapping between coded symbols $\{b_k[i]\}_{i=0}^{M-1}$ and transmitted symbols $\{d_k[i]\}_{i=0}^{M-1}$, the probability density function (pdf) of

$z_k[i]$ conditioned on coded symbols and the phase error compensator is given by

$$p\left(z_k[i]|\{b_k[i]\}_{i=0}^{M-1},\theta_k\right) = \frac{1}{v_k[i]\sqrt{2\pi}} \times \exp\{-\frac{1}{2v_k^2[i]}|z_k[i] - d_k[i]\exp(j\theta_k)|^2\}, \tag{4.50}$$

because the noise samples at the output of the MMSE filter are independent we may write,

$$p\left(\{z_k[i]\}_{i=0}^{n}|\{b_k[i]\}_{i=0}^{M-1},\theta_k\right) = \left(\frac{1}{v_k[i]\sqrt{2\pi}}\right)^{n+1} \times \exp\{-\frac{1}{2v_k^2[i]}\sum_{i=0}^{n}|z_k[i] - d_k[i]\exp(j\theta_k)|^2\}. \tag{4.51}$$

Since θ_k has uniform distribution over $[0, 2\pi)$, the dependence of equation (4.51) on θ_k can be removed by integrating over the pdf of θ_k. Using Bayes' formula and limiting the number of previous samples used by the estimator to the window size W, an approximation for conditional pdf $p\left(z_k[n]|\{b_k[m]\}_{m=0}^{M-1},\{z_k[i]\}_{i=0}^{n-1}\right)$ can be obtained as follows:

$$\begin{aligned} & p\left(z_k[n]|\{b_k[m]\}_{m=0}^{M-1},\{z_k[i]\}_{i=0}^{n-1}\right) \approx \\ & p\left(z_k[n]|\{b_k[n-m]\}_{m=0}^{W-1},\{z_k[n-i]\}_{i=1}^{W}\right) \\ = \; & F_k[n]\frac{I_0\left(\frac{1}{v_k^2[n]}|z_k[n] + \zeta_k[n]\exp\{j\pi\check{b}_k[n]\}|\right)}{I_0\left(\frac{1}{v_k^2[n]}|\zeta_k[n]|\right)}, \end{aligned} \tag{4.52}$$

with

$$\zeta_k[n] = \sum_{\rho=1}^{W} z_k[n-\rho]\exp\{j\pi\sum_{i=1}^{\rho-1}\check{b}_k[n-i]\}, \tag{4.53}$$

where $\check{b}_k[i] \triangleq (b_k[i]+1)/2$, $F_k[n]$ is a quantity that does not depend on $\{\check{b}_k[n-m]\}_{m=0}^{W-1}$, and $I_0(.)$ is the modified Bessel function of order zero. Using the window size of W, different values of the estimate arise only from 2^{W-1} possible values of $\{\check{b}_k[n-m]\}_{m=0}^{W-1}$. As such trellis-based decoding structure can be constructed. It should be noted that this trellis structure is purely artificial and it is not to be confused with the trellis structure associated with the differential encoder. Defining the state at time n as $s_n = \{\check{b}_k[n-m]\}_{m=0}^{W-1}$, the state space $\mathcal{S}$ is the set of 2^{W-1} binary sequences of length $W-1$. From each of the 2^{W-1} states, there are two branches corresponding to the two different values of $\check{b}_k[n]$, for

a total of 2^W branches in a trellis section. The trellis structure is defined by the state transition matrix $ST_W\left[\{\check{b}_k[n-m]\}_{m=1}^{W-2}, \check{b}_k[n]\right] = \{\check{b}_k[n-m]\}_{m=0}^{W-2}$ and the "code symbol" generation matrix $SG_W\left[\{\check{b}_k[n-m]\}_{m=1}^{W-1}, \check{b}_k[n]\right] = \{\check{b}_k[n-m]\}_{m=0}^{W-1}$. Associated with the branch corresponding to the specific sequence of code symbols, $\{\check{b}_k[n-m]\}_{m=0}^{W-1}$, is the branch metric defined in (4.52).

With this trellis structure and the *a priori* log-likelihood ratios, $\{\lambda_2[b_k[i]]\}$, the standard APP algorithm can be used to calculate the *a posteriori* LLRs, $\{\Lambda_2[b_k[i]]\}$ at the output of the differential decoder. The extrinsic LLRs $\lambda_1[b_k[i]]$ at the output of the differential decoder are formed by subtracting the *a priori* LLRs $\{\lambda_2[b_k[i]]\}$ from the corresponding *aposteriori* LLRs $\{\Lambda_2[b_k[i]]\}$ as shown in Fig.4.2. The extrinsic LLRs are then deinterleaved and sent back to the channel decoder to serve as the *a priori* LLRs $\{\lambda_1[b_k[j]]\}$ for the next inner iteration between the channel decoder and the differential decoder. The inner iterative process between channel decoder and differential decoder proceeds until the condition of a certain number of inner iterations is fulfilled. At this point if the constraint on the number of external iteration is also satisfied, the *a posteriori* LLRs at the output of differential decoder are sent to a decision device after appropriate deinterleaving, and the process is terminated. Otherwise the soft estimate of complex symbols $c_k[i]$ for $k = 1, ..., K$ and $i = 0, ..., M-1$ is formed and is sent to the channel estimator and soft interference cancellation unit for the next iteration.

Using the *a posteriori* log-likelihood ratios $\{\Lambda_2[b_k[i]]\}$, the soft estimate of transmitted symbols is given by [65]

$$\hat{b}_k[i] = E\{b_k[i]\} = \tanh\left(\frac{1}{2}\Lambda_2[b_k[i]]\right), \tag{4.54}$$

for $k = 1, ..., K$ and $i = 0, ..., M-1$. The soft estimate of complex symbols $\{c_k[i]\}$ is then formed using the method introduced in [102],

$$\hat{c}_k[i] = \frac{1}{2}\left(z_k[i] + \hat{b}_k[i]z_k[i-1]\right) \tag{4.55}$$

for $k = 1, ..., K$ and $i = 0, ..., M-1$. It should be noted that the norm of the soft estimate of the complex symbol $c_k[i]$ should always be equal or less than one. Thus we may normalize the result obtained in (4.55) if $|\hat{c}_k[i]| > 1$.

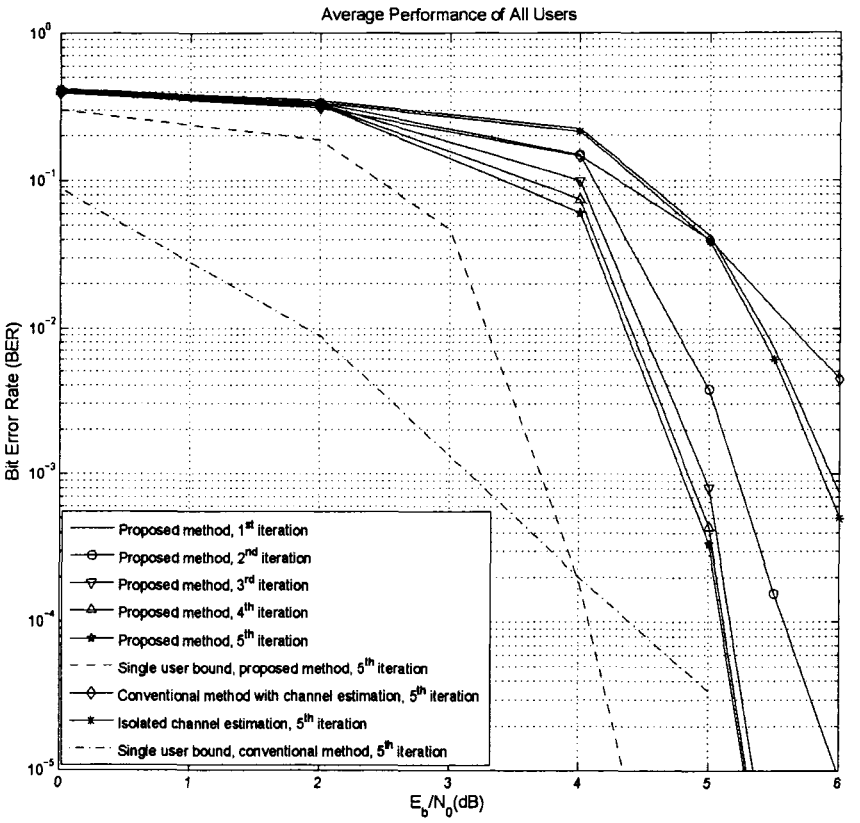

Figure 4.3: Average performance of all users for the proposed receiver structure in four-user multipath channel, number of internal iterations= 3, number of external iterations= 5, block length of $M' = 512$

4.3 Simulation Results

We present bit error rate (BER) performance results by simulating data transmission using the receiver introduced in Section III.

We consider an asynchronous CDMA system with four or eight users ($K = 4$ or $K = 8$). The user spreading sequences are sequences of length 15 and the same set of spreading sequences is used for all simulations. The multipath channel model is given by (4.4). The number of paths between each user and the base station is $L_k = 3$, and the delay of each path $\tau_{l,k}$ is uniformly distributed on $[0, 10T_c]$. In Table 4.1 we list the signature sequence $\{s_k[j']\}$, path delay $\{\tau_{l,k}\}$ and complex path gain $\{g_{l,k}\}$ for each user k. The multipath delays are in terms of number of chip intervals (T_c). The complex path gains for each user are normalized such that the composite signature of each user (i.e user k) satisfies $||\mathbf{He}_{\tilde{K}\iota+k}|| = 1$. All users employ the same rate 1/2 constraint length 5 recursive systematic convolutional encoder with generator matrix $g = [23, 35]$ in octal notation, where the first element in the matrix is the feedback part. The size of the window for differential decoder is $W = 3$. Each user uses a different interleaver generated randomly. The block size of information bits for all users is either 512 or 256 bits as noted on the figures. In the simulation, all users have equal power, chip pulse waveform is a raised cosine with roll-off factor of 0.5, and the over-sampling rate p at the output of the matched filter is set to be one except for the case of eight users ($K = 8$) where the over-sampling factor is increased to two in order to be able to accommodate all users in the system. In each figure, we have included the performance of the proposed method for the first five iterations; furthermore, in order to demonstrate the performance gain achieved by our proposed iterative channel estimation method, we have also included the performance of a similar structure which performs one time blind channel estimation and then performs five external iterations between the multiuser detector and single-user channel decoders. We refer to this method in our simulation as the isolated channel estimation method. Also the performance of the system after five iterations is shown for the case when the single-users' differential decoders are eliminated. This structure is similar to the conventional turbo multiuser detector proposed in [65], with additional blocks consist of the proposed channel estimation and the SISO differential detection; we refer to

it as the conventional method. Finally, for systems with four users, the figures also show the single-user bounds for our proposed method and the conventional method after five iterations. The single-user bounds refer to the performance of our proposed method as well as the conventional method when the channel is known to the receiver and only one user is present in the system (i.e. no multiple access interference). These are the lower bounds for our proposed algorithm and the conventional algorithm.

Fig.4.3 illustrates the average bit error rate performance of the system after five iterations for a block length of 512 bits. In each iteration, after passing the information from the first stage to the second stage of the receiver, three inner iterations are performed between the RSC decoders and the differential decoders. It is observed that very close performance to the single-user bound is achieved. When comparing the performance of the proposed system and that of the conventional system to their respective single-user bound, one could observe that our proposed method is less susceptible to the effects of the channel estimation error and the multiple access interference. Slight degradation in performance is observed as the block length is decreased from 512 to 256 bits as shown in Fig.4.4. This is in part due to the finite length of the signal frame, from which the channel is estimated. Fig.4.5 shows the performance of the proposed method when eight users are present in the system. We have performed one internal iteration and five external iterations. Also in Fig.4.5 we have provided the performance of the proposed receiver when the channel is perfectly known to the receiver. it can be seen that even with one internal iteration the performance of the proposed method outperforms that of the conventional method. The effectiveness of the proposed iterative channel estimation scheme may become more clear by comparing the performance of our proposed method with that of the isolated channel estimation scheme. It can be seen that the isolated channel estimation scheme is unable to improve its performance after five iterations while our proposed scheme exhibits great improvement in performance after the same number of iterations. Further improvement is made to our method by the serial concatenation of the RSC channel decoders and the differential decoders. This is clear as we compare the performance of our proposed method with that of the conventional turbo multiuser detector which does not employ the differential decoders.

4.4 Summary

We have proposed an iterative uplink receiver for multiuser differentially coded CDMA systems in multipath channels.

The iterative receiver consists of a first stage of channel estimation, soft interference cancellation and SISO multiuser filtering based on the MMSE criterion, followed by the second stage that consists of a bank of serially concatenated single-user channel decoders and differential decoders.

The proposed receiver is able to estimate the channel and to improve the estimation via iteration. For the first iteration the channel is estimated using a subspace blind method, while for later iterations the channel is estimated using the soft estimate of complex symbols provided by combining the output of the differential decoders and the MMSE multiuser filter.

The power of the proposed receiver resides in two parts. First, due to different users' spreading codes, it is able to estimate the channel without using the pilot sequences, thus increasing the bandwidth efficiency. Furthermore by improving the accuracy of the estimation in each iteration, the performance degradation due to imperfect channel estimation is minimal. Second, the performance is further improved by exploiting the serial concatenation of an RSC channel decoder with a differential decoder. It should be noted that the differential encoder has a coding rate of one, thus it does not introduce any redundancy and yet significantly improves the BER performance. Simulation results demonstrate that the proposed receiver offers performance approaching that of the single-user bound at high SNR.

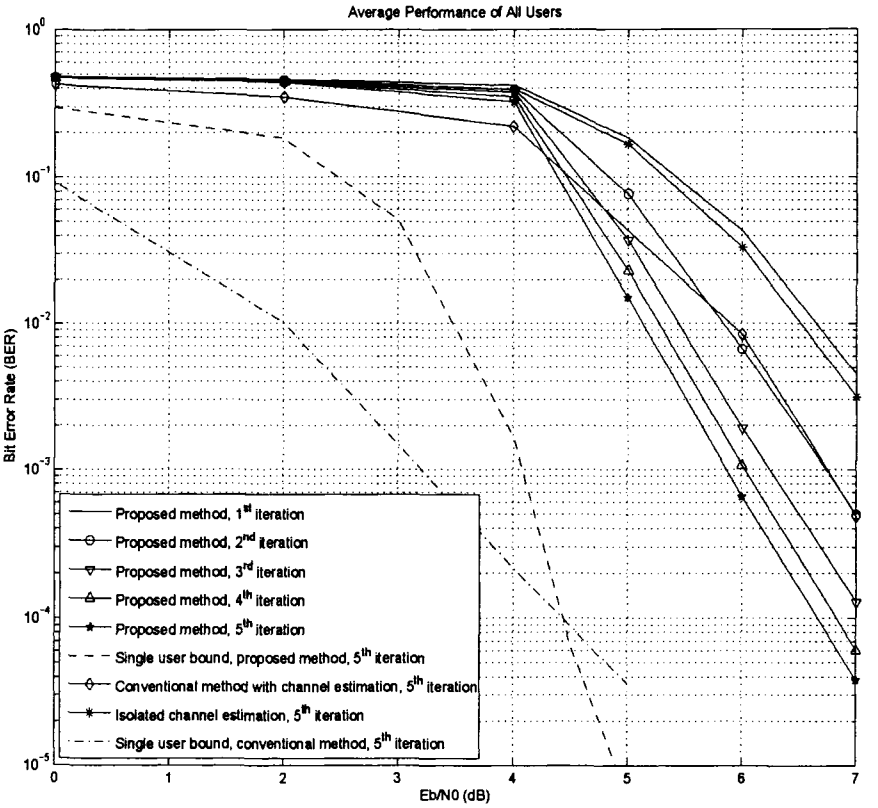

Figure 4.4: Average performance of all users for the proposed receiver structure in four-user multipath channel, number of internal iterations= 3, number of external iterations= 5, block length of $M' = 256$

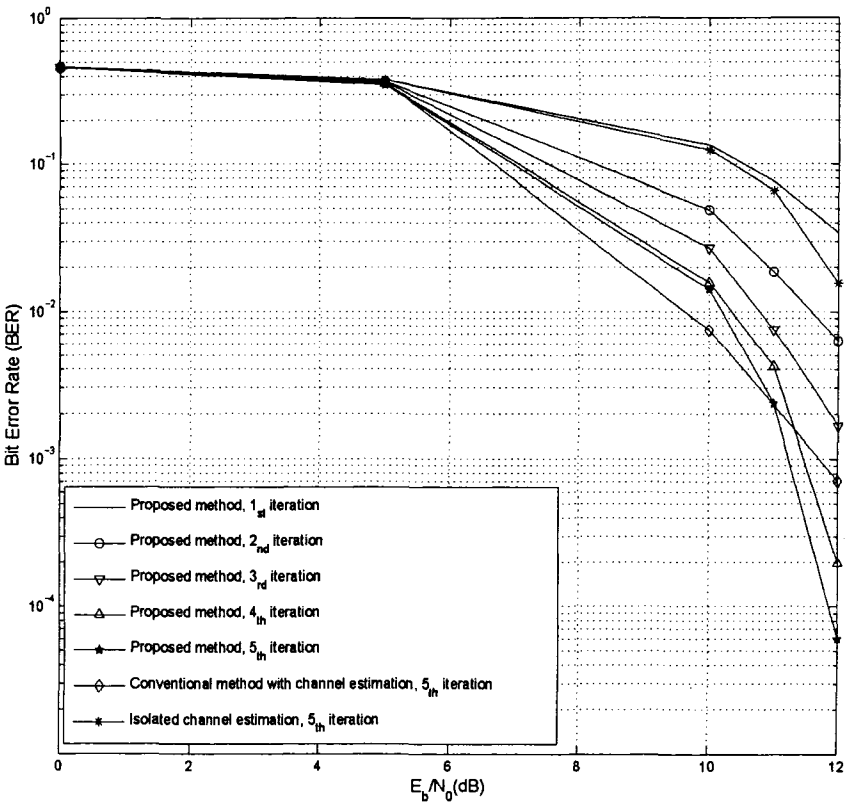

Figure 4.5: Average performance of all users for the proposed receiver structure in eight-user multipath channel, number of internal iterations= 1, number of external iterations= 5, block length of $M' = 512$

Chapter 5

Concluding Remarks

5.1 Summary of Contributions

The main concern of this work has been to address some practical issues in wireless communication systems and to propose efficient receiver structures to combat different impairments that communication systems can face in practice. We have addressed some of these issues both in single-user and in multiuser environments; however, the focus has been on the multiuser scenario.

In Chapter 2, we propose a receiver structure which is able to estimate the SNR without using pilot symbols. Our proposed estimator is able to estimate the SNR and improve the estimation via iteration. In the first iteration an eigen-decomposition is performed on the received signal. By separating the signal subspace from the noise subspace and choosing the largest eigen-value of the noise subspace, an estimate for the variance of the noise is obtained. For the first iteration we exploit the estimated variance in the Log-MAP equalization and decoding algorithm. For later iterations, if the quality of the extrinsic information at the output of the decoder improves, this information is utilized as an alternative to the original subspace method to mitigate any mismatch between the actual SNR and the estimated SNR at the receiver. A hypothesis testing criterion is introduced to decide whether or

not this transition is beneficial in terms of the receiver performance. Simulation results demonstrate identical performance with optimal algorithm even for very short block lengths. Furthermore, the estimator performance in terms of the normalized bias is investigated and it is shown that our proposed method is unbiased. This is in contrast with the method proposed in [55] where it demonstrates an error floor in terms of the estimator bias by increasing the SNR. We have also included the normalized root mean-square error (RMSE) of the proposed estimator and it is shown that the RMSE of the estimator is decreased as the iteration proceeds.

Multiuser detection in the presence of unknown interference is considered in Chapter 3. We first consider the scheme proposed in [73] and we mathematically show that the detection algorithm does not provide robust performance in CDMA uplinks since the algorithm fails to converge when the extrinsic information at the input of the multiuser detector is large enough. We then propose a robust group blind multiuser detection scheme that combines the concept of group-blind detection and turbo multiuser detection for asynchronous CDMA systems. Specifically, it consists of two stages similar to those of [65] for recursive systematic convolutionally encoded CDMA systems. The first stage consists of soft interference cancellation and combined group blind MMSE filtering, whereas the second stage consists of channel decoding. The combined group blind MMSE filtering tries to suppress the interference from known users based on the signature waveforms and the channel characteristic of these users and to suppress the interference from other unknown users using subspace-based blind methods. Simulation results show that this method preserves its advantage in performance over the conventional turbo multiuser detection method even in the case of high intercell interference. It is also shown that because of the exploitation of the subspace method we can easily estimate the variance of the noise at the receiver; therefore, the knowledge of SNR is not necessary at the receiver. Furthermore, based on the statistic properties of the signal and the channel, we propose an estimation algorithm to estimate the number of unknown users which is much faster, less complex and is able to provide the number of unknown users in white and nonwhite noise environments with high probability. Simulation results show that the proposed estimator is not sensitive to parameters such as

SNR, over sampling factor, or processing gain.

In Chapter 4, we have proposed an iterative receiver that performs channel estimation without using pilot symbols. We will do the channel estimation in conjunction with symbol detection at each iteration. For the first iteration, we perform the blind channel estimation procedure to estimate the channel. Since the blind channel estimator has an arbitrary phase ambiguity, we employ differential encoding and decoding [88]. We exploit the result of recent research on the class of error correcting codes generated by the serial concatenation of a recursive systematic convolutional (RSC) encoder, an interleaver and a differential encoder [96]- [101] for each user. These codes are attractive because they combine the performance gain of error correcting coding with the robustness of noncoherent demodulation [101].

In Appendix A, we have proposed a method to modify the Max-Log-MAP algorithm. In terms of performance, the proposed algorithm has a very close performance to the Log-MAP algorithm, even in high loss ISI channels where there is a wide gap between the performance of the Max-Log-MAP algorithm compared to that of the Log-MAP algorithm. In terms of implementation, the proposed algorithm is simply implementable using adders and comparators. This is in contrast with the Log-MAP algorithm implementation in which direct implementation is almost impossible, and using table lookup increases the area and power while decreasing the overall speed.

5.2 Impact and Conclusions

We first proposed an improved Max-Log-MAP algorithm for turbo decoding and turbo equalization. The proposed algorithm utilizes the MacLaurin Series to expand the logarithmic term in the Jacobian logarithmic function of the Log-MAP algorithm. This approach is quite promising in terms of performance compared to the optimal Log-MAP algorithm while its complexity is comparable with the suboptimal Max-Log-MAP algorithm. Simulation results demonstrate that the proposed algorithm has a performance very close to the Log-MAP algorithm for turbo equalization over frequency selective channels. Furthermore, it is shown than even in a high loss inter-symbol interference (ISI) channel, the proposed algorithm preserves its performance close to that of the Log-Map algorithm while there is

a wide gap between the performance of the Log-MAP and Max Log-MAP turbo equalizers.

The only drawback to the proposed algorithm is its sensitivity to signal to noise ratio. While the Max-Log-MAP algorithm, as shown in our work, is insensitive to any mismatch between the actual SNR and the estimated SNR at the receiver, the Log-MAP algorithm as well as the proposed algorithm shows substantial sensitivity to the mismatch which inevitably degrades the performance of the system.Therfore, the SNR estimation is crucial in equalization and decoding based on the maximum *a posteriori* algorithm. Any mismatch between the estimated SNR and the actual SNR may substantially degrade the performance of the system. In practice, different approaches based on known pilot symbols or unknown data symbols are proposed to estimate the SNR. The hard or soft decision of the output of the decoder is then utilized to obtain a long sequence of virtual pilot symbols to estimate the SNR. Due to the fact that the output of the decoder is not error free, a correction of the estimated SNR may be required. All the existing methods in the literature are based on an exhaustive search. Unfortunately, the amount of bias depends on the coding rate, the frame length, the employed modulation scheme and the constraint length of the code. This is not a practical approach for new technologies such as CDMA high speed downlink packet access (HSDPA) where any of the above parameters might change depending on the various parameters of the channel or the user requirements. The significance of our proposed method lies in the fact that we were able to derive an analytical closed form solution that can replace the exhaustive search method. The simulation results confirm our expectation, and the amount of bias asymptotically becomes zero as the iteration proceeds. The proposed receiver is able to estimate the signal-to-noise ratio (SNR) and to improve the estimation via iteration. Initially a subspace-based method is exploited to estimate the SNR. During the iterative process of equalization and decoding if the quality of the *a posteriori* information at the output of the decoder improves, it is possible to utilize this information as an alternative to the original subspace method to mitigate any mismatch between the actual SNR and the estimated SNR at the receiver. A hypothesis testing criterion is introduced to decide whether or not this transition is beneficial in terms of the receiver performance. Simulation results demonstrate that the proposed receiver structure

is able to yield a performance similar to that of the known SNR at the receiver.

We have then considered multiuser scenarios. Specifically, the direct-sequence code-division multiple-access (DS-CDMA) is taken into consideration. A turbo receiver structure is proposed for the uplink of coded CDMA systems in the presence of unknown interference. The proposed receiver consists of a first stage that performs soft interference cancellation and group-blind linear minimum mean-square-error (MMSE) filtering, followed by a second stage that performs channel decoding. The proposed group-blind linear MMSE filter suppresses the residual multiple-access interference (MAI) from known users based on the spreading sequences and the channel characteristics of these users, while suppressing the interference from other unknown users using a subspace-based blind method. The proposed receiver is suitable for suppressing inter-cell interference in heavily loaded CDMA systems. A novel estimator is also proposed to estimate the number of unknown users in the system by exploiting the statistical properties of the received signal, since the knowledge of the number of unknown users is crucial for the proposed receiver structure. Simulation results demonstrate that the proposed estimator can provide the number of unknown users precisely, and also the proposed group-blind receiver integrated with the new estimator can significantly outperform the conventional turbo multiuser detector in the presence of inter-cell interference. Furthermore, we proposed a receiver structure that performs joint iterative multiuser detection and channel estimation for the uplink of differentially coded asynchronous CDMA systems in unknown multipath channels without using pilot symbols. This approach considerably increases the bandwidth efficiency and hence the throughput of the system without sacrificing the performance. This is an interesting result because before this work it has been always assumed that blind channel estimators cannot be employed in coded CDMA systems due to their poor performance in low signal to noise ratio (SNR). In this work we demonstrated that if the process of channel estimation is integrated to the iterative process of multiuser detection and channel decoding, the system performance could be substantially improved. Additionally, we introduced a powerful concatenation of recursive systematic convolutional encoder and differential encoder for each user at the transmitter side, and a turbo style decoding at the receiver side. The combination of these two inno-

vative approaches resulted in a receiver performance in terms of bit error rate (BER) that approaches that of the single-user bound at high SNR. Specifically, the proposed receiver consists of two stages. The first stage performs channel estimation, soft interference cancellation and soft-in-soft-out (SISO) multiuser filtering, and the second stage consists of a bank of serially concatenated single-user channel decoders and differential decoders. The single user iterative decoder for each user consists of a powerful combination of a recursive systematic convolutional (RSC) decoder with a differential decoder, working together in an iterative fashion.

In terms of channel estimation for the first iteration, the multipath channel is estimated blindly by exploiting the orthogonality between the signal and noise subspaces. For later iterations the channel is estimated using the soft estimates of the coded bits of each user provided by single user iterative decoders in conjunction with the output of the multiuser detector. By exchanging soft information between different stages, the receiver performance is improved through the iteration process. Simulation results demonstrate that the performance of the proposed iterative multiuser detector with integrated channel estimator approaches the single-user bound at high SNR.

5.3 Future Works

The results of this thesis can serve as the basis for the following further research:

- *Joint channel estimation and turbo equalization*: In Chapter 2, we have assumed that the channel coefficients are known to the receiver. Since in a practical system, the system is unkown, it is very important that the proposed method in Chapter 2, which jointly performs turbo equalization and SNR estimation, has to be integrated with a channel estimator to estimate the coefficients of the mutipath channel.

- *Long-code DS-CDMA systems*: one of the key features of the next-generation CDMA-based wireless networks standards is the adoption of long (aperiodic) spreading codes. The use of long codes ensures that all the users achieve on the average the same performance, thus avoiding the unpleasant situation that in an asynchronous environment

two or more users have highly correlated signature waveforms for several bit intervals. On the other hand, long codes destroy some of the bit-interval cyclostationarity properties of the CDMA signals and, thus, make ineffective many of the advanced signal processing techniques that have been developed for blind multiuser detection and adaptive channel estimation in short-code (periodic) DS-CDMA systems. In Chapter 3, we have employed periodic spreading sequences and employed a subspace-based blind method to remove the interference from unknown users. The extension of this method to include the aperiodic spreading sequences poses new challenges and is novel and largely unexplored research topic.

- *Hybrid Channel Estimation*: In Chapter 4, we have employed a blind channel estimator in order to estimate the channel. It has been shown that the proposed algorithm performs well for a moderate frame length. Whereas, for a small frame length this type of channel estimator does not perform very well. Since in a practical system, a frame usually consists of both pilot and data symbols, one possible approach for making the receiver more suitable for small frame lengths is to develop a hybrid channel estimation scheme that employs both a limited number of pilots and data symbols.

- *Group-blind multiuser detection with integrated channel estimation*: The combination of the group blind receiver proposed in Chapter 3 with the channel estimation scheme proposed in Chapter 4 is an interesting topic.

- *Near-Far Problem*: In Chapter 4, we have assumed a perfect power control scheme is in place; therefore, all users signals arrive at the receiver with equal power. Generalizing the method to include a near-far situation is an interesting research topic.

Appendix A

An Improved Max-Log-MAP Algorithm for Turbo Decoding and Turbo Equalization

In this chapter we propose an improved Max-Log-MAP algorithm for turbo decoding and turbo equalization. The proposed algorithm utilizes the MacLaurin Series to expand the logarithmic term in the Jacobian logarithmic function of the Log-MAP algorithm.

In terms of complexity the proposed algorithm can easily be implemented by means of adders and comparators as this is the case for the Max-Log-MAP algorithm. Also, simulation results show that the proposed algorithm has performance very close to the Log-MAP algorithm for both turbo decoding over additive white Gaussian noise (AWGN) channels and turbo equalization over frequency selective channels. Further it is shown than even in a high loss intersymbol interference (ISI) channel, the proposed algorithm preserves its performance close to that of the Log-Map algorithm while there is a wide gap between the performance of the Log-MAP and Max Log-MAP turbo equalizers.

This chapter is organized as follows. After reviewing the turbo decoding and turbo detection schemes in Section A.1, the Log-MAP and the Max-Log-MAP algorithms are

presented in Section A.2. The proposed method is presented in Section A.3. In section A.4 we compare the performance of the proposed algorithm among the Log-MAP and the Max-Log-MAP turbo decoders and turbo equalizers. Section A.5 provides detailed implementation block diagrams for this algorithm. Finally, summary of this chapter is given in Section A.6.

Throughout this chapter, Binary phase shift keying (BPSK) modulation is considered, and it is assumed that in the case of ISI channel, the channel coefficients are known at the receiver.

A.1 Turbo Principles

We briefly review the concepts of turbo decoding and turbo equalization. Detailed explanations are given in [2], [12] and [13] for turbo decoding and in [4] - [7] for turbo equalization.

A.1.1 Turbo Decoder

At the transmitter the information bits u_k first are encoded through the parallel concatenation of two recursive systematic (RSC) codes. It is possible to increase the rate of the overall code by puncturing parity bits in a suitable pattern [2]. In case of turbo decoding, we assume the codes are transmitted over an AWGN, binary input, memory less channel and the rate of the code is equal to 1/2. Corresponding to each data bit u_k, two bits $x_{k,1}$ and $x_{k,2}$ are transmitted, where $x_{k,1}$ is equal to the information bit u_k and $x_{k,2}$ is equal to the parity of one of the component encoders.

A turbo decoder as shown in Fig.A.1 consists of two component decoders that both employ the MAP algorithm to compute *a posteriori* probabilities for information bits, using the trellis structure of encoder as it has been described in [1]. The decoding procedure starts by assuming *a priori* log likelihood ratios (also called L-values) of information bits for *Decoder1*, $L_{D1}^{pri}(\hat{u})$, are equal to zero. Observing scaled output of the channel values $L_c y$, *Decoder1* evaluates the *a posteriori* L-values of information bits. By subtracting the scaled channel values and the *a priori* L-values from output *a posteriori* L-values, the

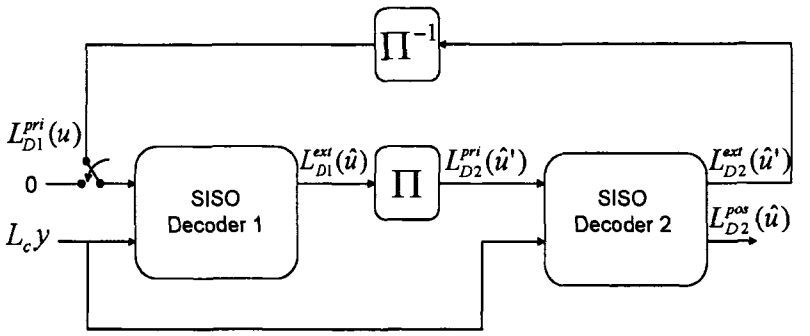

Figure A.1: Turbo decoder

extrinsic information $L_{D1}^{ext}(\hat{u}')$ is obtained. This extrinsic information is interleaved using the same interleaver pattern in the encoder, and is passed to *Decoder2* as the *a priori* L-values $L_{D2}^{pri}(\hat{u}')$. Analogous to the first decoder, the second decoder also computes the new *a posteriori* likelihood ratios, $L_{D2}^{pos}(\hat{u}')$ using updated *a priori* densities and scaled output of the channel values. The extrinsic information is determined, exactly in the same way and is fedback to the *Decoder1* after passing through the deinterleaver. The decoding algorithm proceeds iteratively until the condition of a predetermined number of iterations is satisfied. The output *a posteriori* L-values of *decoder2* $L_{D2}^{pos}(\hat{u})$ are sent to a decision device and the process is terminated.

A.1.2 Turbo Equalizer

In case of turbo equalization the information bits u_k are encoded by an RSC encoder and are interleaved before transmission over an ISI channel. The transmitter filter, the impulse response of the channel and whitening match filter of the receiver can be regarded as a

finite impulse response (FIR) filter [14] [15]. If the channel coefficients are known at the receiver, the channel can be decoded using the MAP symbol estimator. In this manner the encoder and the channel form serially concatenated codes which can be decoded using the turbo scheme shown in Fig.A.2.

The *SISO equalizer* observes channel values y and then it provides *a posteriori* probability L-values $L_E^{pos}(\hat{x})$ for all coded bits using the *a priori* information $L_E^{pri}(\hat{x})$. For the first iteration we assume $L_E^{pri}(\hat{x})$ to be zero. The extrinsic information $L_E^{ext}(\hat{x})$ is obtained by subtracting the *a priori* probabilities from the *a posteriori* L-values. After deinterleaving, the extrinsic information is passed to the *SISO decoder* as priori L-values $L_D^{pri}(\hat{x'})$. The decoder does not have access to the channel values. The decoder provides *a posteriori* L-values for both the information bits and parity bits $L_D^{pos}(\hat{x'})$ using the *a priori* probabilities provided by the *SISO equalizer*. Again, the extrinsic information $L_D^{ext}(\hat{x'})$ is formed after eliminating the effect of *a priori* L-values. After interleaving, this extrinsic information is delivered to the *SISO equalizer* as the *a priori* L-values. The iterative equalization and decoding proceed until the condition of a certain number of iterations is satisfied. At this point the *a posteriori* L-values of the information bits, at the output of the decoder $L_D^{pos}(\hat{u})$, are sent to a decision device and the process is terminated.

A.2 Optimum and Suboptimum MAP Algorithms for Equalization and Decoding

We consider the RSC encoder and tapped delay line model of channel for equalization and decoding. Given a binary input alphabet $\{-1, 1\}$, the encoder (or the channel) can be in one of 2^M states corresponding to different contents of encoder (or channel) memories. The trellis structure is exploited to compute the *a posteriori* L-values:

$$L(\hat{x_k}) = \log \frac{P(x_k = 1|\mathbf{y})}{P(x_k = -1|\mathbf{y})} = \log \frac{\sum\limits_{(s',s),x_k=1} p(s', s, \mathbf{y})}{\sum\limits_{(s',s),x_k=-1} p(s', s, \mathbf{y})}, \tag{A.1}$$

where s' and s represent the states of the encoder (or channel) at time $k-1$ and k and y is the received sequence of length N respectively. Dividing the received sequence into three

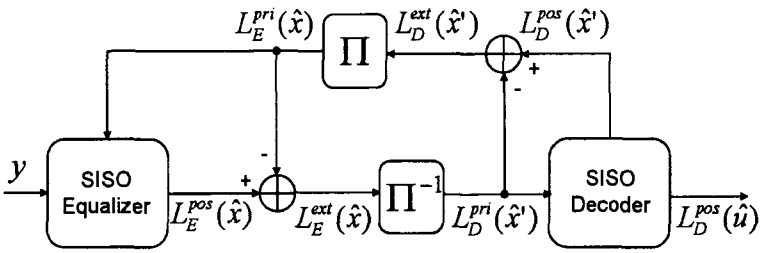

Figure A.2: Turbo Equalizer

separate terms and applying the chain rule we get:

$$p(s', s, \mathbf{y}) = p(s', y_1, ..., y_{k-1}).p(s, y_k|s').p(y_{k+1}, ..., y_N|s). \tag{A.2}$$

This results in decomposition of the numerator and the denominator of equation (A.1) into three terms that can be evaluated recursively, using the forward/backward algorithm.

$$\alpha_k(s') = p(s', y_1, ..., y_{k-1}) \tag{A.3}$$

$$\beta_{k+1}(s) = p(y_{k+1}, ..., y_N|s) \tag{A.4}$$

$$\gamma_k(s', s) = p(s, y_k|s'), \tag{A.5}$$

where $\alpha_{k+1}(s)$ and $\beta_k(s')$ for both the MAP equalizer and the MAP decoder can be computed through the following forward and backward recursions [1]:

$$\alpha_{k+1}(s) = \sum_{s'} \alpha_k(s')\gamma_k(s', s) \tag{A.6}$$

$$\beta_k(s') = \sum_{s} \beta_{k+1}(s)\gamma_k(s', s), \tag{A.7}$$

with boundary conditions $\alpha_0(0)$=1, $\alpha_0(m)$=0 for $m \neq 0$; and $\beta_N(0)$=1, $\beta_N(m)$=0 for $m \neq 0$. However, the calculation of $\gamma_k(s', s)$ in (A.5) for the equalizer and the decoder will be different. According to (A.5)

$$\begin{aligned} \gamma_k(s', s) = p(s, y_k|s') &= p(y_k|s', s)P(s|s') \\ &= p(y_k|s', s)P(x_k), \end{aligned} \tag{A.8}$$

whenever there is a path on trellis between states s' and s; otherwise, $\gamma_k(s', s)$ will be zero. For the decoder, (A.8) can be obtained as follows, [4]:

$$\gamma_k(s', s) = \exp(\sum_{v=1}^{2} \frac{1}{2} x_{k,v} L(\hat{x}_{k,v}) + \frac{1}{2} u_k L(u_k)). \tag{A.9}$$

In the case of the turbo decoding over AWGN channel without ISI, $L(\hat{x}_{k,v})$ is equal to $L_c.y_{k,v} = \frac{4E_b}{N0}.y_{k,v}$, while in the case of the turbo equalization $L(\hat{x}_{k,v})$ is the extrinsic LLR from equalizer at the input of the decoder, and $L(u_k)$ is the *a priori* information for the information bit u_k.

For the equalizer (A.8) can be obtained as follows, [4]:

$$\gamma_k(s', s) = \exp(-\frac{1}{2\sigma_{ch}^2} |y_k - \sum_{i=0}^{M-1} g_i x_{k-i}|^2 + \frac{1}{2} x_k L(x_k)), \tag{A.10}$$

where $\sigma_{ch}^2 = N_0/2$, is the variance of the noise and M denotes the memory length of the channel. y_k is the symbol value received at time k, g_i values correspond to the channel coefficients, and $L(x_k)$ is the *a priori* information for the coded bit x_k.

The Log-MAP algorithm introduced in [52] evaluates $\alpha_{k-1}(s')$, $\beta_k(s)$ and $\gamma_k(s', s)$ in logarithmic terms using the Jacobian logarithmic function. Using this approach the forward/backward recursion in (A.6) and (A.7) will change to,

$$\bar{\alpha}_k(s) = \widehat{\max}(\bar{\alpha}_{k-1}(s') + \bar{\gamma}_k(s', s)) \tag{A.11}$$

$$\bar{\beta}_{k-1}(s') = \widehat{\max}(\bar{\beta}_k(s) + \bar{\gamma}_k(s', s)), \tag{A.12}$$

where

$$\widehat{\max}(z_1, z_2) = \max(z_1, z_2) + \log(1 + \exp(-|z_1 - z_2|)) \tag{A.13}$$

and $\bar{\alpha}_k(s)$, $\bar{\beta}_k(s)$ and $\bar{\gamma}_k(s',s)$ represent the logarithmic values of $\alpha_k(s)$, $\beta_k(s)$ and $\gamma_k(s',s)$ respectively. Finally, the soft output maximum *a posteriori* log likelihood ratio of the decoder can be determined as follows:

$$L(\hat{x}_k) = \widehat{\max}_{(s',s),x_k=1}(\bar{\alpha}_{k-1}(s') + \bar{\gamma}_k(s',s) + \bar{\beta}_k(s)) - \widehat{\max}_{(s',s),x_k=-1}(\bar{\alpha}_{k-1}(s') + \bar{\gamma}_k(s',s) + \bar{\beta}_k(s)), \tag{A.14}$$

the $\widehat{\max}$ operation in the first and second part of equation (A.14) applied only to those existing transitions in the trellis structure where the coded bit x_k is 1 or -1 respectively.

The Max-Log-MAP algorithm in [53] is obtained, by omitting the logarithmic part of equation (A.13). Using this approximation, the Max-Log-MAP algorithm is suboptimal and gives an inferior performance compared to that of the Log-MAP algorithm. In the next section we introduce a new approximation for the Log-MAP algorithm that provides a solution to a number of difficulties that Log-MAP algorithm introduces in practice.

A.3 Improved Max-Log-MAP Algorithm: The Log-MAP Extension

On the one hand evaluation of theLog-MAP algorithm by exploiting the Jacobian logarithmic function in (A.13) results in high complexity. On the other hand, saving the results of $\log(1+\exp(-|z_1 - z_2|))$ in a lookup table would introduce a quantization error caused by truncation of the input of the lookup table (this truncation is necessary because otherwise the size of the lookup table becomes extremely large and the implementation is infeasible). Another problem with the Log-MAP algorithm is that multiple lookup tables are required for a wide range of operating signal to noise ratios, thus increasing hardware cost. Moreover in order to evaluate each maximum *a posteriori* L-value at the output of the equalizer or the decoder, correction terms should be added to the intermediate results from lookup tables recursively. Reading data from these tables is a time consuming process and thus it is not desirable; however, high speed adders and comparators can be implemented effectively thereby reducing power, area and increasing the overall speed which desperately is needed by communication systems. It should be noted that the logarithmic term of equa-

tion (A.13) is effective when $|z_1 - z_2|$ is around zero, otherwise the effect of this term is negligible. Therefore MacLaurin Series expansion is employed to describe the logarithmic term around zero. By neglecting orders greater than one we come up with:

$$\log(1 + \exp(-x)) \approx \log 2 - \frac{1}{2}x, \tag{A.15}$$

since the logarithmic term of equation (A.13) is always greater than zero, we rewrite equation (A.13) using (A.15) as follows,

$$\widehat{\max}(z_1, z_2) \approx \max(z_1, z_2) + \max(0, \log 2 - \frac{1}{2}|z_1 - z_2|). \tag{A.16}$$

Equation (A.16) can be easily implemented using comparators, adders and a shift register. It can be shown that the expression $\log(\exp z_1 + \exp z_2 + \ldots + \exp z_n)$ can be computed recursively. It is evident that the complexity of the proposed algorithm is much lower than the Log-MAP algorithm. In the next section we will show that the performance of the proposed algorithm is very close to the Log-MAP algorithm.

A.4 Simulation results

The performance results for turbo decoding and turbo equalization are shown in Fig.A.3 to A.5. A recursive systematic encoder with two memories and the generator matrix $g = [1, \frac{5}{7}]$ is employed. For turbo code over AWGN channel we considered block length of N=1024 bits, while for turbo equalization over ISI channels two different block lengths N=250 and N=2048 are employed. For turbo detection it is assumed that data is transmitted over two different time invariant channels B and C with tap coefficients $B = \{.407, .815, .407\}$ and $C = \{.227, .460, .688, .460, .227\}$ corresponding to moderate and high loss channels [15] respectively. From these figures it is evident that for turbo decoding over the AWGN channel and turbo detection over moderate loss channel B the Max-Log-MAP algorithm has close performance to the Log-MAP algorithm and the proposed method; however, in the high loss channel the proposed method outperforms the Max-Log-MAP algorithm by a factor of about 1dB gain in the low bit error rate region. Also in all considered channels the proposed method has very close performance to the Log-MAP algorithm.

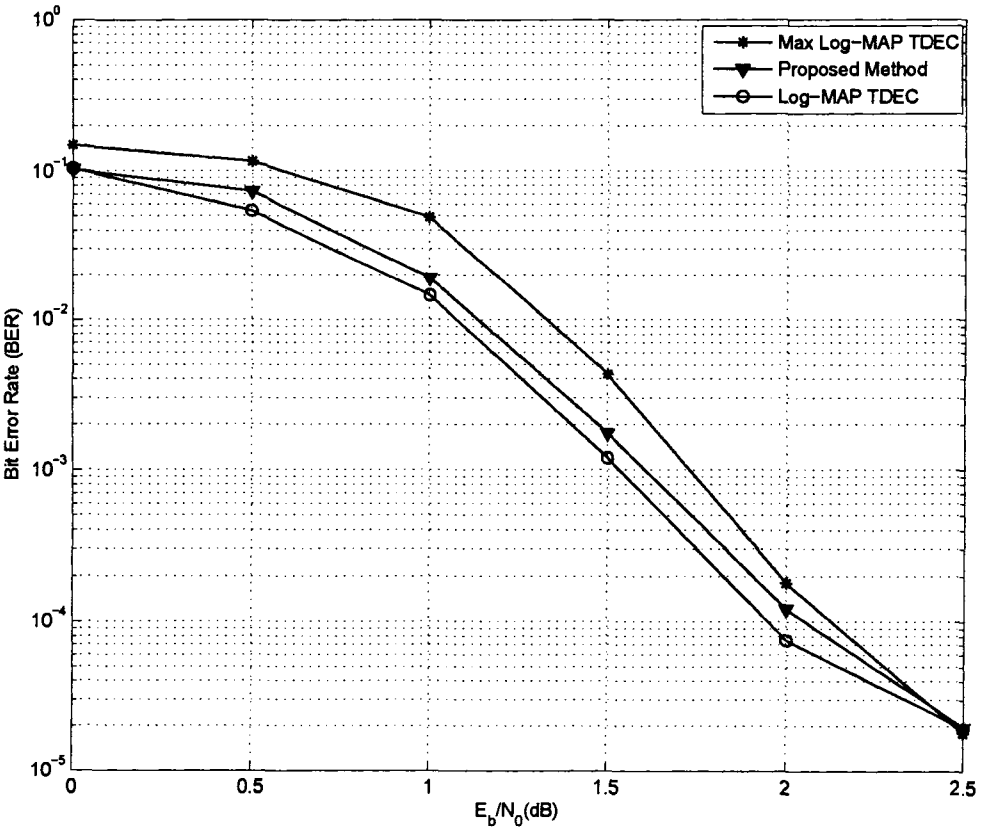

Figure A.3: Turbo decoding Performance, N=1024, No. of Iteration=5, AWGN Channel

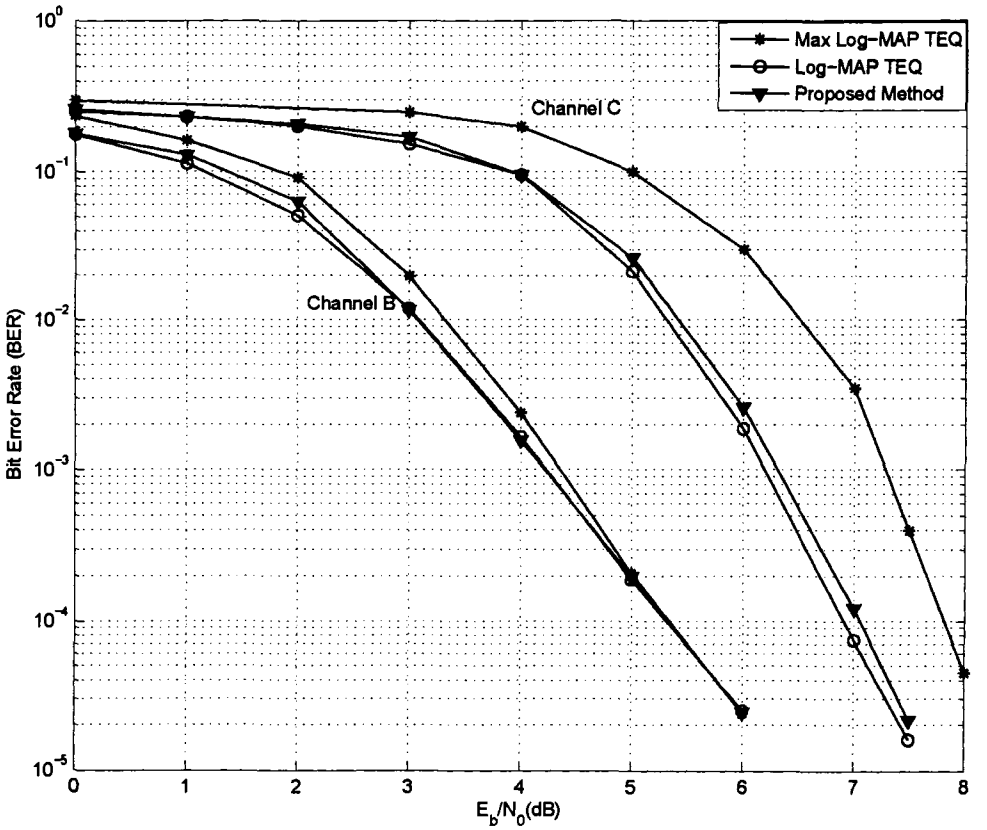

Figure A.4: Turbo Equalization Performance, N=250, No. of Iteration=5

A.5 Design Architecture

The block diagram in Fig.A.6 shows the node metric calculation units. In this figure s_j refers to the state j at time k, while s'_j and s''_j refer to those pervious states at time $k-1$ which enter to the state s_j at time k. The delay elements shown by "D" in this figure are employed in order to provide the node metric values at time $k-1$. The values of $\alpha_k(s)$, in this figure are computed for a turbo decoder (or a turbo equalizer) with n different states using equation (A.11). It should be noted that $\beta_k(s)$ is determined using the same structure in backward recursion. As is evident from this figure, node metrics are computed in parallel. Fig.A.7 shows the detailed architecture of each block in Fig.A.6. It is evident from this figure that the implementation of the additional part in (A.16) in this method is very simple and needs a smaller chip area size compared to the additional part in the Log-MAP algorithm in (A.13) that needs multiple look-up tables for a wide range of SNRs, which increases the chip area and consequently the implementation cost.

A.6 Summary

A novel implementation of the Log-MAP algorithm has been proposed which results in almost equivalent performance to the optimum algorithm and avoids implementation difficulties. The performance of the proposed method is compared with that of the Log-MAP and the Max-Log-MAP algorithms and it is shown that the proposed method has obvious advantages over the Max Log-MAP algorithm, especially where turbo detection over high loss channels is considered. The difference between the proposed method and the Log-MAP algorithm is that the proposed algorithm exploits the MacLaurin Series expansion instead of the logarithmic term in the Jacobian logarithmic function. This replacement enables the direct implementation of the Jacobian logarithmic function employing adders and comparators. As is apparent from the simulation results the proposed method is particularly attractive for turbo detection over high loss ISI channels, since in this challenging application we need to maintain the simplicity of the Max-log-MAP algorithm (because of the overall complexity of the system), yet manage not to compromise the performance.

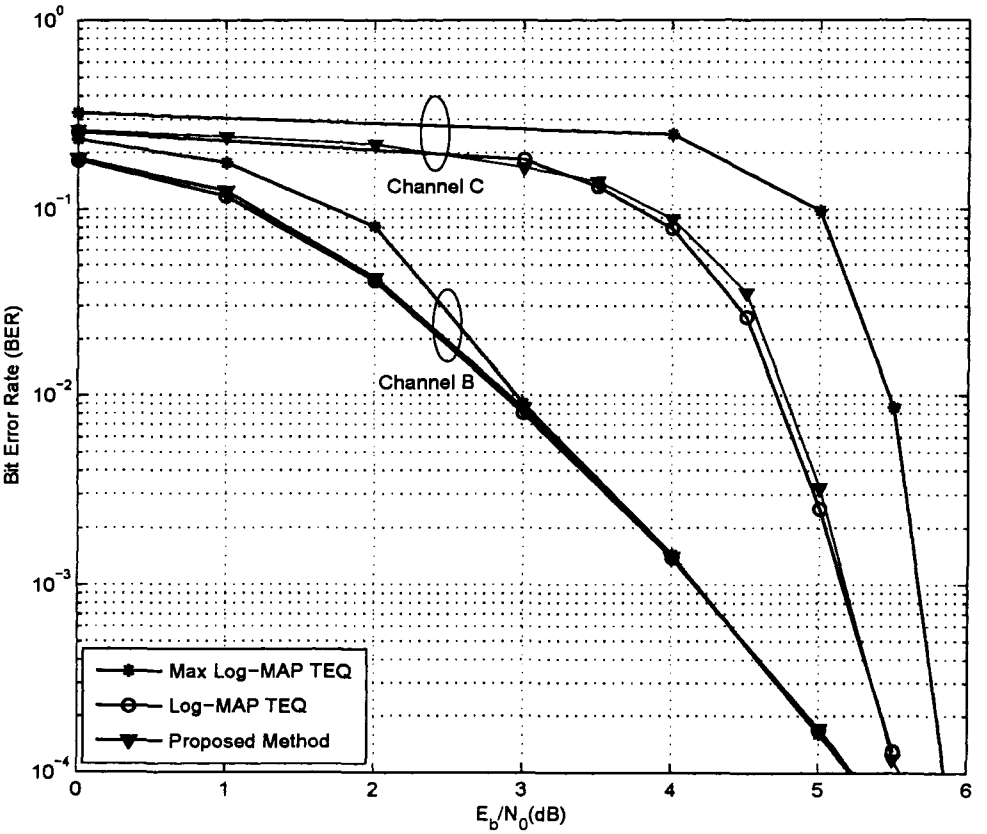

Figure A.5: Turbo Equalization Performance, N=2048, No. of Iteration=5

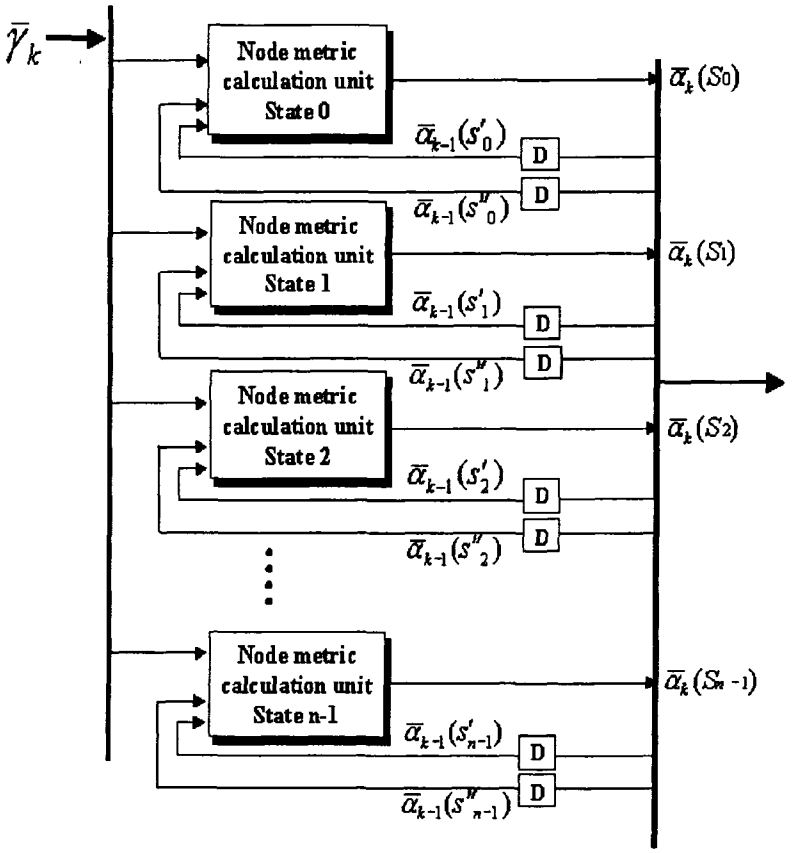

Figure A.6: Node metric calculation unit for n different states

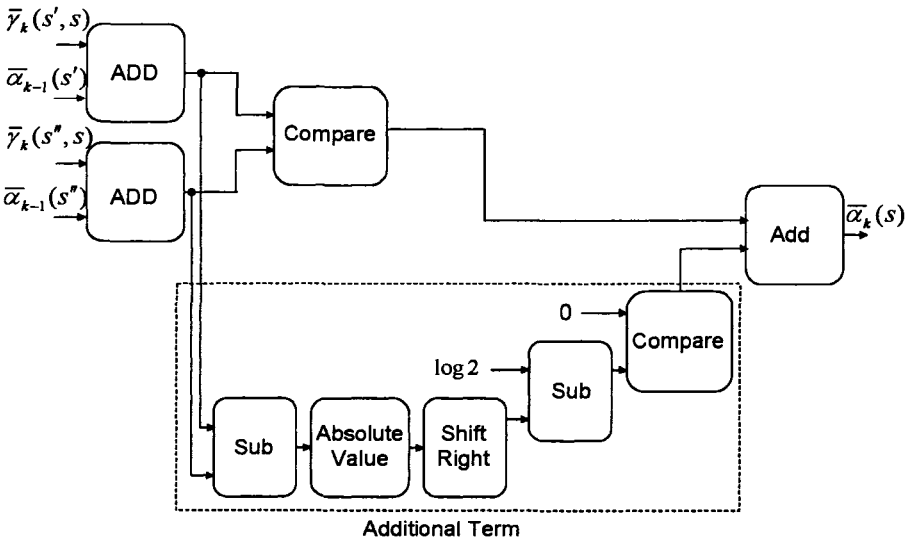

Figure A.7: detailed architecture of proposed method

Appendix B

Proof of (3.3)

As shown in Fig. 3.1, in order to convert the continous-time received signal $r(t)$ into a discrete-time signal at the receiver, $r(t)$ is passed through a matched filter with impulse response $g(t)$, $0 \leq t \leq \frac{T_c}{p}$, and its output is sampled every T_c/p seconds. The output of the matched filter is

$$\begin{aligned} y(t) = r(t) \star g(t) &= \int_{-\infty}^{\infty} r(\tau) g(t-\tau) d\tau, \\ &= \frac{1}{\sqrt{E_p}} \int_{t-\frac{T_c}{p}}^{t} r(\tau) \psi(\frac{T_c}{p} - t + \tau) d\tau, \end{aligned} \tag{B.1}$$

which follows because $g(t) = \frac{1}{\sqrt{E_p}} \psi(\frac{T_c}{p} - t)$, $0 \leq t \leq \frac{T_c}{p}$, and zero otherwise.

Now, if we sample the output of the filter at $t = iT + (q+1)\frac{T_c}{p}$, we obtain

$$r_q[i] \triangleq y(t)|_{t=iT+(q+1)\frac{T_c}{p}} = \frac{1}{\sqrt{E_p}} \int_{iT+q\frac{T_c}{p}}^{iT+(q+1)\frac{T_c}{p}} r(\tau) \psi(\tau - (iT + q\frac{T_c}{p})) d\tau \tag{B.2}$$

for $i = 0, \cdots, M-1$ and $q = 0, \cdots, P-1$. Substituting (3.1) into (B.2) gives

$$\begin{aligned} r_q[i] &= \sum_{k=1}^{K} \sum_{m=0}^{M-1} d_k[m] \frac{1}{\sqrt{N}} \sum_{j'=0}^{N-1} s_k[j'] \sum_{l=1}^{L} g_{l,k} \\ &\times \frac{1}{\sqrt{E_p}} \int_{iT+q\frac{T_c}{p}}^{iT+(q+1)\frac{T_c}{p}} \psi(\tau - mT - \tau_{l,k} - j'T_c) \psi(\tau - iT - q\frac{T_c}{p}) d\tau + \sigma n_q[i], \end{aligned} \tag{B.3}$$

where $n_q[i] = \frac{1}{\sqrt{\sigma^2 E_p}} \int_{iT+q\frac{T_c}{p}}^{iT+(q+1)\frac{T_c}{p}} n(\tau)\psi(\tau - iT - q\frac{T_c}{p})d\tau$.

Operating a change of variable $t = \tau - iT - q\frac{T_c}{p}$ turns (B.3) into the following:

$$\begin{aligned} r_q[i] &= \sum_{k=1}^{K} \sum_{n=i-M+1}^{i} d_k[i-n] \frac{1}{\sqrt{N}} \sum_{j'=0}^{N-1} s_k[j'] \sum_{l=1}^{L} g_{l,k} \\ &\times \frac{1}{\sqrt{E_p}} \int_0^{T_c/p} \psi(t)\psi(t - (\tau_{l,k} - nT + j'T_c - q\frac{T_c}{p}))dt + \sigma n_q[i], \end{aligned} \tag{B.4}$$

where the substitution $n = i - m$ has also been employed.

The integral (B.4) is nonzero only when $\psi(t)$ and $\psi(t-(\tau_{l,k}-nT+j'T_c-q\frac{T_c}{p}))$ overlap on $[0, T_c/p]$. Since $\psi(t) = 0$ outside of the interval $0 \le t \le T_c$, the integral is nonzero for

$$-T_c < \tau_{l,k} - nT + j'T_c - q\frac{T_c}{p} < \frac{T_c}{p}, \tag{B.5}$$

or

$$j'T_c + \tau_{l,k} - q\frac{T_c}{p} - \frac{T_c}{p} < nT < T_c + j'T_c + \tau_{l,k} - q\frac{T_c}{p}. \tag{B.6}$$

The upper bound of n is obtained when $j' = N-1$, $\tau_{l,k} = \iota T$, and $q = 0$, while the lower bound can be obtained when $j' = 0$, $\tau_{l,k} = 0$, and $q = P-1$. Substituting the corresponding values of j', $\tau_{l,k}$ and q into (B.6) yields

$$-T < nT < (\iota + 1)T. \tag{B.7}$$

Using (B.7), it can be concluded that the signals in the integral above overlap only for $n = 0, \cdots, \iota$, since n is a positive integer. Then (B.4) can be rewritten as follows:

$$\begin{aligned} r_q[i] &= \sum_{k=1}^{K} \sum_{n=0}^{\iota} d_k[i-n] \frac{1}{\sqrt{N}} \sum_{j'=0}^{N-1} s_k[j'] \sum_{l=1}^{L} g_{l,k} \\ &\times \frac{1}{\sqrt{E_p}} \int_0^{T_c/p} \psi(t)\psi(t - (\tau_{l,k} - nT + j'T_c - q\frac{T_c}{p}))dt + \sigma n_q[i], \end{aligned} \tag{B.8}$$

which agrees with the result given in (3.3).

□

References

[1] L. Bahl, J. Cocke, F. Jelinek, and J. Raviv, "Optimal Decoding of linear codes for minimizing symbol error rate," *IEEE Trans. Inform. Theory,* vol. It-20,pp. 284-287, March 1974.

[2] C. Berrou, A.Glavieux, and P. Thitimajshima, "Near Shannon limit error-correcting coding and decoding: Turbo-codes," in *Proc. ICC '93,* pp. 1064-1070, May 1993.

[3] C.Douillard, M. Jezequel, C. Berrou, A. Picart, P. Didier, and A. Glavieux, "Iterative correction of Intersymbol interference: Turbo-equalization," *European Transactions on Telecommunications,* vol. 6, pp. 507-511, September-October 1995.

[4] G. Bauch, H. Khoram, and J. Haganauer, "Iterative equalization and decoding in mobile communications systems," in *The Second European Personal Mobile Communications Conference (2.EPMCC'97) together with 3.ITG-Fachtagung "Mobile Kommunikation",* pp. 307-312, VDE/ITG, September/October 1997.

[5] G. Bauch and V. Franz, "A comparison of soft-in/soft-out algorithms for 'Turbo detection'," in *Proc. Intern. Conf. on Telecomm.,* pp. 259-263, June 1998.

[6] G. Bauch and V. Franz, "Iterative equalization and decoding for the GSM - system,"

[7] R. Koetter, A. C. Singer, and M. Tuchler, "Turbo Equalization," *Signal Processing Magazine,* vol. 21, no. 1, pp. 67-80, Jan. 2004.

[8] A.Worm, P. Hoeher, and N. When, "Turbo decoding without SNR estimation," *IEEE Commun. Lett.,* vol. 4, pp. 193-195, June 2000.

[9] M.A. Khalighi, "Effect of mismatched SNR on the performance of Log-MAP turbo detector," *IEEE Trnas. on Vehicular Technology,* vol. 52, No. 5, pp. 1386-1397, September 2003.

[10] M.A. Khalighi,"Sensitivity to SNR mismatch in interference canceling based turbo equalizers," in *Proc. 13th IEEE Int. Symp. Personal, Indoor, and Mobile Radio Communication (PIMRC),* pp. 379-383, September 2002.

[11] T.A. Summers and S.G Wilson, "SNR mismatch and online estimation in turbo decoding," *IEEE Trans. on Commun.,* vol. 46, pp. 421-423, April 1998.

[12] J. Hagenauer, E. Offer, and L. Papke, "Iterative decoding of binary block and convolutional codes," *IEEE Trans on Information Theory,* vol. 42, pp. 429-445, March 1996.

[13] B. Sklar, "A primer on turbo code concepts," *IEEE Commu. Magazine,* vol. 35, no. 12, pp. 94-102, Dec. 1997.

[14] G. Stüber, *Principle of mobile communication,* 2nd ed. Kluwer Academic Publishers, 2001.

[15] J. G. Proakis, *Digital communications,* 4th ed. New York: McGraw-Hill, 2001.

[16] W. C. Y. Lee, *Mobile Cellular Telecommunications*, New York: McGraw-Hill, 1995.

[17] T. S. Rappaport, *Wireless Communications*, Englewood Cliffs, NJ: Prentice-Hall, 2002.

[18] IS-95-A, "Mobile Station-Base Station Compatibility Standard for Dual-Mode Wideband Spread Spectrum Cellular System," 1995.

[19] R. Prasad, W. Mohr, and W. Konhauser, *Third Generation Mobile Communication Systems*, Norwood, MA: Artech House, 2000.

[20] IS-2000, "Physical Layer Standard for cdma2000 Spread Spectrum Systems," 2000.

[21] 3GPP, "Physical Channels and Mapping of Transport Channels onto Physical Channels (fdd)," *3G TS 25.211*, 1999.

[22] T. Ojanpera and R. Prasad, *WCDMA: Towards IP Mobility and Mobile Internet*, Norwood, MA: Artech House, 2000.

[23] R. Prasad, *CDMA for Wireless Personal Communications*, Norwood, MA: Artech House, 1996.

[24] F. Adachi, M. Sawahashi, and H. Suda, "Wideband DS-CDMA for Next-Generation Mobile Communications Systems," *IEEE Communications Magazine*, vol. 36, no. 9, pp. 5669, 1998.

[25] S. Dehghan, et al., "W-CDMA Capacity and Planning Issues," *Electronics and Communication Engineering Journal*, pp. 101118, 2000.

[26] R. Qiu, W. Zhu, and Y. Zhang, "Third-Generation and Beyond (3.5g) Wireless Networks and its Applications," *IEEE Proc. of ISCAC, 2002*, pp. I-41I-44, 2002.

[27] J. M. Hernando, and F. Perez-Fontan, *Introduction to Mobile Communications Engineering, Norwood*, MA: Artech House, 1999.

[28] H. Hammuda, *Cellular Mobile Radio Systems (Designing Systems for Capacity Optimization)*, New York: John Wiley and Sons, 1997.

[29] W. Lee, "Overview of Cellular CDMA," *IEEE Trans. on Vehicular Technology*, vol. 40, no. 2, pp. 291302, 1991.

[30] R. Kohno, R. Meidan, and L. Milstein, "Spread Spectrum Access Methods for Wireless Communications," *IEEE Commun. Mag.*, vol. 33, no. 1, pp. 5867, 1995.

[31] A. J. Viterbi, "The orthogonal-random waveform dichotomy for digital mobile personal communications," *IEEE Personal Commun.*, vol. 1, no. 1, pp. 1824, 1st Qtr. 1994.

[32] R. L. Pickholtz, L. B. Milstein, and D. L. Schilling, "Spread spectrum for mobile communications," *IEEE Trans. Veh. Technol.*, vol. 40, pp. 313322, May 1991.

[33] S. Moshavi, "Multi-user detection for DS-CDMA communications," *IEEE Commun. Mag.*, vol. 34, pp. 132136, Oct. 1996.

[34] R. Lupas and S. Verdú, "Near-far resistance of multiuser detectors in asynchronous channels," *IEEE Trans. Commun.*, vol. 38, pp. 496-508, April 1990.

[35] C. Sankaran and T. Ephremides, "Solving a class of optimum multiuser detection problems with polynomial complexity," *IEEE Trans. Inform. Theory*, vol. 44, pp. 1958-1961, Sept. 1998.

[36] S. Ulukus and R. D. Yates, "Optimum multiuser detection is tractable for synchronous CDMA using m-sequences," *IEEE Commun. Letters*, vol. 2, pp. 8991, April 1998.

[37] C. Schlegel and A. Grant, "Polynomial complexity optimal detection of certain multiple-access systems," *IEEE Trans. Inform. Theory*, vol. 46, pp. 22462248, Sept. 2000.

[38] R. Nilsson, F. Sjöberg, O. Edfors, P. Ödling, H. Eriksson, S. K. Wilson, and P. O. Börjesson, "A low complexity threshold detector making MLSD decision in a multiuser environment," in *Proc. IEEE Veh. Techno. Conf.*, pp. 333337, Ottawa, Canada, May 1998.

[39] P. Nèmeth, L. K. Rasmussen, and T. M. Aulin, "Maximum-likelihood detection of block coded CDMA using the A algorithm," in *Proc IEEE Int. Symp. Inform. Theory*, p. 88, Washington, USA, June 2001.

[40] R. Lupas and S. Verdú, "Linear multiuser detectors for synchronous code-division multiple-access systems," *IEEE Trans. Inform. Theory*, vol. 35, pp. 123-136, Jan. 1989.

[41] Z. Xie, R. T. Short, and C. K. Rushforth, "A family of suboptimum detectors for coherent multiuser communications," *IEEE J. Selected Areas Commun.*, vol. 8, pp. 683-690, May 1990.

[42] S. Haykin, *Adaptive Filter Theory*. Prentice-Hall, Englewood Cliffs, NJ, 1996.

[43] T. J. Lim and S. Roy, "Adaptive filters in multiuser cdma detection," *Baltzer Wireless Networks*, vol. 4, pp. 307-318, April 1998.

[44] M. Honig and M. K. Tsatsanis, "Adaptive techniques for multiuser CDMA receivers," *IEEE Signal Processing Magazine*, vol. 17, pp. 49-61, May 2000.

[45] L. K. Rasmussen, *Iterative detection methods for multi-user direct sequence CDMA systems*, ch. online in subject category Multiuser Communications, online April 2003. The Wiley Encyclopedia of Telecommunications, Wiley and Son, 2004.

[46] P. Patel and J. Holtzman, "Analysis of a simple successive interference cancellation scheme in a DS/CDMA system," *IEEE J. Selected Areas Commun.*, vol. 12, pp. 1713-1724, June 1994.

[47] M. K. Varansi and B. Aazhang, "Multi-stage detection in asynchronous code-division multiple access communications," *IEEE Trans. Commun.*, vol. 38, pp. 509-519, April 1990.

[48] P. H. Tan, L. K. Rasmussen, and T. J. Lim, "Constrained maximum-likelihood detection in CDMA," *IEEE Trans. Commun.*, vol. 49, pp. 142153, Jan. 2001.

[49] F. Tarköy, "MMSE-optimal feedback and its applications," in *Proc. Int. Symp. Inform. Theory*, p. 334, Whistler, B.C., Canada, Sept. 1995.

[50] S. Gollamudi and Y.-F. Huang, "Iterative nonlinear MMSE multiuser detection," in *Proc. Int. Conf. Acoustics, Speech and Sig. Proc.*, pp. 25952598, Phoenix, USA, March 1999.

[51] R. Müller and J. Huber, *Iterative soft-decision interference cancellation for CDMA*, pp. 110115, Broadband Wireless Communications, Springer, London, U.K., 1998.

[52] P. Robertson, P. Hoeher, and E. Villebrun, "Optimal and sub-optimal maximum a posteriori algorithms suitable for turbo decoding," *Eur. Trans. Telecommun.*, vol. 8, no. 2, pp. 119-125,1997.

[53] J.A. Erfanian, S. Pasupathy, and G. Gulak, "Reduced complexity symbol detectors with parallel structures for ISI channels," *IEEE Trans. Commun.*, vol. 42, pp. 1661-1671, February/March/April 1994.

[54] S. Talakoub and B. Shahrrava, "Turbo equalization with iterative online SNR estimation," *IEEE Wireless Communications and Networking Conference*, vol. 1, pp. 267 - 272, March 2005.

[55] Y. Chen and N C. Beaulieu, "An approximate maximum likelihood estimatior for SNR jointly using pilot and data symbols," *IEEE Commun. Lett.*, vol. 9, pp. 517-519, June 2005.

[56] M. A. Dangl and J. Lindner, "Turbo equalization with parametric uncertainties: comparison of SNR estimation algorithms," *Proc. 2nd COST 289 workshop,* pp. 129-133, Antalya, Turkey, July 6-7, 2005.

[57] C. Berrou and A. Glavieux, "Near optimum error-correcting coding and decoding:turbo codes," *IEEE Trans. Commun.*, vol. 44, pp. 1261-1271, Oct. 1996.

[58] P. D. Alexander, A. J. Grant, and M. C. Reed, "Iterative detection in code-division multiple-access with error control coding," *Eur. Trans. Telecommun.*, vol. 9, no. 5, pp. 419-426, Sept.- Oct. 1998.

[59] M. Moher, "An iterative multiuser decoder for near capacity communications," *IEEE Trans. Commun.*, vol. 46, no. 7, pp. 870880, July 1998.

[60] P. D. Alexander, M. C. Reed, J. A. Asenstorfer, and C. B. Schlegel, "Iterative multiuser interference reduction: Turbo CDMA," *IEEE Trans. Commun.*, vol. 47, pp. 1008-1014, July 1999.

[61] M. C. Reed, C. B. Schlegel, P. D. Alexander and J. A. Asenstorfer, "Iterative multiuser detection for CDMA with FEC: Near single user performance," *IEEE Trans. Commun.*, vol. 46, no. 12, pp. 16931699, Dec. 1998.

[62] H. El Gamal and E. Geraniotis, "Iterative multiuser detection for coded CDMA signals in AWGN and fading channels," *IEEE J. Selec. Areas Commun.*, vol. 18, pp. 30-41, Jan 2000.

[63] Y. Zhang and R. S. Blum, "Multistage multiuser detection for CDMA with space-time coding," in *Proc. IEEE Workshop on Statistical and Array Processing*, Aug. 2000.

[64] H. V. Poor, "Iterative multiuser detection," *IEEE Signal Processing Magazine*, vol. 21, no. 1, pp. 8186, 2004.

[65] X. Wang and H. V. Poor, "Iterative (Turbo) soft interference cancellation and decoding for coded CDMA," *IEEE Trans. Commun.*, vol. 47, pp. 1046-1061, July 1999.

[66] A. Høst-Madson, "Semi-blind multiuser detectors for CDMA: Subspace methods," Technical Report. TR Labs, University of Calgary, Calgary, Alberta, Canada, 1997.

[67] A. Høst-Madson and K. S. Cho. "MMSE/PIC multi-user detection for DS-CDMA systems with inter- and intra- interference," *IEEE Trans. Commun.*, vol. 47(2), pp. 291-299, Feb. 1999.

[68] A. Høst-Madson and J.Yu. "Hybrid semi-blind multiuser detection: Subspace tracking method," in *Proc. IEEE Int. Conf. Acoustic, Speech and Signal processing"*, pp. III.352-III.355, 1999.

[69] X. Wang and A. Høst-Madson, "Group blind multiuser detection for uplink CDMA," *IEEE J. Select. Areas Commun.*, vol. 17, pp. 1971-1984, Nov. 1999.

[70] P. Spasojevic, X. Wang, and A. Høst-Madsen, "Nonlinear group-blind multiuser detection," *IEEE Trans. Commun.*, vol.49(9), pp. 1631 - 1641, Sept. 2001.

[71] L. Wu, G. Liao, and Hui Huang, "A novel nonlinear group-blind multiuser detection technique," in *Proc. IEEE Int. Conf. Acoustic, Speech and Signal processing"*, vol. 4, pp. IV.49-IV.52, April 2003.

[72] L. Wu, G. Liao, C. Wang, and Y. Shang, "Bayesian multiuser detection for CDMA system with unknown interference," in *Proc. IEEE Int. Conf. on Communications"*, vol. 4, pp. 2490 - 2493, May 2003.

[73] D. Reynolds and X. Wang, "Turbo multiuser detection with unknown interferences," *IEEE Trans. Commun.*, vol. 50, pp. 616-622, July 1999.

[74] H. V. Poor and S. Verdú,"Probability of error in MMSE multiuser detection," *IEEE Trans. Inform. Theory*, vol. 44, pp. 858-871, May 1997.

[75] S. Verdú, "Minimum probability of error for asynchronous Gaussian multiple-access channels," *IEEE Trans. Inform. Theory*, vol. 32, pp. 8596, Jan. 1986.

[76] S. Verdú, *Multiuser Detection*, Cambridge University Press, Cambridge, UK, 1998.

[77] M. Wax and T. Kailath, "Detection of signals by information theoretic criteria," *IEEE Trans. Acoust., Speech, Signal Processing*, vol. 33, pp. 387-392, April 1985.

[78] Z. Xu and R. S. Cheng, "A robust rank estimation algorithm of group-blind MMSE multiuser detectors for CDMA systems," *IEEE Trans. Commun.*, vol. 51, pp. 547-552, April 2003.

[79] M. H. Moghari and Behnam Shahrrava, "Group blind multiuser detection for CDMA using a Gaussian approximation," in *Proc. IEEE Wireless Communication and Networking Conference"*, vol. 1, pp. 267 - 272 , March 2005.

[80] J. Hagenauer, "The turbo principle: tutorial introduction and state of the art," in *Proc. Int. Symp. Turbo Codes Related Topics*, Brest, France, pp. 1-11, Sept. 1997.

[81] H. V. Poor, "Turbo multiuser detection: A primer," *J. Commun. Networks*, vol. 3, pp. 196-201, Sept. 2001.

[82] S. E. Bensley and B. Aazhang, "Maximum likelihood synchronization of a single user for Code division multiple access communication systems," *IEEE Trans. Commun.*, vol.46, no. 3, pp. 392-399, March 1998.

[83] G. Caire and U. Mitra, "Structured multiuser channel estimation for block-synchronous DS/CDMA," *IEEE Trans. on Commun.*, vol. 49, no. 9, pp. 1605-1617, Sept. 2001.

[84] E. Ertin, U. Mitra, and S. Siwamogsatham, "Maximum-likelihood based multipath channel estimation for code-division multiple-access systems," *IEEE Trans Commun.*, vol. 49, no. 2, pp. 290-302, Feb. 2001.

[85] C. Sengupta, J.R. Cavallaro, and B. Aazhang, "On multipath channel estimation for CDMA systems using multiple sensors," *IEEE Trans. Commun.*, vol. 49, no. 3, pp. 543-554, Mar. 2001.

[86] Z. Xie, C. K. Rushforth, R. T. Short, and T. K. Moon, "Joint signal detection and parameter estimation in multiuser communications," *IEEE Trans. Commun.*, vol. 41, no. 8, pp. 1208-1216, Aug. 1993.

[87] D. Zheng, J. Li, S. L. Miller, and E. Strom, "Efficient code-timing estimator for DS-CDMA signals," *IEEE Trans. Signal Process.*, vol. 45, no. 1, pp. 82-89, Jan. 1997.

[88] X. Wang and H.V. Poor, "Wireless communication systems: Advanced techniques for signal detection," 1st ed., Prentice-Hall, 2004.

[89] S. E. Bensley and B. Aazhang, "Subspace-based channel estimation for code division multiple access communication systems," *IEEE Trans. Commun.*, vol. 44, no. 8, pp. 1009-1020, Aug. 1996.

[90] H. Liu and G. Xu, "A subspace method for signature waveform estimation in synchronous CDMA systems," *IEEE Trans. Commun.*, vol. 44, no. 10, pp. 1346-1354, Nov. 1996.

[91] M. Torlak and G. Xu. "Blind multiuser channel estimation in asynchronous CDMA systems," *IEEE Trans. Signal Process.*, vol. 45, no. 1, pp. 137-147, Jan. 1997.

[92] X. Wang and H.V. Poor, "Blind equalization and multiuser detection in dispersive CDMA channels," *IEEE Trans. Commun.*, vol. 45, no. 9, pp. 91-103, Jan. 1998.

[93] X. Wang and H.V. Poor, "Blind joint equalization and multiuser detection for DS-CDMA in unknown correlated noise," *IEEE Trans. Circuits Syst.II: Analog and Digital Signal Processing*, vol. 46, no. 7, pp. 886-895, July 1999.

[94] A. Lampe, "Iterative multiuser detection with integrated channel estimation for coded DS-CDMA," *IEEE Trans. Commun.*, vol. 50, no. 8, pp. 1217-1223, Aug. 2002.

[95] P. Alexander and A. Grant, "Iterative decoding and channel estimation," in *Proc. IEEE Int. Symp. Inform. Theory (ISIT)*, Sorrento, Italy, June 2000, p. 171.

[96] M. Peleg, S. Shamai (Shitz), and S. Galan, "On iterative decoding for coded noncoherent MPSK communications over block-noncoherent AWGN channel," in *Proc. Int. Conf. Telecommunications (ICT'98)*, Porto Carras, Greece, June 1998, pp. 109-114.

[97] J. Lodge and M. Gertsman, "Joint detection and decoding by turbo processing for fading channel communications," in *Proc. Int. Symp. Turbo Codes*, Brest, France, Sept. 1997, pp. 88-95.

[98] P. Hoeher and J. Lodge, "Iterative decoding/demodulation of coded DPSK systems," in *Proc. IEEE Global Conf. Communications (GLOBECOM'98)*, Sydney, Australia, Nov. 1998, pp. 598-603. B.

[99] B. Petersen and D. Falconer, "Suppression of Adjacent Channel, Co-channel, and Intersymbol Interference by Equalizers and Linear Combiners," IEEE Trans. on Comm., Vol. 42, No. 12, pp. 3109-3118, Dec. 1994.

[100] I. D. Marsland, P. T. Mathiopoulos, and S. Kallel, "Noncoherent turbo equalization for frequency selective Rayleigh fast fading channels," in *Proc. Int. Symp. Turbo Codes*, Brest, France, Sept. 1997, pp. 196-199.

[101] I. D. Marsland and P. T. Mathiopoulos, "On the performance of iterative noncoherent detection of coded M-PSK signals," *IEEE Trans. Commun.*, vol. 48, no. 4, pp. 588-596, April 2000.

[102] C. J. Hegarty and B. Vojcic, "Two-stage multiuser detection for noncoherent CDMA," in *Proc. 33rd Annual Allerton Conf. communication, Control, Computing*, Monticello, IL, pp. 132-136, Oct. 1995

[103] M. Agarwal, K. Datta, and A.K. Chaturvedi, "Optimal bandwidth allocation to coding and spreading in DS-CDMA systems using LMMSE front-end detector," *IEEE Trans. wireless comm.*, vol.4 no. 6, pp. 2636-2641, November 2005.

[104] O.H. Koymen and T.H. Meng, "Oversampling in a forced-asynchronous CDMA system," *IEEE International Conference on Communications ICC01*, vol. 6, pp. 1890-1894, June 2001.

[105] S. Talakoub, L. Sabeti, B. Shahrrava, and M. Ahmadi, "A Simplified Log-MAP Algorithm for Turbo Decoding and Turbo Equalization," accepted for publication in IEEE Transactions on Instrumentation and Measurement, 5 pages, Aug. 2006.